Characterization of *Parelaphostrongylus tenuis* Excretory Glands and Identification of Alpha-Gal-Modified Excreted/Secreted Proteins.

by

Jennifer Fitzpatrick

B.Sc., Dalhousie University, 2008

A Thesis Submitted in Partial Fulfillment

of the Requirements for the Degree of

Master of Science

in the Graduate Academic Unit of Biology

Supervisor: Michael Duffy, PhD., Department of Biology, UNB
Examining Board: Les Cwynar, PhD., Chair
Michael Duffy, PhD., Department of Biology, UNB
Shawn MacLellan, PhD., Department of Biology, UNB
Sara Eisler, PhD., Department of Chemistry, UNB

This thesis is accepted by the
Dean of Graduate Studies

THE UNIVERSITY OF NEW BRUNSWICK

September, 2013

©Jennifer Fitzpatrick, 2013

ABSTRACT

Adult *Parelaphostrongylus tenuis* induce a concomitant immunity that protects their deer host against subsequent infections. Although this phenomenon is common among long-lived parasitic helminths, molecular mechanisms that mediate concomitant immunity remain unknown. Alpha-Gal is a disaccharide that is stage-restricted, synthesized exclusively by adult stage *P. tenuis*, suggesting a potential role in mediating concomitant immunity. Current studies identified excretory glands as the principle source of alpha-Gal-modified glycoproteins. Secretory granules are the dominant component of these specialized cells, confirming a primary role for excretory glands in protein secretion and, by extension, parasitism. The alpha-Gal epitope is also synthesized within the deer host and so parasite-derived alpha-Gal is poised to promote immune modulation. A model is proposed for alpha-Gal-mediated modulation of host immune responses to promote concomitant immunity. Two-dimensional immunoblots and mass spectrometry identified galectin and/or Ancylostoma-secreted protein homologues as likely candidates for modification by alpha-Gal.

DEDICATION

This thesis is dedicated to my parents, Mary and Lee Fitzpatrick. They emphasized the value of education and supported me throughout my many years of study.

ACKNOWLEDGEMENTS

My MSc. research would have been impossible if it were not for a number of people who helped and guided me along the way. Dr. Bryan Crawford and Dr. Dion Durnford were always available to offer their advice and to encourage me to "think outside the box". Their love for science and incredible dedication to their own research were extremely motivating for me.

A significant portion of my research was completed alongside Susan Belfry. Her patience and knowledge helped refine my skills in microscopy, resulting in a chapter of this thesis that I am very proud of. Dr. Chris Jackson's contribution to my work also warrants recognition. The combination of his expertise, calmness, and ease of explaining difficult concepts enabled me to troubleshoot an intimidating part of this thesis, and for this I am incredibly grateful.

It was a pleasure to collaborate with a number of individuals from the New Brunswick Department of Natural Resources. Gary Moore, Dwayne Sabin, and Gail Duncan ensured that I had access to deer heads whenever I needed them. I am thankful to all of the Rangers who helped me with the collection of deer heads, particularly Hurst Gannon, who went above and beyond to make my project a success. I also appreciate the time and effort that Larry Henderson of Custom Meat Cutting and Troy Grant of Blackie's Meat

Shop dedicated to my project during their busiest time of year.

A number of graduate and undergraduate students of the Duffy research group helped me with deer collections, dissections, and providing valuable criticism to my project. Perhaps more importantly is the great atmosphere they created that I always enjoyed being a part of.

I would like to thank Dr. Michael Burt for offering his sage advice whenever needed, in addition to allowing me the use of his laboratory space. It was also a pleasure to work with Dr. Katharine Barclay and I truly appreciate that she offered me Teaching Assistantships each year.

Finally, my supervisor deserves the greatest acknowledgment of all. Dr. Michael Duffy has been a mentor in every sense of the word. While I value the entire graduate program, I truly believe that my professional growth is a result of having worked with Mike. I doubt I will ever have another opportunity to work with someone as patient, motivated and understanding as he is, and I hope to someday be respected by those I supervise as much as he is by me. Working with Mike has without a doubt been the highlight of my graduate school experience. Thanks Mike, you really are the best!

Table of Contents

ABSTRACT ii

DEDICATION iii

ACKNOWLEDGEMENTS iv

Table of Contents vi

List of Tables ix

List of Figures x

Chapter 1 : General Introduction 1

1.1 Distribution of *Parelaphostrongylus tenuis* 1

1.2 *Parelaphostrongylus tenuis* Life Cycle 2

1.3 Helminth Immune Evasion 3

1.3.1 Concomitant Immunity 4

1.3.2 Alpha-Gal and Immune Evasion 5

1.3.3 Molecular Mimicry 6

1.3.4 Immune Modulation: Glycan Gimmickry 7

1.4 Secreted Proteins and Function of the Excretory Gland 7

1.5 Objectives 9

Bibliography 10

Chapter 2 : Excretory Gland Morphology and Improved Localization of the Alpha-Gal Epitope in *Parelaphostrongylus tenuis* 12

2.1 Introduction 12

2.2 Materials and Methods 14

2.2.1 Deer Collection and Dissection 14

2.2.2 Specimen Preparation for General Morphological Studies 15

2.2.3 Specimen Preparation for Immunogold Labeling 16

2.2.4 Immunogold Labeling 17

2.2.5 Collection of Excreted/Secreted Proteins 18

2.2.6 One-Dimensional Gel Electrophoresis and Western Blot 19

2.3 Results 21

2.3.1 Prevalence and Intensity of *Parelaphostrongylus tenuis* in White-tailed Deer of New Brunswick 21

2.3.2 Structure of the Secretory System of Adult *Parelaphostrongylus tenuis*. 24

2.3.3 Morphology and Ultrastructure of the Cuticle 33

2.3.4 Immunogold Labeling for Detection of alpha-Gal 35

2.3.5 Detection of Alpha-Gal in E/S Products and Somatic Extracts from Adult *P. tenuis* 37

2.4 Discussion 39

Bibliography 46

Chapter 3 : Identification of Alpha-Gal-Modified Excreted/Secreted Proteins From Adult *Parelaphostrongylus tenuis* 49

3.1 Introduction 49

3.2 Materials and Methods 53

3.2.1 Generation of a Transcriptome From Secretory Glands of Adult *P. tenuis* 53

3.2.2 Two-Dimensional Gel Electrophoresis and Western Blot 55

3.2.3 Peptide Identification 58

3.2.4 Identifying *P. tenuis* Proteins Corresponding to Sequenced Peptides 60

3.3 Results 63

3.3.1 Transcriptome Assembly 63

3.3.2 Selection of Alpha-Gal-Modified Excreted/Secreted Proteins for MS/MS Peptide Identification 63

3.3.3 nano LC-MS/MS 66

3.4 Discussion 78

3.4.2 Rationale for Galectin-5 and ASPs as Alpha-Gal-Modified E/S Proteins 96

Bibliography 99

Chapter 4 : Implications and Future Prospects 107

4.1 Alpha-Gal at the Host-Parasite Interface 107

4.2 Defining the Role for Alpha-Gal in Parasitism 108

4.3 Secretory Glands as Unique Organs for Protein Secretion 110

Bibliography 112

Appendix 1 113

Appendix 2 120

Curriculum Vitae

List of Tables

Table 2.1 Solutions and processing times used for tissue dehydration and resin infiltration to prepare *Parelaphostrongylus tenuis* specimens for immunogold labeling..... 18

Table 2.2 Prevalence and intensity of adult *Parelaphostrongylus tenuis* in white-tailed deer (*Odocoileus virginianus*)..... 23

Table 3.1 Adult *P. tenuis* Excreted/Secreted Proteins Identified from Tandem Mass Spectrometry Analysis..... 75

Table 3.2 Protein Composition of Alpha-Gal-Modified Spots Identified from 2D Gels. Summary of Predicted Molecular Mass, Extracellular Secretion and N-Glycosylation..... 76

List of Figures

Figure 1.1 Life Cycle of *Parelaphostrongylus tenuis*.1. First-stage larvae (L1) are shed in the feces of the deer host. 2. L1s penetrate a slug or snail, and subsequently develop into infective third-stage larvae (L3). 3. Once ingested by the deer, the L3s enter the alimentary canal and migrate to the lumbar spinal cord. The L3 migrate to the subdural space and travel to the cranium where they mature into adult worms. 4. Female worms release eggs into the blood, enabling eggs to travel to the lungs where they hatch, releasing L1s. The L1 are carried up the mucociliary escalator of the lungs, are swallowed, and are then passed with host feces. 3

Figure 1.2 Structure of galactose-alpha 1,3-galactose (alpha-Gal) 5

Figure 2.1 Adult *Parelaphostrongylus tenuis* contain two large excretory glands that occupy up to 10% of the length of the worm. The excretory glands occur adjacent to the digestive tract (pharynx and intestine). Red arrowheads delineate the anterior end and posterior end of one excretory gland. 25

Figure 2.2 Adult *Parelaphostrongylus tenuis* contain two large excretory glands packed with secretory granules. Light micrographs of a cross-section 2 mm from the anterior tip of the worm stained with toluidine blue and basic fuchsin show two excretory glands housing secretory granules (purple spheres)[A]. Increased magnification view of secretory granules within one excretory gland, and longitudinal ridges that occur as part of the exterior cuticle [B]. c = cuticle, eg = excretory gland, i = intestine, lm = longitudinal muscle, lr = longitudinal cuticular ridges. 26

Figure 2.3 An excretory duct connects the excretory glands with the excretory pore.

Light micrograph of a longitudinal section through adult *Parelaphostrongylus tenuis* stained with toluidine blue and basic fuchsin showing the excretory pore, excretory duct and excretory gland (eg). Also shown are the anterior muscular pharynx and the more posterior glandular pharynx. 27

Figure 2.4 The glandular secretory system of adult *Parelaphostrongylus tenuis* consists of a glandular region in the pharynx and two excretory gland cells. Light micrograph of a longitudinal section through adult *Parelaphostrongylus tenuis* stained with toluidine blue and basic fuchsin showing the components of the secretory system. mp = muscular pharynx, gp = glandular pharynx, eg = excretory gland (only one excretory gland is shown). The excretory pore is also shown. 28

Figure 2.5 The glandular pharynx and excretory glands of *Parelaphostrongylus tenuis* possess large nuclei. Light micrographs of longitudinal sections from the anterior end of adult female *Parelaphostrongylus tenuis* stained with toluidine blue and basic fuchsin show the presence of large nuclei containing a number of nucleoli. One of many large nuclei (n), approximately 30 μm in diameter, found in the glandular pharynx contains 2 darkly stained nucleoli (nu) [A]. Excretory gland cells contain one large nucleus (n), approximately 30 μm in diameter, each with darkly stained nucleoli (nu) [B]..... 29

Figure 2.6 In some instances, the nucleus of each excretory gland was closely associated with the cell membrane via furrows. Light micrographs of longitudinal sections 2-4 mm [A] and 4-6 mm [B] from the anterior end of adult female *Parelaphostrongylus tenuis* show furrows associated with each nucleus. A furrow connects the nucleus with the excretory gland membrane. The nucleoli are absent in one micrograph, but

were located in subsequent sections. All sections were stained with toluidine blue and basic fuchsin. f = furrow, hyp = hypodermis, n = nucleus, nu = nucleoli..... 30

Figure 2.7 Endoplasmic reticulum and mitochondria are abundant in the cytoplasm of the excretory gland cells from adult *Parelaphostrongylus tenuis*. Transmission electron micrographs of the excretory glands showing secretory granules (sg), endoplasmic reticulum (er), and the excretory gland cell membrane (egm) [A]. Mitochondria (m) were found dispersed throughout the excretory gland cells [B]. 31

Figure 2.8 Transmission electron micrograph of secretory granules from the excretory gland cells of adult *Parelaphostrongylus tenuis*. Some granules were clearly enveloped by a membrane (arrowheads) whereas other granules did not have a distinct outer membrane (arrows). 32

Figure 2.9 A transmission electron micrograph through the nucleus of an excretory gland cell of *Parelaphostrongylus tenuis* showing a large nucleolus. The nuclear envelope (ne) is shown enclosing one of the nucleoli (nu), approximately 3 μm in diameter. A mitochondrion (m) and secretory granule (sg) is also shown [A]. Increased magnification highlights the absence of a nucleolar membrane and the presence of a dense fibrillar component (dfc) and a granular component (gc) characteristic of eukaryotic nucleoli [B]. 33

Figure 2.10 The cuticle of adult *Parelaphostrongylus tenuis* is modified with longitudinal cuticle ridges. A transverse section transmission electron micrograph shows the layers of the cuticle that include the epicuticle (ep), the cortical zone (co), the medial zone (md) and the basal zone (bs). The epicuticle (ep) has longitudinal ridges spaced approximately 0.5 μm apart. Other features labeled for orientation include the

hypodermis (hyp), basal lamina (bl) and longitudinal muscle (lm)..... 34

Figure 2.11 Immunogold localization of alpha-Gal to the contents of secretory granules of the excretory gland in adult *Parelaphostrongylus tenuis*. Gold particles (black dots) indicate the presence of the alpha-Gal epitope and are restricted to secretory granules [A]. Increased magnification of the granule from panel A provides an improved image of the gold particles within the granule [B]. Induction of a white halo artifact around gold particles enabled confirmation that alpha-Gal is restricted to contents of secretory granules and absent from the intergranular space [C]. Gold particles were absent in a negative control section where the primary antibody was omitted [D]..... 36

Figure 2.12 Immunoblot detection of alpha-Gal in somatic extracts and E/S products of adult *P. tenuis*. Alpha-Gal was detected in a smear of proteins with apparent molecular masses of 45-145 kDa in E/S products from adult female worms. Alpha-Gal was also detected in a smear of somatic proteins with an apparent molecular masses of 30-105 kDa from the anterior 10% of both female and male worms, and one protein of apparent molecular mass of 55-kDa from the posterior 10% of the adult female. Alpha-Gal was not detected in the posterior region of the male worm. 38

Figure 3.1 The Two-Dimensional Polyacrylamide Gel profile of E/S proteins from adult female *P. tenuis*. Proteins were separated on a 12% homogenous tris-glycine gel with an IPG strip with a pH range of 3-10NL. The gel was stained with Coomassie Brilliant Blue..... 64

Figure 3.2 Immunoblot detection of alpha-Gal on 40-50 kDa E/S proteins from adult

female *P. tenuis* in a 2D SDS-PAGE blot. Spots 2-6 correspond with those in Figure 3.3 selected for MS/MS sequencing. 65

Figure 3.3 Adult female *P. tenuis* E/S proteins were selected for MS/MS sequencing. Spots 2-6 were alpha-Gal-modified, whereas spot 1 was selected as a negative control (See Figure 3.2). 66

Figure 3.4 Pt-ENO-1. *P. tenuis* Enolase from the TIM phosphate binding superfamily.. 67

Figure 3.5 Pt-CTL-2. *P. tenuis* Catalase from the catalase-like superfamily. 68

Figure 3.6 Pt-RNR-2. *P. tenuis* Ribonucleotide Reductase from the ferritin-like superfamily. Red amino acids are from peptides found in spot 6. A predicted N-glycosylation site is located on the asparagine (amino acid 348) in the box. No signal peptide cleavage site was predicted..... 68

Figure 3.7 Pt-Act-3. *P. tenuis* Actin from the NBD sugar-kinase HSP70 actin superfamily. Green amino acids are from a peptide found only in spot 2; red amino acids are from a peptide found only in spot 3; orange amino acids are from a peptide found in both spot 2 and 3; and, blue amino acids are from peptides found in spots 2, 3 and 4. A predicted N-glycosylation site is located on the asparagine in the box (amino acid 13). No signal peptide cleavage site was predicted. 69

Figure 3.8 Pt-EIF-4A-III. *P. tenuis* Eukaryotic Initiation Factor from the P-loop NTPase superfamily. Red amino acids are from a peptide found in spots 5 and 6. A predicted N-glycosylation site is located on the asparagine in the box (amino acid 294). No signal peptide cleavage site was predicted..... 69

Figure 3.9 Pt-EIF-4A. *P. tenuis* Eukaryotic Initiation Factor from the P-loop NTPase superfamily. Red amino acids are from a peptide found in spots 5 and 6. Predicted

N-glycosylation sites are located on the asparagines in the boxes (amino acids 102, 175). No signal peptide cleavage site was predicted. 69

Figure 3.10 Pt-VIT-2. *P. tenuis* vitellogenin from the domain of unknown function superfamily. Red amino acids are from a peptide found in spots 2 and 3. No N-glycosylation sites were predicted. A vertical line between amino acids 19 and 20 indicates the predicted signal peptide cleavage site..... 70

Figure 3.11 Pt-ALDO-2. *P. tenuis* Fructose-1, 6-bisphosphate Aldolase from the TIM phosphate-binding superfamily. Green amino acids are from a peptide found in spot 5; blue amino acids are those from peptides in spots 5 and 6; and red amino acids are those from a peptide identified in spots 2, 3, 4, 5 and 6. No N-glycosylation sites were predicted. No signal peptide cleavage site was predicted. 70

Figure 3.12 Pt-Galectin-5. *P. tenuis* Galectin from the GLECT superfamily. Red amino acids are those from peptides in spots 5 and 6 and blue amino acids are those from a peptide identified only in spot 5. A predicted N-glycosylation site is located on the asparagine in the box (amino acid 110). A vertical line between amino acids 14 and 15 indicates the predicted signal peptide cleavage site..... 71

Figure 3.13 Pt-cGST-1. *P. tenuis* Glutathione-S-transferase from the Thioredoxin-like superfamily and the GST-C family superfamily. Red amino acids are those from a peptide found in spots 2, 5 and 6. No N-glycosylation sites were predicted. No signal peptide cleavage site was predicted..... 71

Figure 3.14 Pt-GST-2. *P. tenuis* Glutathione-S-transferase from the Thioredoxin-like superfamily and the GST-C family superfamily. Red amino acids are those from a peptide found in spots 2, 5 and 6. No N-glycosylation sites were predicted. No

signal peptide cleavage site was predicted..... 71

Figure 3.15 Pt-HPD-1. *P. tenuis* 4-hydroxyphenylpyruvate dioxygenase from the Glo EDI_BRP-like superfamily. Red amino acids are those from peptides found in both spots 5 and 6. The black underlined amino acids represent a peptide from spots 5 and 6 that differs only at the first amino acid (a leucine was identified by mass spectrometry instead of the isoleucine shown here). A predicted N-glycosylation site is located on the asparagine in the box (amino acid 230). No signal peptide cleavage site was predicted..... 72

Figure 3.16 Pt-HPD-1a. *P. tenuis* 4-hydroxyphenylpyruvate dioxygenase from the Glo EDI_BRP-like superfamily. Red amino acids are those from peptides found in spots 5 and 6. The black underlined amino acids represent a peptide from spots 5 and 6 that differs only at the first amino acid (a leucine was identified by mass spectrometry instead of the isoleucine shown here). A predicted N-glycosylation site is located on the asparagine in the box (amino acid 230). No signal peptide cleavage site was predicted..... 72

Figure 3.17 Pt-ASP-16a. *P. tenuis* Venom Allergen/Ancylostoma Secreted Protein from the SCP superfamily. Red amino acids are those from a peptide found in spots 2, 5 and 6. Predicted N-glycosylation sites are located on the asparagines in the boxes (amino acids 63, 99, 118, 148). A vertical line between amino acids 19 and 20 indicates the predicted signal peptide cleavage site..... 73

Figure 3.18 Pt-ASP-16b. *P. tenuis* Venom Allergen/Ancylostoma Secreted Protein from the SCP superfamily. Red amino acids are those from a peptide found in spots 2, 5 and 6. Predicted N-glycosylation sites are located on the asparagines in the boxes

(amino acids 51, 141). A vertical line between amino acids 19 and 20 indicates the predicted signal peptide cleavage site. 73

Figure 3.19 Pt-ASP. *P. tenuis* Ancylostoma Secreted Protein from the SCP superfamily. Red amino acids are those from a peptide found in spot 2. Predicted N-glycosylation sites are located on the asparagines in the boxes (amino acids 96, 107, 160, 165, 207). A vertical line between amino acids 19 and 20 indicates the predicted signal peptide cleavage site. 73

Figure 3.20 Pt-ASP_ANCCA. *P. tenuis* Ancylostoma Secreted Protein from the SCP superfamily. Green amino acids are from a peptide found in spot 4; blue amino acids are those from peptides found in Spots 2 and 4; and red amino acids are from peptides found in Spot 2, 3 and 4. No N-glycosylation sites were predicted. A vertical line between amino acids 18 and 19 indicates the predicted signal peptide cleavage site. 74

Figure 3.21 Mechanism of eosinophil-mediated killing of parasitic helminth larvae via antibody-dependent cell-mediated cytotoxicity (ADCC). Galectin-3 on eosinophils is required for attachment to vascular cell adhesion molecule 1 (VCAM-1) to enable extravasation to the site of infection. Galectin-3 also provides stabilization for binding of Immunoglobulin E (IgE) to Fcε receptors on eosinophils in the tissue, a process required for degranulation and subsequent killing of the parasitic helminth via ADCC 83

Figure 3.22 Proposed model for inhibition of eosinophil extravasation to site of infection by parasite alpha-Gal. Soluble alpha-Gal-modified E/S proteins released from adult *P. tenuis* bind to host galectin-3 before it is expressed on the surface of circulating

eosinophils. This interaction inhibits pentamerization and simultaneous binding of galectin-3 to VCAM-1 on host endothelial cells. Eosinophils will not extravasate to site of infection in host tissue, enabling persistence of *P. tenuis* infection. 84

Figure 3.23 Proposed model for blocking ADCC via alpha-Gal mediated inhibition of the interaction between Immunoglobulin E (IgE) and Fcε receptors on eosinophils. Should eosinophils arrive at the site of P. *tenuis* infection, soluble alpha-Gal-modified E/S proteins released from adult P. *tenuis* will bind to host galectin-3. This inhibits the interaction between galectin-3 and the Fc portion of IgE. The binding of galectin-3 to the galectin-3 binding protein on the surface of the eosinophils would also be inhibited. The lack of the stabilizing interaction of IgE with the Fcε receptor will result in blocking of degranulation and promotion of parasitic helminth survival. 84

Figure A1-1 LC-MS/MS total ion current (TIC) chromatogram for Spot 1..... 114

Figure A1-2 LC-MS/MS total ion current (TIC) chromatogram for Spot 2..... 115

Figure A1-3 LC-MS/MS total ion current (TIC) chromatogram for Spot 3..... 116

Figure A1-4 LC-MS/MS total ion current (TIC) chromatogram for Spot 4..... 117

Figure A1-5 LC-MS/MS total ion current (TIC) chromatogram for Spot 5..... 118

Figure A1-6 LC-MS/MS total ion current (TIC) chromatogram for Spot 6..... 119

Figure A2-1 *P. tenuis* enolase has 92% identity with enolase of *Haemonchus contortus*. Alignment of Pt-ENO-1 with *H. contortus* enolase (ADK47524.1) was performed using the BLASTp program from NCBI. The amino acids displayed are in standard

single-letter code and identical residues are in red..... 121

Figure A2-2 *P. tenuis* catalase has 81% identity with catalase of Haemonchus contortus. Alignment of Pt-CTL-2 with H. contortus catalase (AAT28330.1) was performed using the BLASTp program from NCBI. The amino acids displayed are in standard single-letter code and identical residues are in red..... 122

Figure A2-3 *P. tenuis* ribonucleotide reductase has 74% identity with ribonucleotide reductase of *Caenorhabditis brenneri*. Alignment of Pt-RNRR2 with *C. brenneri* ribonucleotide reductase (EGT45534.1) was performed using the BLASTp program from NCBI. The amino acids displayed are in standard single-letter code and identical residues are in red..... 123

Figure A2-4 *P. tenuis* actin has 100% identity with actin of *Caenorhabditis elegans*. Alignment of Pt-ACT-3 with *C. elegans* actin (NP_505817.1) was performed using the BLASTp program from NCBI. The amino acids displayed are in standard single-letter code and identical residues are in red..... 124

Figure A2-5 *P. tenuis* eukaryotic initiation factor has 90% identity with eukaryotic initiation factor of *Loa loa*. Alignment of Pt-EIF-4A-III with *Loa loa* eukaryotic initiation factor (EFO21014.2) was performed using the BLASTp program from NCBI. The amino acids displayed are in standard single-letter code and identical residues are in red..... 125

Figure A2-6 *P. tenuis* eukaryotic initiation factor has 90% identity with eukaryotic initiation factor of *Ascaris suum*. Alignment of Pt-EIF-4A with *A. suum* eukaryotic initiation factor (ADY42814) was performed using the BLASTp program from NCBI and graphic developed using the MultAlin sequence alignment program. The

amino acids displayed are in standard single-letter code and identical residues are in red..... 126

Figure A2-7 *P. tenuis* eukaryotic initiation factor paralogues have 69% identity with each other. The alignment graphic of Pt-EIF-4A with Pt-EIF-4A-III was developed using the MultAlin sequence alignment program. The amino acids displayed are in standard single-letter code and identical residues are in red.....127

Figure A2-8 *P. tenuis* vitellogenin has 39% identity with vitellogenin of *Caenorhabditis elegans*. Alignment of Pt-VIT-2 with *C. elegans* vitellogenin (NP_508868) was performed using the BLASTp program from NCBI. The amino acids are displayed in standard single-letter code and identical residues are in red..... 128

Figure A2-9 *P. tenuis* vitellogenin has 39% identity with vitellogenin of *Caenorhabditis elegans*. Alignment of Pt-VIT-2 with *C. elegans* vitellogenin (NP_508868) was performed using the BLASTp program from NCBI. The amino acids are displayed in standard single-letter code and identical residues are in red. (con'd).....129

Figure A2-10 *P. tenuis* vitellogenin has 39% identity with vitellogenin of *Caenorhabditis elegans*. Alignment of Pt-VIT-2 with *C. elegans* vitellogenin (NP_508868) was performed using the BLASTp program from NCBI. The amino acids are displayed in standard single-letter code and identical residues are in red. (con'd).....130

Figure A2-11 *P. tenuis* fructose-1,6-bisphosphate (FBP) aldolase has 87% identity with FBP aldolase of *Caenorhabditis remanei*. Alignment of Pt-ALDO-2 with *C. remanei* FBP aldolase (XP_003110723.1) was performed using the BLASTp program from NCBI. The amino acids are displayed in standard single-letter code and identical residues are in red.....131

Figure A2-12 *P. tenuis* galectin has 94% identity with galectin of *Angiostrongylus cantonensis*. Alignment of Pt-Galectin-5 with *A. cantonensis* galectin (AEK98127) was performed using the BLASTp program from NCBI. The amino acids are displayed in standard single-letter code and identical residues are in red..... 132

Figure A2-13 *P. tenuis* cytosolic glutathione-S-transferase (GST) has 71% identity with cytosolic GST of *Oesophagostomum dentatum*. Alignment of Pt-cGST-1 with *O. dentatum* cytosolic GST (ACA30414) was performed using the BLASTp program from NCBI. The amino acids are displayed in standard single-letter code and identical residues are in red.....133

Figure A2-14 *P. tenuis* glutathione-S-transferase (GST) has 68% identity with GST of *Heligmosomoides polygyrus*. Alignment of Pt-GST-2 with *H. polygyrus* GST (1TW9_A) was performed using the BLASTp program from NCBI. The amino acids are displayed in standard single-letter code and identical residues are in red..... 134

Figure A2-15 *P. tenuis* glutathione-S-transferase paralogues have 86% identity with each other. The alignment graphic of Pt-cGST-1 with Pt-GST-2 was developed using the MultAlin sequence alignment program. The amino acids displayed are in standard single-letter code and identical residues are in red..... 135

Figure A2-16 *P. tenuis* 4-hydroxyphenylpyruvate dioxygenase (HPPD) has 77% identity with HPPD of *Caenorhabditis briggsae*. Alignment of Pt-HPD-1 with *C. briggsae* HPPD (XP_002642363.1) was performed using the BLASTp program from NCBI. The amino acids are displayed in standard single-letter code and identical residues are in red..... 136

Figure A2-17 *P. tenuis* 4-hydroxyphenylpyruvate dioxygenase (HPPD) has 76% identity with HPPD of *Caenorhabditis briggsae*. Alignment of Pt-HPD-1a with *C. briggsae* HPPD (XP_002642363.1) was performed using the BLASTp program from NCBI. The amino acids are displayed in standard single-letter code and identical residues are in red..... 137

Figure A2-18 *P. tenuis* 4-hydroxyphenylpyruvate dioxygenase (HPPD) paralogues have 98% identity with each other. The alignment graphic of Pt-HPD-1 with Pt-HPD-1a was developed using the MultAlin sequence alignment program. The amino acids displayed are in standard single-letter code and identical residues are in red..... 138

Figure A2-19 *P. tenuis* Ancylostoma secreted protein (ASP) has 32% identity with ASP of *Heligmosomoides polygyrus bakeri*. Alignment of Pt-ASP-16a with *H. polygyrus bakeri* ASP (AEP82932.1) was performed using the BLASTp program from NCBI. The amino acids are displayed in standard single-letter code and identical residues are in red..... 139

Figure A2-20 *P. tenuis* Ancylostoma secreted protein (ASP) has 32% identity with ASP of *Heligmosomoides polygyrus bakeri*. Alignment of Pt-ASP-16b with *H. polygyrus bakeri* ASP (AEP82932.1) was performed using the BLASTp program from NCBI. The amino acids are displayed in standard single-letter code and identical residues are in red..... 140

Figure A2-21 *P. tenuis* Ancylostoma secreted protein (ASP) paralogues have 88% identity with each other. The alignment graphic of Pt-ASP-16a with Pt-ASP-16b was developed using the MultAlin sequence alignment program. The amino acids displayed are in standard single-letter code and identical residues are in red..... 141

Figure A2-22 *P. tenuis* Ancylostoma secreted protein (ASP) has 28% identity with ASP of *Ascaris suum.* Alignment of Pt-ASP with *A. suum* ASP (ADY48180.1) was performed using the BLASTp program from NCBI. The amino acids are displayed in standard single-letter code and identical residues are in red..... 142

Figure A2-23 *P. tenuis* Ancylostoma secreted protein (ASP) has 42% identity with ASP of *Ancylostoma caninum.* Alignment of Pt-ASP_ANCCA with *A. caninum* ASP (Q16937.1.1) was performed using the BLASTp program from NCBI. The amino acids are displayed in standard single-letter code and identical residues are in red..... 143

Chapter 1 : General Introduction

Helminths are parasitic worms that commonly infect humans in developing countries and animals worldwide. These infections can lead to decreased quality of human life (DALY; Hotez *et al.,* 2008) and incredible economic expenditures to promote the health of companion animals and livestock species (van Stijn *et al.,* 2010; Hotez *et al.,* 2008). Accordingly, substantial efforts have been made to develop and implement protocols to prevent infections and to alleviate morbidity and mortality that accompany infections. A critical approach includes identifying molecules that facilitate infection and promote survival of helminths (Hewitson *et al.,* 2011). Specifically, defining secreted helminth products and the organs from which they originate provides insight into complex host-parasite interactions that are the product of co-evolution. Understanding the molecules that mediate infectious processes is key to the rational development of strategies to control disease associated with helminth infections. *Parelaphostrongylus tenuis* is a parasitic nematode of white-tailed deer (*Odocoileus virginianus*) that induces a debilitating neurologic disease in numerous other wildlife and domestic livestock species (Anderson, 2000). The excreted/secreted products of *P. tenuis*, and the organs from which they originate, were studied to provide insight into factors that are required for establishment and persistence of infection.

1.1 Distribution of *Parelaphostrongylus tenuis*

Dougherty (1945) originally described *Parelaphostrongylus tenuis* from white-tailed

deer. It is a neurotropic nematode of the superfamily Metastrongyloidea within the order Strongylida. All strongylids are bursate nematodes, and they are often referred to as lungworms because most species have a life stage that occupies the lungs of its vertebrate host (Anderson, 2000). Prevalence of *P. tenuis* infection is over 90% in some regions with an average infection intensity of 3.4 adult worms per deer (Duffy, 2000).

1.2 *Parelaphostrongylus tenuis* Life Cycle

The life cycle of *P. tenuis* consists of two hosts: the intermediate terrestrial gastropod host; and, the definitive white-tailed deer host. Deer become infected by ingesting third-stage larvae (L3) that develop in terrestrial gastropods. Once ingested by deer, the larvae penetrate the alimentary canal and migrate to the lumbar spinal cord. After 30-40 days of development within the parenchyma of the spinal cord, the larvae enter the subdural space and migrate to the cranium where they mature into adults. Adult worms are found within either the cranial blood vessels or the cerebrospinal fluid surrounding the brain. Gravid female worms deposit eggs into the venous blood and eggs embolize in capillaries of the lungs where they hatch as first-stage larvae (L1) that penetrate the surrounding alveoli. The L1 are carried up the mucociliary escalator of the lungs, are swallowed, and are then passed with host feces. The L1 infect gastropods as they graze on the fecal matter, resulting in the continuation of the life cycle (Anderson, 2000).

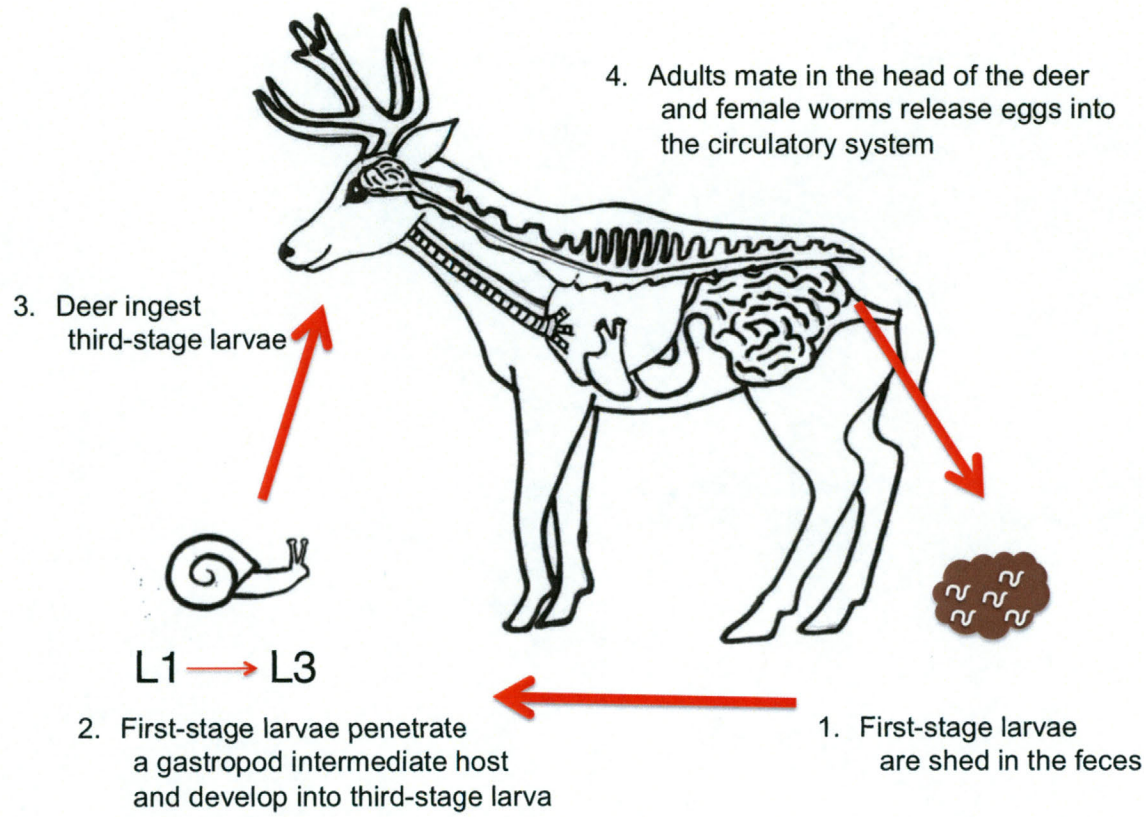


Figure 1.1 Life Cycle of *Parelaphostrongylus tenuis*.1. First-stage larvae (L1) are shed in the feces of the deer host. 2. L1s penetrate a slug or snail, and subsequently develop into infective third-stage larvae (L3). 3. Once ingested by the deer, the L3s enter the alimentary canal and migrate to the lumbar spinal cord. The L3 migrate to the subdural space and travel to the cranium where they mature into adult worms. 4. Female worms release eggs into the blood, enabling eggs to travel to the lungs where they hatch, releasing L1s. The L1 are carried up the mucociliary escalator of the lungs, are swallowed, and are then passed with host feces.

1.3 Helminth Immune Evasion

The co-evolution of parasites with their vertebrate hosts has required a balance whereby parasites avoid elimination by host immune responses but also limit severe pathology associated with infections (Anthony *et al.,* 2007). Parasites have adapted a number of mechanisms to exploit the host immune response. One of the most well known examples

is that of antigenic variation in African trypanosomes (Damian, 1997) where variant surface glycoproteins (VSGs) are displayed one variant at a time, thereby avoiding detection by adaptive immune responses. Another form of evasion is molecular mimicry, defined as passive evasion via display of epitopes common to those found in their host (Damian, 1997). While multiple mechanisms of immune evasion by helminths are being investigated, interest in a role for glycans is a current focus. Immune responses of antigen presenting cells to most helminth infections leads to polarization to a T helper 2 (Th2) response, and recent research has discovered that this may be facilitated by the interactions of helminth glycans with key host immune cells (Thomas and Harn, 2004).

1.3.1 Concomitant Immunity

Adult *P. tenuis* are known to survive and proliferate within their deer host for up to six years (Duffy *et al.*, 2004), evidence that they are accomplished at immune evasion. Infected deer are also known to resist challenge infection with L3 (Duffy *et al.*, 2004). The ability of a host to mount an effective immune response against larval stages, while at the same time not able to clear an established infection of adult worms, is known as concomitant immunity. Restricting the burden size prevents overcrowding in the host and can allow for persistence of infection (Brown and Grenfell, 2001). Infections with adult *P. tenuis* are typically of low intensity ($x = 3.4$, range = 1-31; Duffy, 2000). Neurologic signs are reported only rarely in white-tailed deer and are restricted to high intensity infections (Prestwood, 1970).

1.3.2 Alpha-Gal and Immune Evasion

As mentioned earlier, immune evasion within the host may be explained by the presence of parasite glycoconjugates. Interestingly, previous research on *P. tenuis* discovered that adult parasites produce a novel glycan (Galα1-3Gal; alpha-Gal). Alpha-Gal is a terminal disaccharide of N-linked glycans and is found in all mammals except old world primates, where a mutation in the α1,3 galactosyltransferase resulted in loss of the epitope (Galili U *et al.*, 1988).

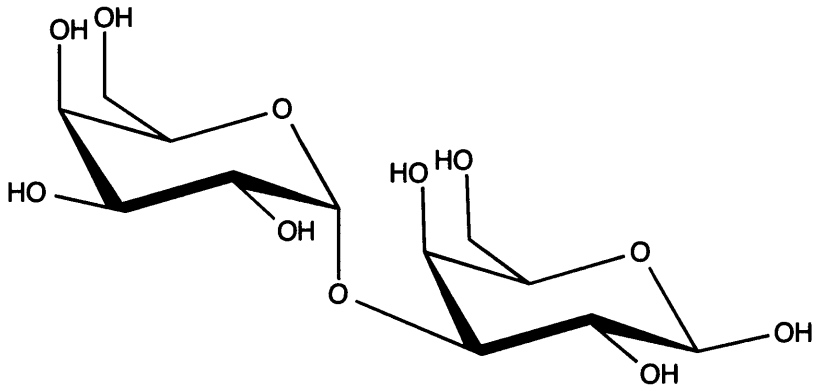


Figure 1.2 Structure of galactose-alpha 1,3-galactose (alpha-Gal).

Inactivation of the α1-3 galactosyltransferase enzyme likely resulted from evolutionary selection that benefited individuals with decreased expression of the α-galactosyl epitope. It has been proposed that a pathogen that utilized alpha-Gal to mediate infection of Old World primates served as the selective pressure (Galili and Swanson, 1991). The use of alpha-Gal by pathogens that infect deer, and other mammals that possess this glycan, is

compatible with the definition of molecular mimicry. The display of epitopes common to those found in the host is suggestive that alpha-Gal might have a role in immune evasion.

The identification of alpha-Gal in *P. tenuis* was the first report of this glycan from any metazoan parasite (Duffy *et al.*, 2006), however, the recent discovery of this glycan in another parasitic nematode, *Haemonchus contortus* (van Stijn *et al.*, 2010) and other members of the superfamily Metastrongyloidea (*P. andersoni, P. odocoilei, Elaphostrongylus rangiferi,* and *Crenosoma vulpis*) (Bedford, 2010) suggests that this sugar might be employed more broadly by parasitic nematodes. Synthesis of alpha-Gal is restricted to the adult stage of *P. tenuis*, the only life-stage that occurs exclusive within the mammalian deer host. Alpha-Gal is localized to glycoproteins from the excretory glands within *P. tenuis*, in addition to within the uteri of female worms (Duffy *et al.*, 2006).

1.3.3 Molecular Mimicry

The original localization of alpha-Gal in the uteri of *P. tenuis* was not of sufficient resolution to determine if it was on the surface of eggs, within the uterine matrix, or a combination of both. It was intriguing to speculate that alpha-Gal on the egg surface would facilitate a molecular mimicry-type of immune evasion by eggs developing within the deer lungs (Duffy *et al.*, 2006). Recent work using immunogold labelling localized alpha-Gal to unknown structures that associate with the egg surface but that are much more abundant within the uterine matrix (Rideout, 2012). These structures are not

presumed to remain associated with the eggs following oviposition. Accordingly, it seems unlikely that alpha-Gal has a role in disguising the eggs as "self" molecules in the host (Rideout, 2012).

1.3.4 Immune Modulation: Glycan Gimmickry

While alpha-Gal likely does not have a role in molecular mimicry with *P. tenuis* eggs, this leaves open questions about the function of the abundant alpha-Gal-modified proteins released from the excretory gland. Recent discoveries regarding interactions between host-like helminth glycans and host glycan-binding proteins have shown that glycans may have a role in modulating host immune responses. Researchers named this concept "glycan gimmickry", and define it as an "active strategy of parasites to use their glycans to target glycan-binding proteins within the host to promote their survival" (van Die and Cummings, 2010)

1.4 Secreted Proteins and Function of the Excretory Gland

The excretory glands of *P. tenuis* were originally identified by Anderson (1956). These glands are each single-celled, occupy up to 10% of worm length and were described as granular (Anderson, 1956). Secretory glands are also found in plant parasitic nematodes and have been the focus of many studies investigating host-parasite interactions because of their secreted products (Hussey, 1989). Negative consequences from plant parasitic nematode infections to agricultural crop species are of equal concern to those caused by

animal parasitic nematodes due to production losses.

Morphological adaptations related to host-parasite interactions are often seen in nematode secretory cells such as esophageal glands, and likely also include amphidial glands and excretory-secretory glands (Jasmer *et al.,* 2003). A substantial amount of research has been devoted to secreted products from both plant and mammalian parasitic nematodes; however, the secretory glands of plant-parasitic nematodes have been studied more than those of animal-parasitic nematodes (Hussey *et al.*, 2002). The knowledge of both the secreted products, and their glandular origin, in plant parasitic nematodes has led to a better understanding of parasitism. This provides insight for new methods to overcome obstacles surrounding resistance to plant parasitic nematicides, and other strategies to reduce the use of nematicides due to environmental issues (Jasmer *et al.*, 2003). In the case of animal parasitic nematodes, a similar understanding of both their secreted products and their secretory organs should prove helpful for the identification of drug and vaccine targets to help control helminth infections of animals. The specific identification of secreted products is an initial step to gaining a better understanding of how parasite molecules interact with those of the host. For example, it would be impossible to develop an effective vaccine without first knowing what parasite molecules are interacting with the host immune response, and how they promote persistence of infection (Anthony *et al.*, 2007). Insight into the ultrastructural morphology of the excretory glands of the *P. tenuis* secretory system and specific identification of parasite glycoproteins modified by alpha-Gal will aid in determining a functional role for the excretory glands and alpha-Gal, and could also provide insight into broader concepts in immune modulation by animal parasitic nematodes.

1.5 Objectives

This research program had 2 main objectives as follows:

1. Describe excretory gland morphology of adult *P. tenuis* and refine ultrastructural localization of the alpha-Gal epitope (Chapter 2).
2. Identify select alpha-Gal modified proteins from E/S products of adult *P. tenuis* (Chapter 3).

Bibliography

Anderson, R. C. (2000). Nematode parasites of vertebrates : their development and transmission. CABI Pub., Wallingford, Oxon, UK; New York, NY.

Anderson, R. C. (1956). *Elaphostrongylus odocoilei* Hobmaier and Hobmaier, 1934 in the cranial case of *Odocoileus virginianus* borealis miller. " *Can. J. Zool.,* 34(3), 167-173.

Anthony RM, Rutitzky LI, Urban JF Jr, Stadecker MJ, and Gause WC. (2007). "Protective immune mechanisms in helminth infection." *Nat. Rev. Immunol.,* 7(12), 975-987.

Bedford, R.O. (2010). Molecular conservation of a novel glycan used by parasitic nematodes in immune evasion. Honours Thesis. University of New Brunswick, Fredericton, New Brunswick, Canada, 53 pp.

Brown, S., and Grenfell, B. (2001). "An unlikely partnership: parasites, concomitant immunity and host defence." *Proc. Biol. Sci.,* 268(1485), 2543-2549.

Damian RT. (1997). "Parasite immune evasion and exploitation: reflections and projections." *Parasitology,* 115(7), 169-175.

Duffy MS, Greaves TA, and Burt MD. (2004). "Establishment of adult *Parelaphostrongylus tenuis,* patent infections, and acquired immunity after experimental infection of white-tailed deer (*Odocoileus virginianus*) and red deer (*Cervus elaphus elaphus).*" *J.Parasitol.,* 90(2), 245-254.

Duffy, M. S., Morris, H. R., Dell, A., Appleton, J. A., and Haslam, S. M. (2006). "Protein glycosylation in *Parelaphostrongylus tenuis*-first description of the Galα1-3Gal sequence in a nematode." *Glycobiology,* 16(9), 854-862.

Duffy, M. S. (2000). "Life history studies of *Parelaphostrongylus tenius* and *Elaphostrongylus cervi* with investigations into the potential for reliable antemortem immunodiagnosis". University of New Brunswick, Fredericton, N.B.

Galili U, Shohet SB, Kobrin E, Stults CL, and Macher BA. (1988). "Man, apes, and Old World monkeys differ from other mammals in the expression of alpha-galactosyl epitopes on nucleated cells." *J. Biol. Chem.,* 263(33), 17755-17762.

Galili, U., and Swanson, K. (1991). "Gene Sequences Suggest Inactivation of α-1,3-Galactosyltransferase in Catarrhines after the Divergence of Apes from Monkeys." *Proc. Natl. Acad. Sci. U.S.A.,* 88(16), 7401-7404.

Hewitson, J. P., Harcus, Y., Murray, J., van Agtmaal, M., Filbey, K. J., Grainger, J. R., Bridgett, S., Blaxter, M. L., Ashton, P. D., Ashford, D. A., Curwen, R. S., Wilson, R. A., Dowle, A. A., and Maizels, R. M. (2011). "Proteomic analysis of secretory products from the model gastrointestinal nematode *Heligmosomoides polygyrus* reveals dominance of Venom Allergen-Like (VAL) proteins." *J. Proteomics,* 74(9), 1573-1594.

Hotez PJ, Brindley PJ, Bethony JM, King CH, Pearce EJ, and Jacobson J. (2008). "Helminth infections: the great neglected tropical diseases." *J. Clin. Invest.,* 118(4), 1311-21.

Hussey, R. (1989). "Disease-Inducing Secretions Of Plant-Parasitic Nematodes." *Annu. Rev. Phytopathol.,* 27(1), 123-141.

Hussey, R. S., Davis, E. L., and Baum, T. J. (2002). "Secrets in secretions: genes that control nematode parasitism of plants." *Braz. J. Plant Physiol.,* 14(3), 183-194.

Jasmer, D. P., Goverse, A., and Smant, G. (2003). "Parasitic Nematode Interactions with Mammals and Plants." *Annu. Rev. Phytopathol.,* 41(1), 245-270.

Prestwood AK. (1970). "Neurologic disease in a white-tailed deer massively infected with meningeal worm." *J. Wildl. Dis.,* 6(1), 84-86.

Rideout, E.G.W. (2012). Localization of glycosylated reproductive proteins from *Parelaphostrongylus tenuis* with a potential role in immune evasion. Honours Thesis. University of New Brunswick, Fredericton, New Brunswick, Canada, 47 pp.

Thomas, P. G., and Harn, D. A. (2004). "Immune biasing by helminth glycans." *Cell. Microbiol.,* 6(1), 13-22.

van Die I., and Cummings R.D. (2010). "Glycan gimmickry by parasitic helminths: A strategy for modulating the host immune response?" *Glycobiology,* 20(1), 2-12.

van Stijn CM, van den Broek M, Vervelde L, Alvarez RA, Cummings RD, Tefsen B, and van Die I. (2010). "Vaccination-induced IgG response to Galalpha1-3GalNAc glycan epitopes in lambs protected against *Haemonchus contortus* challenge infection." *Int. J. Parasitol.,* 40(2), 215-22.

Chapter 2 : Excretory Gland Morphology and Improved Localization of the Alpha-Gal Epitope in *Parelaphostrongylus tenuis*

2.1 Introduction

Parelaphostrongylus tenuis is a parasitic nematode found commonly in white-tailed deer of eastern North America. Adult worms are found within the cranial blood vessels or the cerebrospinal fluid surrounding the brain of the deer (Duffy *et al.*, 2004). A wide variety of wildlife and domestic livestock species are susceptible to *P. tenuis* infection. However, infection in most atypical hosts results in a debilitating neurological disease (Anderson, 2000). Instead of migrating within the sub-dural space, the parasite will remain within the parenchyma or will leave and then re-enter the parenchyma of atypical hosts en route to the cranium. Adult *P. tenuis* can survive and proliferate within their white-tailed deer host for up to six years (Duffy *et al.*, 2004), evidence that they have evolved effective mechanisms of immune evasion. Furthermore, these parasites induce a concomitant immunity that protects against subsequent exposures to *P. tenuis* (Duffy *et al.*, 2004). The molecular basis of concomitant immunity remains undefined but this parasite has evolved molecular mechanisms to counteract the complex suite of cells and molecules of the immune system of their mammalian host. While the specific molecules remain largely undefined, so do the organs that serve as the source of immunomodulatory molecules.

Parasites have adapted many ways to promote their survival by evading host immune

responses. Molecular mimicry involves the display of molecular epitopes that are common to the host (Damian, 1997). There has been a significant amount of research devoted to helminth glycans, because they occur commonly at the host-parasite interface and are known to modulate host immunity (Terrazas *et al.*, 2001). Interestingly, previous research on *P. tenuis* discovered that adult parasites produce a novel glycan (Galα1-3Gal; alpha-Gal) that is localized to the uterus and to the excretory glands (Duffy *et al.*, 2006). The alpha-Gal epitope is common in the deer host, and so a molecular mimicry type of immune evasion was proposed (Duffy *et al.*, 2006). However, recent research serves to rule out a potential role in molecular mimicry (Rideout, 2012). The specific proteins modified by alpha-Gal remain unknown as does the function of the excretory glands of adult *P.tenuis*.

Early descriptions of excretory glands in parasitic and free-living nematodes have resulted in much confusion with respect to their function. Glands in the anterior pseudocoelom of nematodes have been named "excretory" and "secretory" by different authors. In nematology, the term "excretory" denotes a process that eliminates nitrogenous waste, while "secretory" gland cells house secretions that have biochemical function that can aid in parasitism of a host (Hussey *et al.*, 2002). Many researchers have erroneously associated anterior glands with a role in excretion (Bird, 1971). Leading to confusion in the nomenclature regarding function is the fact that both the tubular excretory system and the glandular "excretory" cells release material through the same duct and pore in some nematodes (Nelson *et al.*, 1983). Tubular canals are known to remove metabolic waste and perform osmoregulatory function (Nelson and Riddle,

1984). Given the proximity of the gland cells to the tubules in many nematodes, it is not surprising that these glands were mistakenly termed excretory glands and thereby indicating a role in excretion. However, the cytoplasm of excretory glands is dominated by large numbers of secretory granules (Lee, 1970) and this alone suggests evidence for a primary role in protein secretion, and not waste excretion (Lee, 1970; Waddell, 1968). The other glands associated with the anterior alimentary canal are referred to as either esophageal or pharyngeal glands. They also are rich in secretory granules with a role in protein secretion (Brunianská *et al.*, 2007).

We investigated the ultrastructure of these gland cells and used immunogold labeling to further define the distribution of alpha-Gal in these cells to help infer a role for this epitope during parasitism. The presence of secretory granules in the excretory glands indicates a role in secretion, not excretion, and thus should be renamed as "secretory" glands.

2.2 Materials and Methods

2.2.1 Deer Collection and Dissection

Heads were collected from 166 hunter-killed and road-killed white-tailed deer (*Odocoileus virginianus*) from southern New Brunswick between October 2010 and November 2011 for retrieval of adult *Parelaphostrongylus tenuis*. Deer were aged by examining the wear and replacement of the premolars and molars of the lower jaw

(Severinghaus, 1949). The head was skinned and the central nervous system (CNS) was accessed by cutting through the skull with a reciprocating saw. Two sagittal cuts were made through the frontal and parietal plates and extending to the lateral edges of the occipital condyles that flank the foramen magnum. A final transverse cut through the frontal plate enabled a section of the skull cap to be removed to allow access to the CNS. The brain was carefully removed to allow examination of the meninges and for removal of worms. Following inspection of the intracranial space, the superior sagittal sinus and cavernous sinus were excised and placed in phosphate buffered saline (PBS; 137 mM NaCl, 2.7 mM KCl, 4.3 mM Na_2PO_4, 1.46 mM KH_2PO_4, pH 7.4). All tissues were examined for parasites using a dissecting microscope (1.6X-40X). Recovered worms were washed three times in sterile PBS and were assessed using a dissecting microscope to confirm that they were intact and alive for use in later downstream applications. All leftover animal materials were discarded following standard animal care protocols for use of the necropsy room at UNB.

2.2.2 Specimen Preparation for General Morphological Studies

Intact female and male worms were fixed in a primary fixative for 12 hours (2% glutaraldehyde, 2% paraformaldehyde, 0.1 M sodium cacodylate buffer, pH 7.4), followed by post-fixation for 2 hours in 1% osmium tetroxide in 0.1 M sodium cacodylate buffer. Prior to dehydration, the anterior region of individual worms that contained the excretory glands were cut into consecutive serial segments, each 2 mm in length, starting from the very tip of the anterior end of the worm and ending at the distal

part of the glands. Individual segments were dehydrated through an ethanol gradient (Table 1) in preparation for infiltration in Spurr's Resin (Ted Pella; via Cedarlane Laboratories, Burlington, ON). Specimens were oriented in flat molds and the resin was left to polymerize at 60°C overnight.

Selected segments were cut in either cross or longitudinal sections (1 μm thick) using a histoknife (Diatome, Biel/Switzerland) on a Leica Ultracut microtome (Leica Microsystems Inc., Concord, ON). One-micrometer sections were collected onto glass slides, stained with Epoxy Tissue Stain (Electron Microscopy Sciences; via Cedarlane Laboratories, Burlington, ON), and images were taken using a DC500 digital camera on a Leica DMR light microscope (Leica Microsystems Inc.; Concord, ON). For transmission electron microscopy, sections were cut at 70 nm with a diamond knife (Diatome, Biel/Switzerland) and collected onto formvar-coated copper grids (Electron Microscopy Sciences). Sections were stained with 5% aqueous uranyl acetate followed by 3% lead citrate (Reynolds, 1963) and were examined in a JEOL 2011 (Scanning) Transmission Electron Microscope operated at 200 KV. Images were captured using a Gatan Ultrascan digital camera and Digital Micrograph software (Gatan; Warrendale, PA, USA).

2.2.3 Specimen Preparation for Immunogold Labeling

Intact female and male worms were fixed overnight in a primary fixative (3% paraformaldehyde, 0.5% glutaraldehyde, 0.1 M sodium cacodylate, pH 7.4). Specimens

were placed in 70% ethanol to cut the segments desired for embedding. The anterior ends were excised to retain intact excretory glands that were then cut into consecutive serial segments, each 2 mm in length, starting from the anterior end of the worm. Selected segments were dehydrated through an ethanol gradient (Table 1) in preparation for infiltration in LR White Resin (Electron Microscopy Sciences). Each segment was embedded in a gelatin capsule and the resin polymerized at 50-55 °C for 12-24 hours. Areas of interest were re-oriented for either transverse or longitudinal sectioning. Ultrathin sections (75-90 nm) were cut using a diamond knife (Diatome; Biel/Switzerland) on a Leica Ultracut microtome (Leica Microsystems Inc.). Sections were collected onto unsupported nickel grids (300 mesh; Electron Microscopy Sciences,).

2.2.4 Immunogold Labeling

Nematode tissues on each grid were blocked with a solution of 5% BSA/TBS (5% bovine serum albumin in TBS; 0.05 M Tris Base, 0.13 M NaCl, pH 7.6) for 30 minutes. Tissues were incubated with diluent without antibody to serve as negative controls or with a monoclonal anti-alpha-Gal IgM antibody (mAb M86; Cedarlane Laboratories). The optimal primary antibody dilution was determined empirically in a preliminary experiment. Grids were incubated with a 1:3, 1:10, or 1:100 dilution of the anti-alpha-Gal antibody in 5% BSA/TBS for 2 hours. All grids were washed three times with TBS and were incubated for 30 minutes in a 1:20 dilution of the gold-conjugated anti-mouse-IgM antibody (12 nm colloidal Gold-AffiniPure; Cedarlane Laboratories, Burlington, ON) diluted in 5% BSA, 10% normal goat serum, in TBS. Grids were post-stained with

2% uranyl acetate for 4 minutes followed by Reynold's lead citrate for 1 minute to provide contrast with the tissue when viewed using the transmission electron microscope. The 1:10 anti-alpha-Gal dilution was used in all subsequent experiments.

Table 2.1 Solutions and processing times used for tissue dehydration and resin infiltration to prepare *Parelaphostrongylus tenuis* specimens for immunogold labeling.

Treatment	Time (hours)
30% EtOH	0.5
50% EtOH	0.5
70% EtOH	0.5
80% EtOH	0.5
90% EtOH	0.5
100% EtOH	0.5
100% EtOH	0.5
1 part resin: 2 parts 100% EtOH	4
2 parts resin: 1 part 100% EtOH	12
100% resin	4
100% resin	4

2.2.5 Collection of Excreted/Secreted Proteins

Adult female and male worms that were intact and alive were maintained *in vitro* for collection of excreted/secreted (E/S) proteins. Worms were washed five times with sterile 1X PBS in a laminar flow hood using aseptic technique, and were then stored in 3 ml of a protein-free culture medium, RPMI 1640 (Sigma-Aldrich; Oakville, ON), at 37°C. Control tubes containing medium, but lacking worms were handled in a similar way to monitor technique. Culture medium from each tube was inspected every 24 hours for the presence of contaminating bacteria that were observed on occasion due to

the nature of extraction methodologies. Each worm was examined every 24 hours to ensure integrity of the body and the corresponding purity of E/S proteins. Worms that became damaged or less active were removed from culture and stored at -80°C in 1X PBS. Once deemed free of bacterial contamination, the medium was pooled based on gender of the worms. Collected culture medium was filtered through a 0.2 μm pore membrane to remove eggs and other matter and then concentrated using Amicon Ultra-15 Centrifugal Filter Units (Millipore, Immobilon, Billerica, MA) by centrifugation at 3000 X g at 4°C for 60 minutes, followed by another centrifugation step of 3000 X g at 4°C for 45 minutes. Protein concentration was determined using the Bio-Rad protein assay (Bio-Rad Laboratories; Mississauga, Ontario, Canada) according to the manufacturer's instructions.

2.2.6 One-Dimensional Gel Electrophoresis and Western Blot

Adult worm E/S and somatic proteins were separated by sodium dodecyl sulfate polyacrylamide gel electrophoresis (SDS-PAGE) using the Laemmli buffer system (Laemmli UK, 1970). Proteins were solubilized in 2X reducing sample preparation buffer (2X SPB; 0.125 M Tris, 4% SDS, 20% Glycerol, 20% 2-Mercaptoethanol, pH 6.8) and resolved in reducing SDS-PAGE discontinuous gels. Separating gels (11%; 37.5 Acrylamide:Bis) of dimensions 0.75 mm x 5.5 cm, were cast and left to polymerize at room temperature for 60 minutes followed by polymerization of stacking gels (4%; 37.5 Acrylamide:Bis) around sample 'combs' (Bio-Rad Laboratories; Mississauga, Ontario, Canada) at room temperature for 30 minutes. Gels were assembled in a Mini-

Protean Tetra Cell System (Bio-Rad; Mississauga, Ontario, Canada) and electrophoresis buffer (0.025M Tris, 0.19 M Glycine, 0.1% SDS) was added to the lower and upper reservoirs of the cell unit. Gels were loaded with 10 µl of protein sample per well and low-range molecular weight markers (97.4-14.4 kDa; Bio-Rad; Mississauga, Ontario, Canada) in specified lanes. Voltage was set at 75 V until the dye front entered the separating gel, after which voltage was increased to 150 V until the dye front reached the bottom of the gel.

Once electrophoresis was complete, the stacking gel was removed from the separating gel. Proteins in the separating gel were transferred to a 0.45 µm PVDF membrane (Millipore; Immobilon, Billerica, MA) in a Trans-Blot SD Semi-Dry Electrophoretic Transfer Cell (Bio-Rad; Mississauga, Ontario, Canada) at a constant voltage of 14 V and a limit of 0.2 A for 50 minutes. The PVDF membrane was stained with Ponceau S (0.2% Ponceau S, 3% trichloro acetic acid, 3% sulfosalicylic acid) to ensure proteins were transferred to the PVDF membrane and then washed in tris-buffered saline (TBS; 0.05 M Tris Base, 0.13 M NaCl, pH 7.6) to remove excess Ponceau S. The membrane was left to dry overnight, labeled, and then placed in 100% methanol for 1 minute before being placed in TBS for 1 hour for rehydration. The membrane was blocked in 5% bovine serum albumin (BSA; Sigma-Aldrich, Oakville, Ontario, Canada) for 1 hour, followed by three, 15-minute rinse steps with TBS. The membrane was then probed with a 1:10 dilution of anti-alpha-Gal antibody (M86; Cedarlane Laboratories, Burlington, ON) in 5% BSA in TBS for 1 hour at room temperature, and then left overnight at 4°C. The membrane was placed on an ADAMS Nutator (ClayAdams;

Parsippany, New Jersey, USA) to rotate for 1 hour at room temperature before it was washed 3 times, 15 minutes each, with 0.05% Tween® 20 in TBS. The PVDF membrane was then placed in a solution containing 5% skim milk (Nestle; North York, Ontario, Canada), 5% normal goat serum (Cedarlane Laboratories; Burlington, Ontario, Canada), and a 1:5000 dilution of horseradish peroxidase-conjugated goat anti-mouse IgM antibody (Cedarlane Laboratories, Burlington, ON) in TBS. After one hour, the rinse and wash protocol described above was repeated. Pierce ECL substrate (Fisher Scientific; Ottawa, ONT) was placed on the membrane in a dark room to develop autoradiographs of the blot (Thermo Scientific CL-XPosure Film; Fisher Scientific, Ottawa, Ontario, Canada) according to manufacturer's recommendations.

2.3 Results

2.3.1 Prevalence and Intensity of *Parelaphostrongylus tenuis* in White-tailed Deer of New Brunswick.

Heads were collected from 166 white-tailed deer. Of these, 151 were used for determination of prevalence and intensity of infection with *P. tenuis*. The remaining 15 heads were excluded because they had severe skull trauma, and thus an accurate determination of infection status and intensity was not possible. Heads from 79% (11/14) of deer aged $\leq$ 0.5 years old were infected with adult *P. tenuis*, whereas 87% (32/37) of those aged >0.5-1.5 years old, and 93% (93/100) of those aged >1.5-yr-old

were infected with adult *P.tenuis*. The deer aged ≤ 0.5 years old had a mean intensity of 3.3 ± 2.9 adult *P. tenuis*, with 1-10 worms found per infected deer. The mean intensity of infection for deer aged 0.5-1.5 years old was 3.8 ± 4.3 with 1-24 worms per deer, and deer aged >1.5-yr-old had a mean intensity of 3.7 ± 3.2 with 1-24 worms per deer (Table 2.1). Overall, 90% (136/151) of deer from all age classes were infected with adult *P. tenuis*, and had a mean intensity of 3.7 ± 3.4 with 1-24 worms per deer. This is higher than previous reports of 83% prevalence of infection within New Brunswick (Duffy, 2000). The overall intensity of infection of 3.7 was slightly lower than the previously reported 4.3 (Duffy, 2000). The differences likely reflect regional differences in prevalence and intensity and the focus of the current study on animals from the south-eastern part of New Brunswick.

Table 2.2 Prevalence and intensity of adult *Parelaphostrongylus tenuis* in white-tailed deer (*Odocoileus virginianus*).

Deer age	Number of deer examined	Number of deer infected	Prevalence (%)	Mean Intensity and Standard Deviation	Range in Intensity
≤ 0.5-yr-old	14	11	78.6	3.3 ± 2.9	1-10
0.5-1.5-yr-old	37	32	86.5	3.8 ± 4.3	1-24
> 1.5-yr-old	100	93	93	3.7 ± 3.2	1-24
All ages	151	136	90	3.7 ± 3.4	1-24

2.3.2 Structure of the Secretory System of Adult *Parelaphostrongylus tenuis*.

2.3.2.1 General Morphology of Secretory System

The glandular secretory system of adult *P. tenuis* consists of two excretory gland cells and the pharynx. The pharynx, approximately 0.71 mm in length, is located at the very tip of the anterior end proximal to the mouth. The large paired excretory glands extend longitudinally alongside the pharynx and intestine, occupying up to 10% of the worm's length (Figure 2.1). Sections through the anterior end of adult *P. tenuis* were collected to examine the secretory system using a light microscope. A representative section 2 mm from the tip of the anterior end was approximately 200 μm in diameter. The contents of the pseudocoelum are comprised primarily of the two excretory glands and the digestive system (Figure 2.2a). The excretory glands are single-celled and are densely populated with spherical secretory granules up to 4 μm in diameter (Figure 2.2a,b) that stained purple with toluidine blue and basic fuchsin stain. The excretory duct is lined with cuticle and it connects the anterior end of each gland to the excretory pore (Figure 2.3). The pharynx has a muscular component found in the more anterior region that leads into a more distal glandular region that contains secretory granules up to ~1 μm in diameter (Figures 2.3, 2.4), smaller than the granules in the excretory gland. Longitudinal sections demonstrate the presence of many large nuclei (30 μm in diameter) with prominent nucleoli distributed through the glandular component of the pharynx (Figure 2.5a). One large nucleus (30 μm in diameter) with prominent nucleoli is located in the posterior region of each excretory gland (Figure 2.5b). Associated with

some nuclei of the excretory glands were 'furrows' that appear to connect the nucleus with the cell membrane of the gland (Figure 2.6). The furrows associated with both nuclei and the excretory gland cell membranes in one worm were not found in others. However, this observation does not appear to be an artifact. Examination of more specimens might provide further insight into this observation.

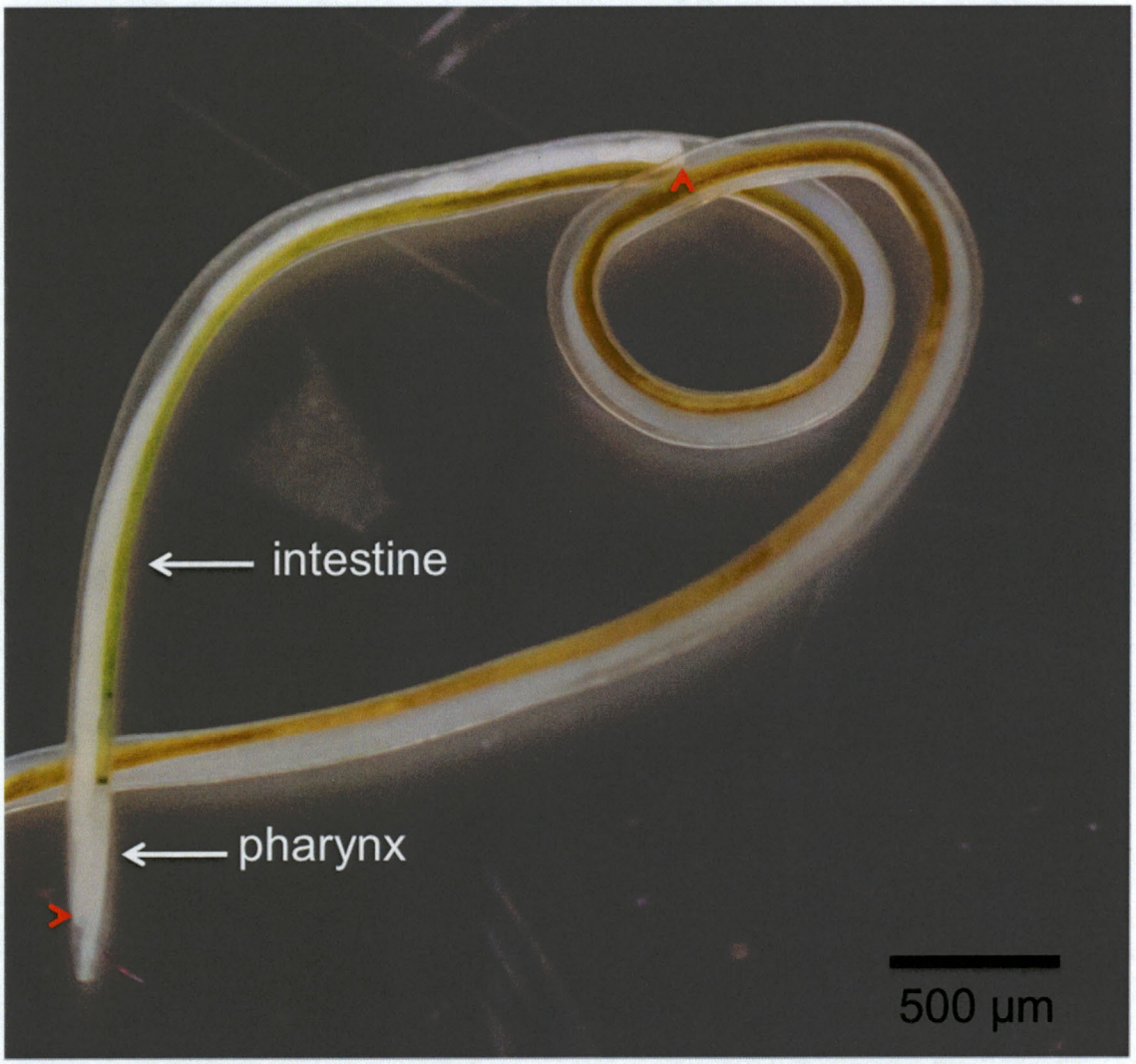


Figure 2.1 Adult *Parelaphostrongylus tenuis* contain two large excretory glands that occupy up to 10% of the length of the worm. The excretory glands occur adjacent to the digestive tract (pharynx and intestine). Red arrowheads delineate the anterior end and posterior end of one excretory gland.

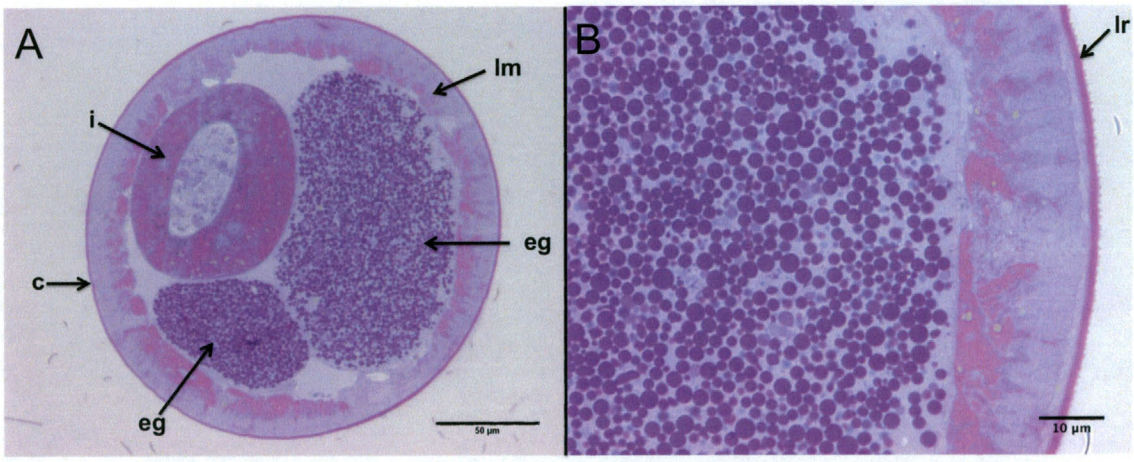


Figure 2.2 Adult *Parelaphostrongylus tenuis* contain two large excretory glands packed with secretory granules. Light micrographs of a cross-section 2 mm from the anterior tip of the worm stained with toluidine blue and basic fuchsin show two excretory glands housing secretory granules (purple spheres)[A]. Increased magnification view of secretory granules within one excretory gland, and longitudinal ridges that occur as part of the exterior cuticle [B]. c = cuticle, eg = excretory gland, i = intestine, lm = longitudinal muscle, lr = longitudinal cuticular ridges.

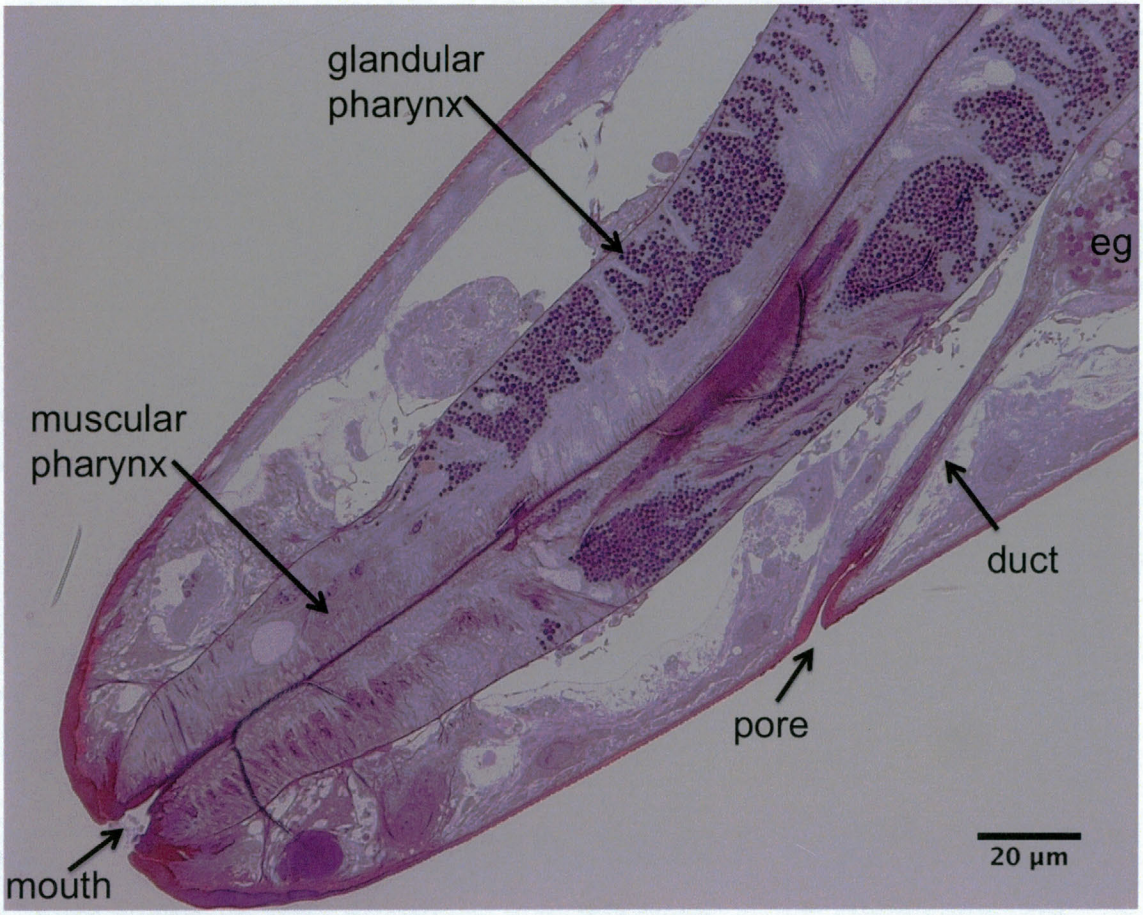


Figure 2.3 An excretory duct connects the excretory glands with the excretory pore. Light micrograph of a longitudinal section through adult *Parelaphostrongylus tenuis* stained with toluidine blue and basic fuchsin showing the excretory pore, excretory duct and excretory gland (eg). Also shown are the anterior muscular pharynx and the more posterior glandular pharynx.

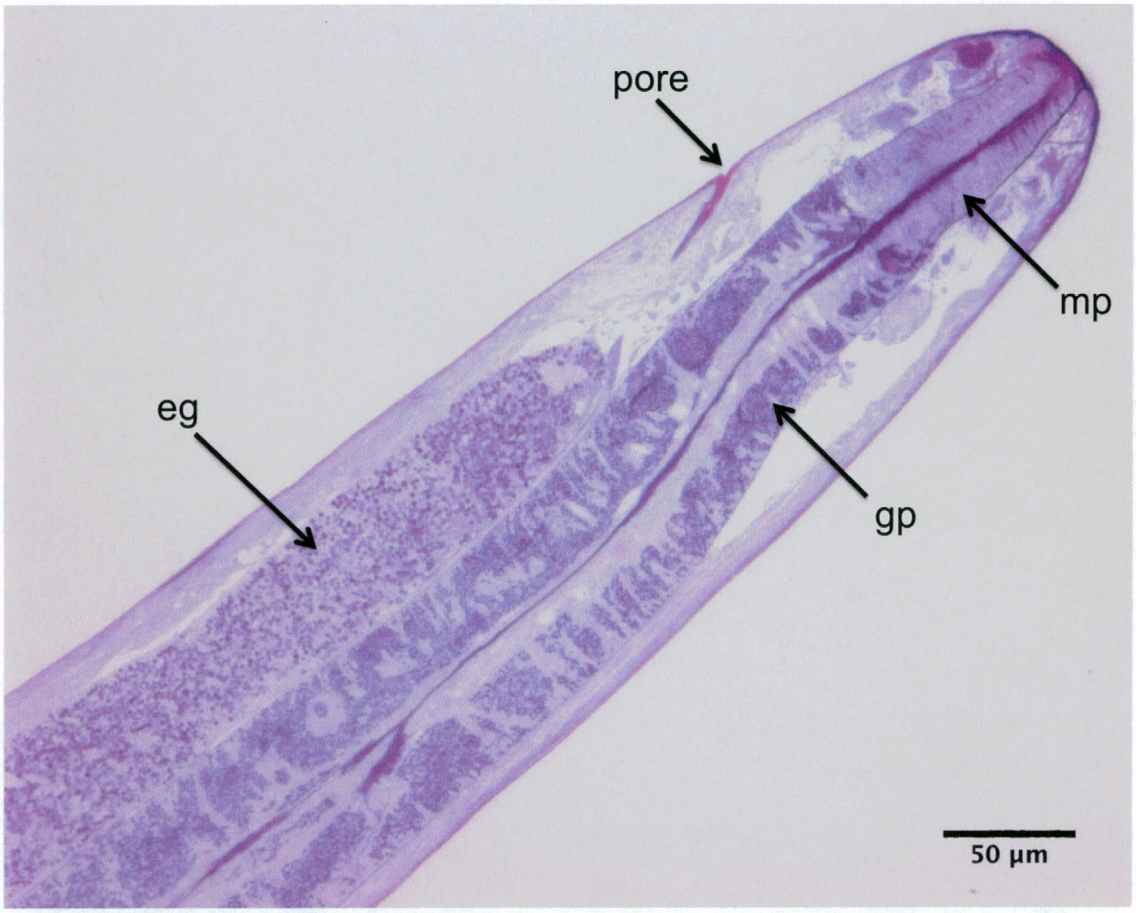


Figure 2.4 The glandular secretory system of adult *Parelaphostrongylus tenuis* consists of a glandular region in the pharynx and two excretory gland cells. Light micrograph of a longitudinal section through adult *Parelaphostrongylus tenuis* stained with toluidine blue and basic fuchsin showing the components of the secretory system. mp = muscular pharynx, gp = glandular pharynx, eg = excretory gland (only one excretory gland is shown). The excretory pore is also shown.

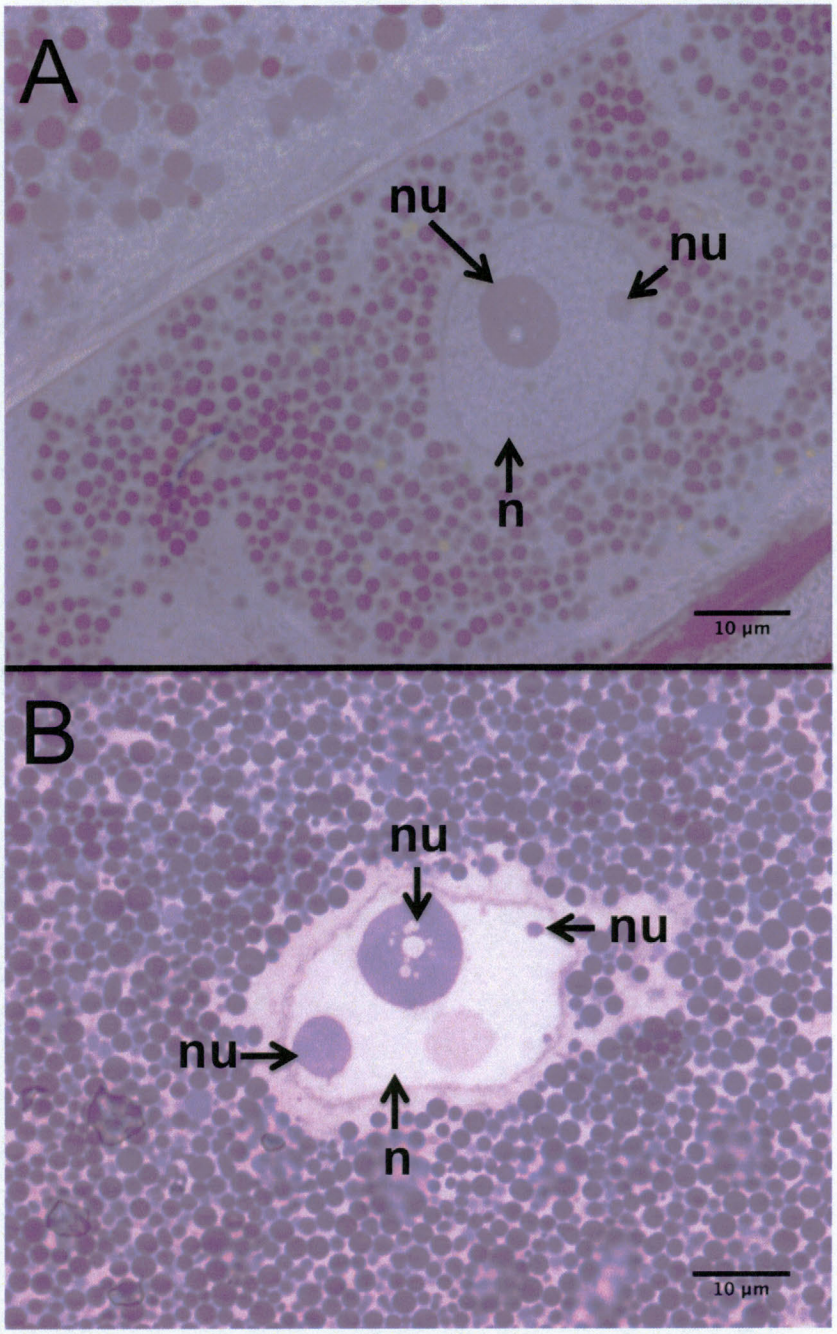


Figure 2.5 The glandular pharynx and excretory glands of *Parelaphostrongylus tenuis* possess large nuclei. Light micrographs of longitudinal sections from the anterior end of adult female *Parelaphostrongylus tenuis* stained with toluidine blue and basic fuchsin show the presence of large nuclei containing a number of nucleoli. One of many large nuclei (n), approximately 30 µm in diameter, found in the glandular pharynx contains 2 darkly stained nucleoli (nu) [A]. Excretory gland cells contain one large nucleus (n), approximately 30 µm in diameter, each with darkly stained nucleoli (nu) [B].

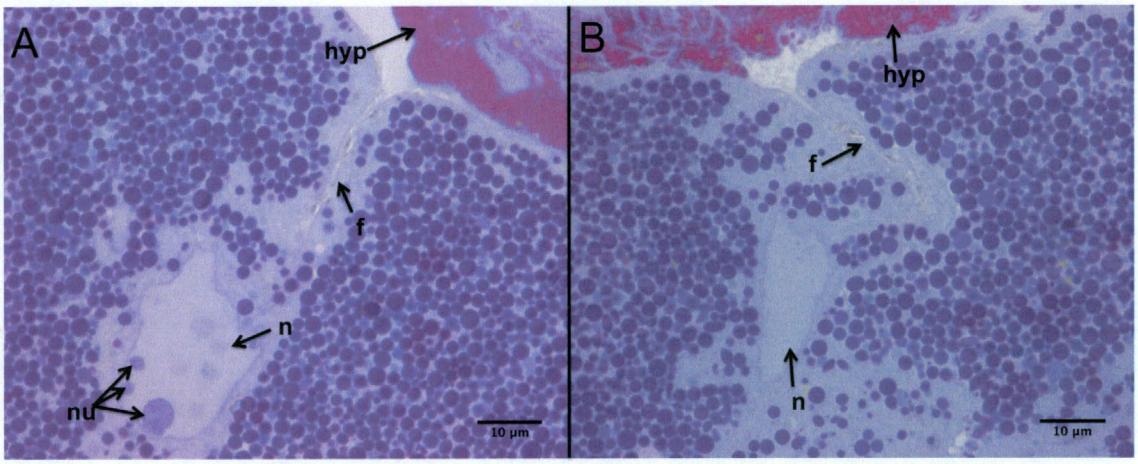


Figure 2.6 In some instances, the nucleus of each excretory gland was closely associated with the cell membrane via furrows. Light micrographs of longitudinal sections 2-4 mm [A] and 4-6 mm [B] from the anterior end of adult female *Parelaphostrongylus tenuis* show furrows associated with each nucleus. A furrow connects the nucleus with the excretory gland membrane. The nucleoli are absent in one micrograph, but were located in subsequent sections. All sections were stained with toluidine blue and basic fuchsin. f = furrow, hyp = hypodermis, n = nucleus, nu = nucleoli.

2.3.2.2 Ultrastructure of the Excretory Glands of the Secretory System

Transmission electron microscopy was used to supplement the light microscopy observations of excretory glands. Each excretory gland contains endoplasmic reticulum (Figure 2.7a), mitochondria (Figure 2.7b), and secretory granules up to 4 µm in diameter (Figure 2.7, Figure 2.8). Increased magnification of the single nucleus in each excretory gland cell highlights features common in eukaryotic nucleoli. The nucleoli lack a membrane and possess both a dense fibrillar component and a granular component (Figure 2.9). Secretory granules with both distinct and indistinct outer membranes were often found in the same region of excretory gland cells (Figure 2.8).

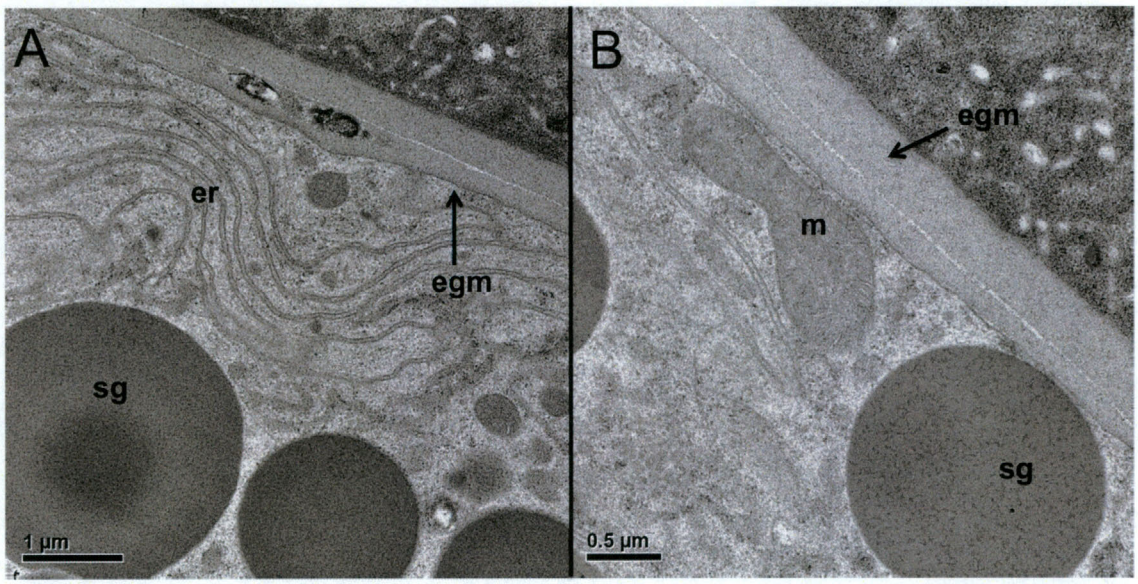


Figure 2.7 Endoplasmic reticulum and mitochondria are abundant in the cytoplasm of the excretory gland cells from adult *Parelaphostrongylus tenuis*. Transmission electron micrographs of the excretory glands showing secretory granules (sg), endoplasmic reticulum (er), and the excretory gland cell membrane (egm) [A]. Mitochondria (m) were found dispersed throughout the excretory gland cells [B].

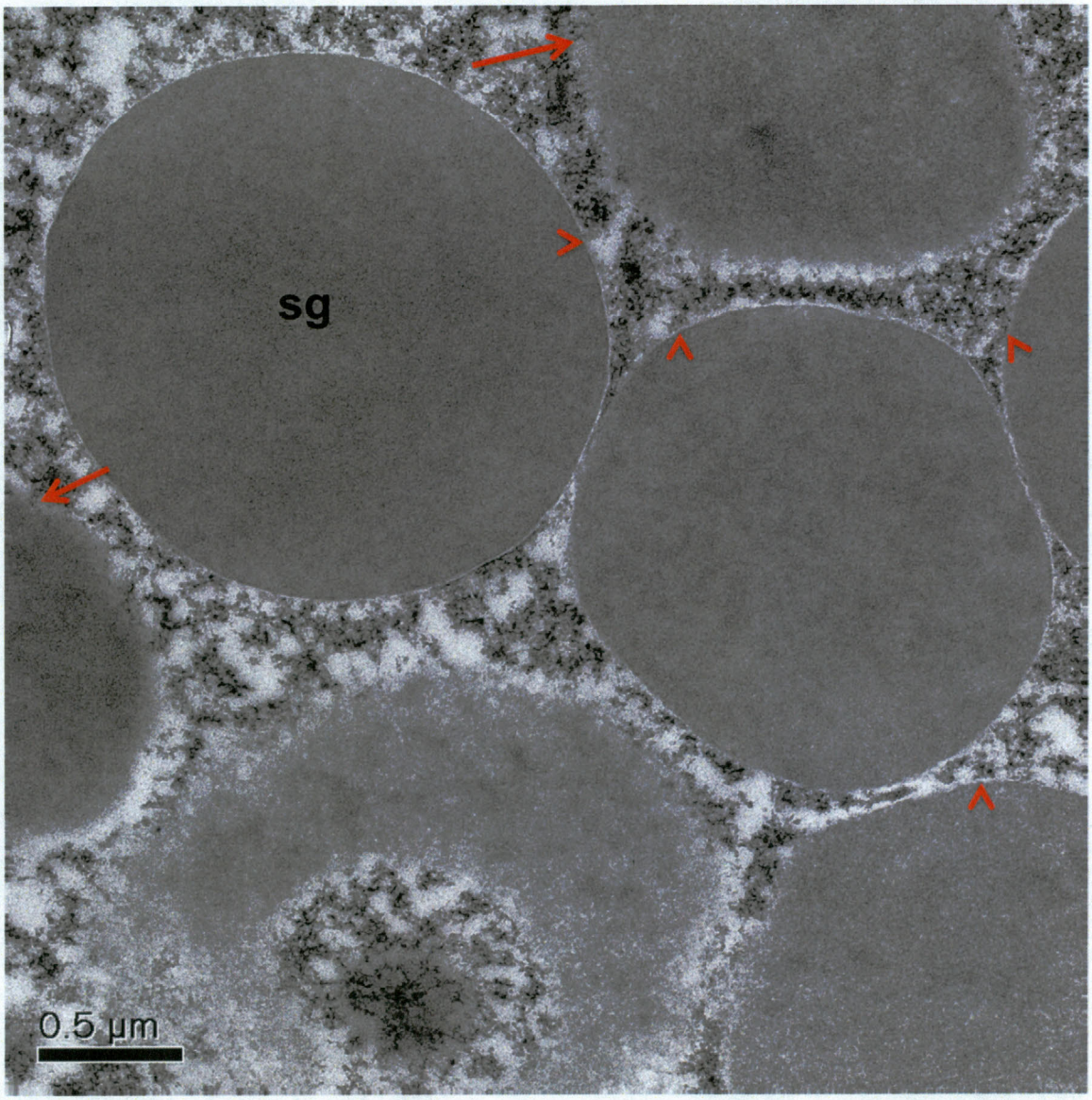


Figure 2.8 Transmission electron micrograph of secretory granules from the excretory gland cells of adult *Parelaphostrongylus tenuis*. Some granules were clearly enveloped by a membrane (arrowheads) whereas other granules did not have a distinct outer membrane (arrows).

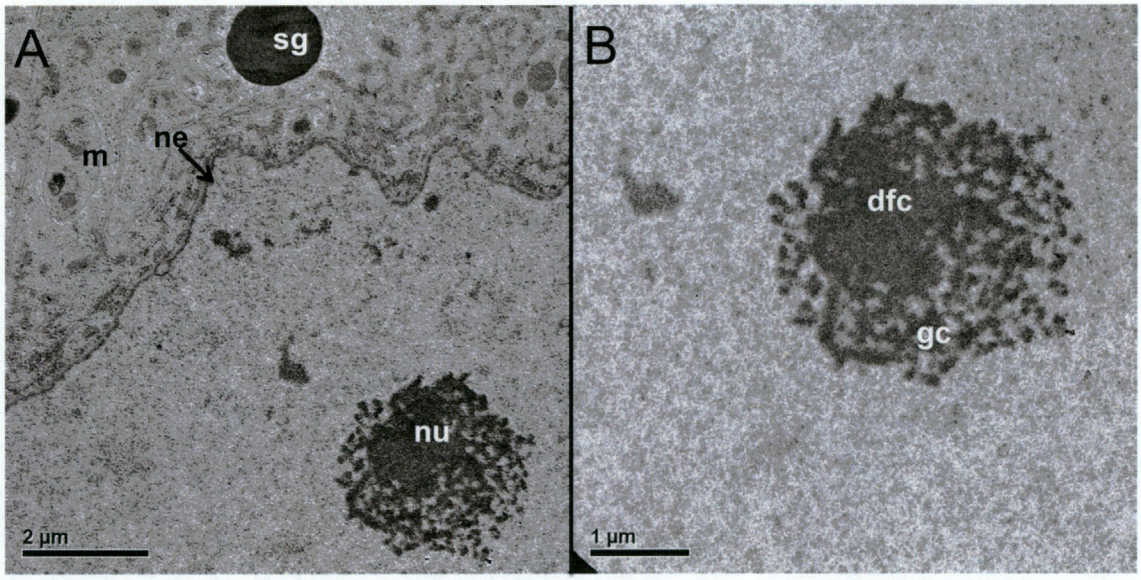


Figure 2.9 A transmission electron micrograph through the nucleus of an excretory gland cell of *Parelaphostrongylus tenuis* showing a large nucleolus. The nuclear envelope (ne) is shown enclosing one of the nucleoli (nu), approximately 3 µm in diameter. A mitochondrion (m) and secretory granule (sg) is also shown [A]. Increased magnification highlights the absence of a nucleolar membrane and the presence of a dense fibrillar component (dfc) and a granular component (gc) characteristic of eukaryotic nucleoli [B].

2.3.3 Morphology and Ultrastructure of the Cuticle

The epicuticle is textured with longitudinal ridges ~0.2-0.3 µm that extend the full-length of the worm (Figure 2.2a, 2.10). The longitudinal ridges are dispersed along the perimeter of the cuticle approximately 0.5 µm apart. The cortical, medial and basal zones of the cuticle are shown, in addition to the hypodermis, basal lamina and longitudinal muscle (Figure 2.10). The identification of the longitudinal ridges of the cuticle of *P. tenuis* does not conform to the 1974 revision of the taxonomic identification keys for nematode parasites of vertebrates, as they state that members of the superfamily Metastongyloidea lack longitudinal cuticular ridges (Commonwealth

Institute of Helminthology. *et al.*, 1974). However, this is the first time that adult *P. tenuis* has been examined at such a high magnification and the possibility that the longitudinal ridges were never seen before simply due to magnification limits is the most likely explanation for the contradiction between this current result and the taxonomic keys.

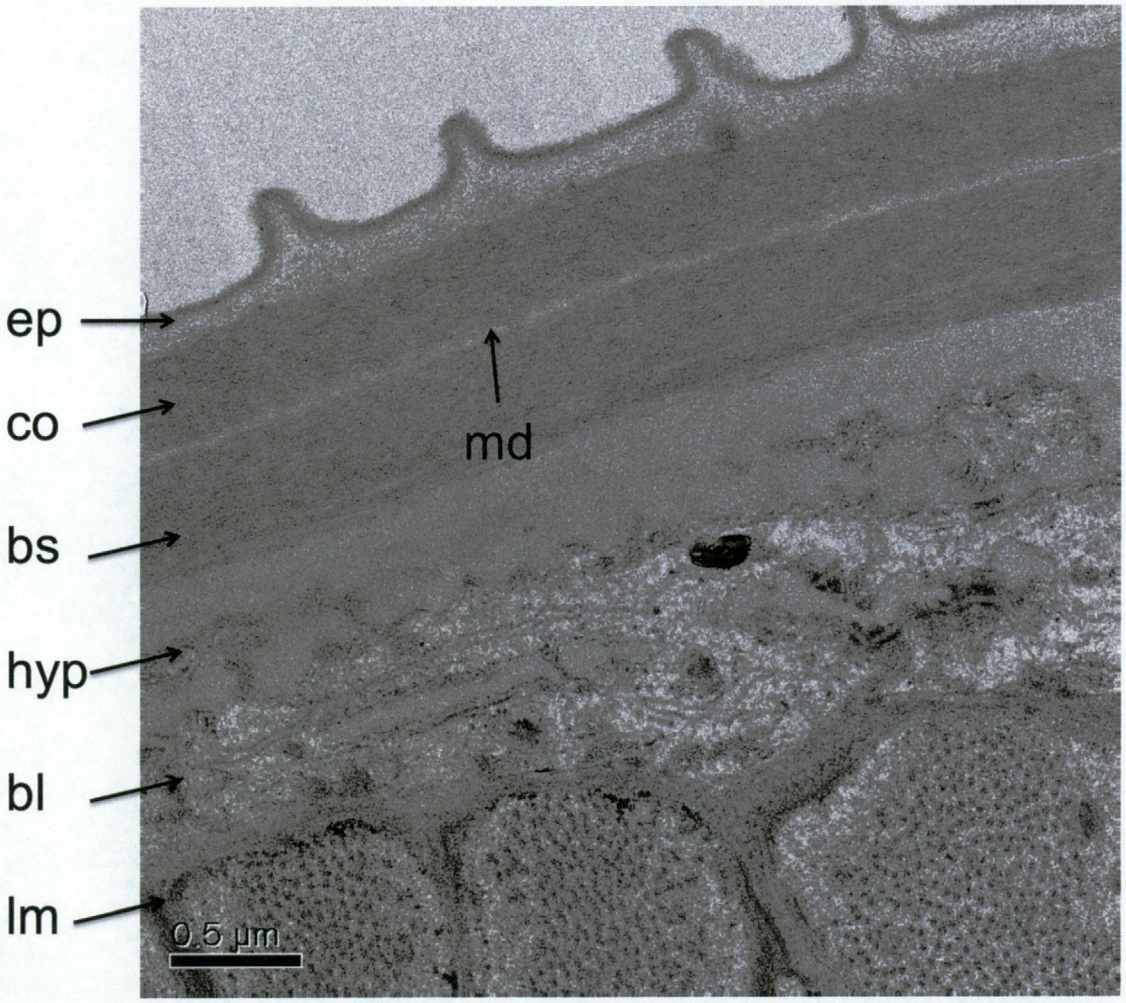


Figure 2.10 The cuticle of adult *Parelaphostrongylus tenuis* is modified with longitudinal cuticle ridges. A transverse section transmission electron micrograph shows the layers of the cuticle that include the epicuticle (ep), the cortical zone (co), the medial zone (md) and the basal zone (bs). The epicuticle (ep) has longitudinal ridges spaced approximately 0.5 µm apart. Other features labeled for orientation include the hypodermis (hyp), basal lamina (bl) and longitudinal muscle (lm).

2.3.4 Immunogold Labeling for Detection of alpha-Gal

High-resolution localization of alpha-Gal within the excretory gland was obtained by transmission electron microscopy and immunogold labeling using a 12-nm gold particle conjugated to a secondary antibody. Gold particles were restricted to the contents of the secretory granules housed within excretory glands (Figure 2.11a, 2.11b). Viewing the specimen slightly out of focus allowed better visualization of gold particles by creating a white halo artifact around each particle. A thorough search of the intergranular space surrounding each granule confirmed the absence of gold particles in this region (Figure 2.11c). Accordingly, alpha-Gal was restricted to the contents of the secretory granules and was absent from the extra-granular spaces of the excretory gland. Gold particles were absent from negative control cross-sections lacking primary antibody (Figure 2.11d).

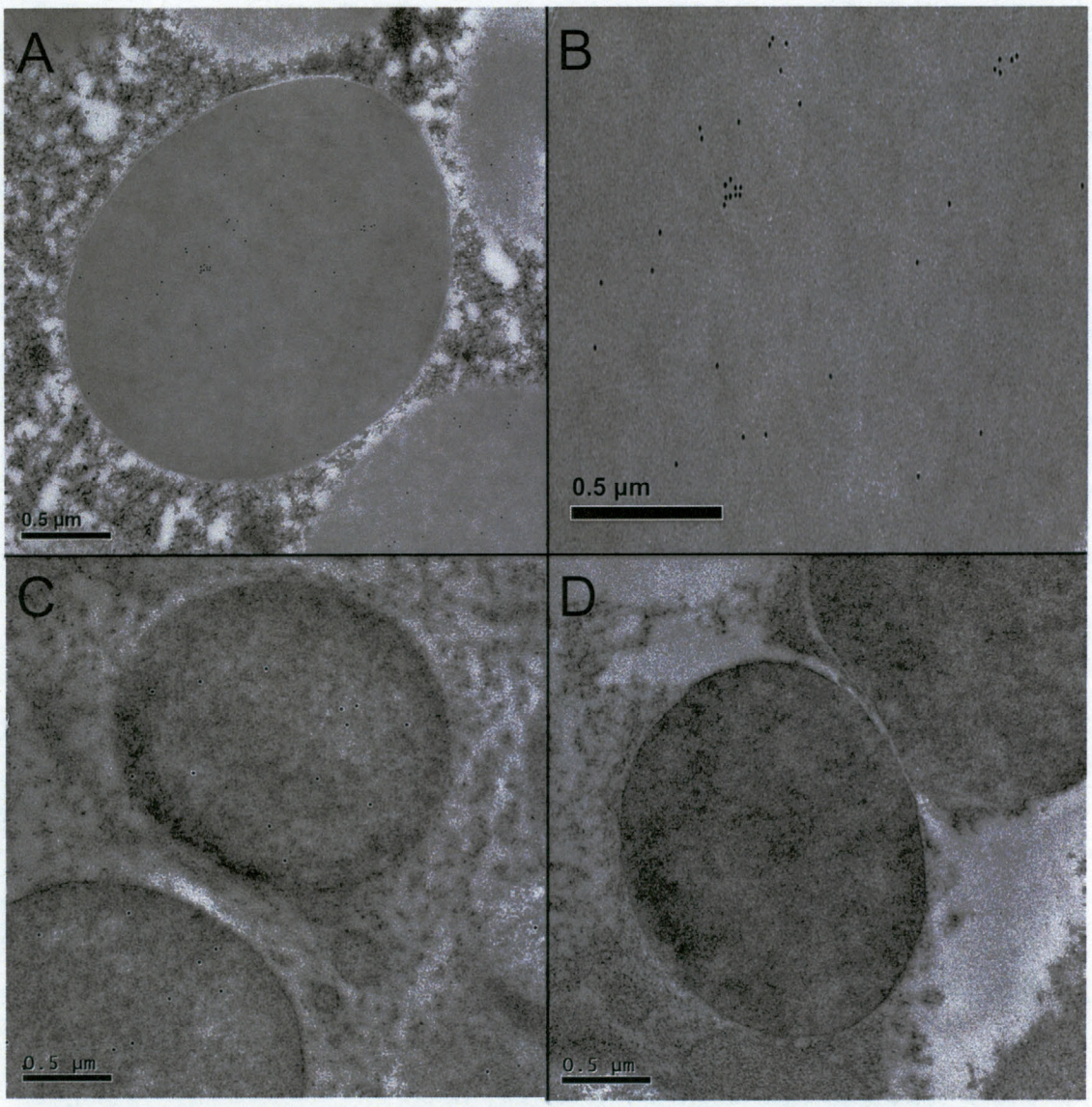


Figure 2.11 Immunogold localization of alpha-Gal to the contents of secretory granules of the excretory gland in adult *Parelaphostrongylus tenuis*. Gold particles (black dots) indicate the presence of the alpha-Gal epitope and are restricted to secretory granules [A]. Increased magnification of the granule from panel A provides an improved image of the gold particles within the granule [B]. Induction of a white halo artifact around gold particles enabled confirmation that alpha-Gal is restricted to contents of secretory granules and absent from the intergranular space [C]. Gold particles were absent in a negative control section where the primary antibody was omitted [D].

2.3.5 Detection of Alpha-Gal in E/S Products and Somatic Extracts from Adult *P. tenuis*

Protein extracts from adult *P. tenuis* were separated by sodium dodecyl sulfate polyacrylamide gel electrophoresis (SDS-PAGE) and blotted to PVDF. Protein abundance was judged to be equivalent in all lanes according to the Ponceau S staining of blotted protiens on the PVDF membrane (data not shown). Alpha-Gal was detected in several E/S proteins from adult *P. tenuis* with apparent molecular masses of 45-145 kDa.(Figure 2.12). Alpha-Gal was also detected in a smear of somatic proteins with apparent molecular masses of 30-105 kDa from the anterior 10% of both female and male worms (Figure 2.12). A single protein with an apparent molecular mass of 55 kDa was modified with alpha-Gal in the posterior region of female *P. tenuis*. Alpha-Gal was not detected in the posterior region of male *P. tenuis* (Figure 2.12).

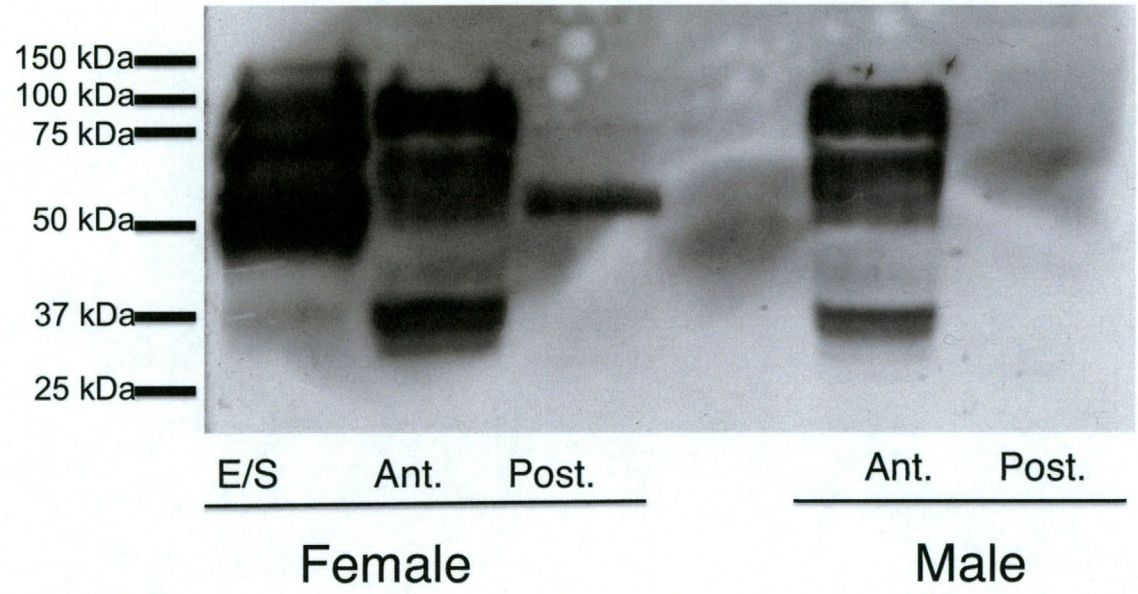


Figure 2.12 Immunoblot detection of alpha-Gal in somatic extracts and E/S products of adult *P. tenuis.* Alpha-Gal was detected in a smear of proteins with apparent molecular masses of 45-145 kDa in E/S products from adult female worms. Alpha-Gal was also detected in a smear of somatic proteins with an apparent molecular masses of 30-105 kDa from the anterior 10% of both female and male worms, and one protein of apparent molecular mass of 55-kDa from the posterior 10% of the adult female. Alpha-Gal was not detected in the posterior region of the male worm.

2.4 Discussion

Helminth glycans are known to have a key role in interacting with immune effector cells at the host-parasite interface (van Die and Cummings, 2010). Early research on *P. tenuis* discovered for the first time in a helminth parasite that this nematode produces a novel glycan (alpha-Gal; Galα1-3Gal) restricted to the adult life stage (Duffy *et al.*, 2006). Alpha-Gal modifies E/S (excreted/secreted) proteins and was localized to excretory glands and uteri of adult *P. tenuis* using immunohistochemistry (Duffy *et al.*, 2006). Alpha-Gal is a terminal disaccharide of some N-linked glycans and it is found in all mammals with the exception of old world primates, where a mutation in the α1,3 galactosyltransferase resulted in loss of the epitope (Galili U *et al.*, 1988). Accordingly, this glycan is present within the deer host of *P. tenuis* and thereby represents a "self" antigen unrecognizable by lymphocyte receptors. The recent discovery of this glycan in closely-related Metastrongyloid nematodes (*P. andersoni, P. odocoilei, Elaphostrongylus rangiferi,* and *Crenosoma vulpis*; Bedford, 2010) and in a Trichostrongyloid nematode (*Haemonchus contortus*; (van Stijn *et al.*, 2010), indicates that this sugar is utilized more commonly in parasitism of mammals. While glycans like mannose are common in nematodes, alpha-Gal has a more restricted distribution in parasitic nematodes (Duffy *et al.,* 2006).

Immunogold labelling of alpha-Gal within excretory glands of the secretory system of *P. tenuis* in the current study improved resolution tremendously. Alpha-Gal is present within secretory granules of the excretory glands but not within the extragranular

cytoplasm of these large cells. The absence of alpha-Gal from some parasitic nematodes argues against a role in basic physiological processes of nematodes. Furthermore, stage restriction of alpha-Gal in adult *P. tenuis* and its conservation in the deer host supports a definitive role in parasitism. Parasite molecules that are also conserved in their host are common and may promote parasite persistence. This molecular mimicry is a type of immune evasion (Damian, 1964) that may enable adult parasites to persist for the life span of their host. If alpha-Gal were employed by the parasite as a camouflage-type of molecular mimicry, one would expect the parasite to be coated externally or their products to be abundantly coated with this glycan. Adult *P. tenuis* induce a concomitant immunity and can persist up to 6 years in their deer host (Duffy e*t al.*, 2004). The life cycle involves release of large numbers of eggs (up to several million per day) into the bloodstream with subsequent development of larvae initiated following embolization in the capillaries of host lungs (Duffy e*t al.*, 2004). Accordingly, eggs must also evade host effector cells during their development in deer lungs. Previous localization of alpha-Gal in the uterus led to speculation that this disaccharide might serve to camouflage parasite eggs developing within host lungs (Duffy *et al.*, 2006). However, improved resolution using immunogold labelling documented that alpha-Gal is not localized to egg surfaces and therefore it does not have an obvious role in immune evasion by camouflage (Rideout, 2012). While a camouflage-type of molecular mimicry has been ruled out, it is possible that an immunomodulatory-type of molecular gimmickry is taking place via alpha-Gal-modified proteins released from adult *P. tenuis*.

The term 'excretory-secretory proteins' is used widely in helminth biology. It

encompasses proteins that are released from the uterus, anus, and a variety of glands in the anterior ends of helminths (pharyngeal, esophageal, amphidial, excretory and secretory glands). Given that the term excretion implies release of waste products, only intestinal contents from the anus represent true excreted proteins. E/S proteins from adult nematodes are required for persistence of infection by means of reproduction, enabling the parasite to feed, immunomodulation and immune evasion (Hewitson *et al.*, 2009). More often than not, molecular characterization of E/S proteins actively released by the worm is completed without knowing which secretory gland the proteins originated from. However, some thoroughly investigated proteins have been localized exclusively to specific glands within parasitic nematodes, similar to alpha-Gal restriction to the excretory system of *P. tenuis*. For example, acetylcholinesterase is secreted to hydrolize host acteylcholine and was localized to amphidial and oesophageal glands of *Necator americanus* (McLaren *et al.*, 1974). A 24 kDa E/S candidate vaccine antigen produced in the oesophagus of *Haemonchus contortus*, is secreted to enable feeding (Schallig *et al.*, 1997). A secreted cellulose binding protein was localized to the dorsal oesophageal gland of the plant parasitic nematode *Heterodera schachtii*. This protein targets plant enzymes to induce cell wall modifications that facilitate parasitism (Hewezi *et al.*, 2008). Identification of specific secreted proteins, and the glands they originate from, has helped to elucidate the functional role of secretory glands in parasitism of the host.

Adult *P. tenuis* were fractionated to determine the relative abundance of alpha-Gal-modified proteins derived from the glandular secretory system in the anterior of worms

as compared to proteins derived from the posterior of worms. Comparatively, the fraction from the anterior portion of the worm showed great diversity and abundance in the number of proteins modified by alpha-Gal. While secretory granules are found in both the glandular pharynx and in the paired excretory glands of the secretory system of *P. tenuis*, immunogold labeling demonstrates definitive absence of alpha-Gal in the pharynx (unpublished data). Accordingly, all alpha-Gal-modified proteins from the anterior 10% of *P. tenuis* are restricted to secretory granules within the excretory gland cells with no involvement of the glandular pharynx. With only 4 alpha-Gal-modified proteins confirmed outside of the secretory system (Rideout, 2012), the excretory gland cells are the principle source of alpha-Gal that is released into the host during parasitism.

The excretory glands of *P.tenuis* were originally described as elongated, faintly granular single-celled glands, each with a large nucleus at the posterior end (Anderson, 1956). A cuticle-lined duct connected the glands with a pore to release contents to the outside environment. The current work by light and electron microscopy confirmed that the two large gland cells occur adjacent to the pharynx and intestine, that an excretory pore that opens to a cuticle-lined duct is associated with these glands, and a large nucleus is present in the posterior region of each cell. The large nucleus of each *P. tenuis* excretory gland cell was up to 30 μm in diameter. This is not surprising since, according to the karyoplasmic ratio (the proportioned ratio of nuclear to cellular volume; (Huber and Gerace, 2007), one would expect large gland cells that are up to 10% of the length of the worm to require a large nucleus. Similar large nuclei were also observed

in the glandular pharynx of *P. tenuis*. Interestingly, throughout the parasitic nematode literature, there are many references to large nuclei being associated with large gland cells in the anterior end: the three mononucleate gland cells of the pharynx of *Anguillicoloides crassus* (Brunianská *et al.*, 2007); all seven anterior glands (amphidial, oesophageal and excretory glands) of *Necator americanus* (McLaren, 1974): and, the three oesophageal gland cells of the Tylenchid plant parasites (Hussey *et al.*, 2002). While these authors provide little insight for a role for large nuclei in secretory cells, nematode cell size shows positive correlation with cell ploidy, as seen in hypodermal cells of many worms in the order Rhabditida (Flemming *et al.*, 2000). Polyploidization by endoreduplication causes nuclear enlargement, and increased DNA copy number can be beneficial for cells that require high metabolic activity (Comai, 2005). A role for endoreduplication in nematode secretory organs should be studied as a potential explanation for the large nuclei found in *P. tenuis* excretory glands.

While *P. tenuis* excretory glands were originally described as 'faintly granular' (Anderson, 1956), this is the first time that secretory granules have been demonstrated specifically. According to Burgess and Kelly (1987), a cell specialized for storage of vast amounts of protein is required to have secretory granules. Secretory granules have high electron density and look granular when viewed with an electron microscope. The contents of the secretory granules are only released when triggered by an extracellular stimulus and so this type of granular protein secretion is called regulated secretion. The use of secretory granules for long-term storage allows for condensation of proteins at concentrations higher than what is found in early Golgi cisternae. This feature enables

secretory cells to release large amounts of protein immediately upon receiving an external signal, without having to synthesize new proteins (Burgess and Kelly, 1987). Our observation of granules with and without membranes is not unique to *P. tenuis*; both have been observed in subventral oesophageal glands of *Meloidogyne javanica* during different life-stages (Bird, 1968). Granules with membranes are most common in preparasitic larvae and granules lacking a membrane were observed in parasitic larvae (Bird, 1968). Granules lacking a distinct membrane were thought to be releasing their contents into the duct.

Previous work had identified the presence of alpha-Gal within excretory gland cells (Duffy *et al.*, 2006). One focus of this current study was to clarify the localization of the alpha-Gal epitope within the excretory glands. The current work established that the glands are full of secretory granules, and thus are designed to respond to an extracellular stimulus to release large quantities of protein. I have confirmed earlier work that *P. tenuis* secretes glycoproteins from the secretory system in the anterior end of the worm (Duffy *et al.*, 2006). It is now established that these alpha-Gal-modified proteins originate from secretory granules housed in the excretory glands. The presence of secretory granules in the excretory glands indicates a role in secretion, and not excretion. It was suggested previously that the term "excretory glands" was truly a misnomer given their role (Lee, 1970; Bird, 1971). Ultrastructural features of these glands in *P. tenuis* provide compelling evidence that the *P. tenuis* excretory glands should be renamed "secretory glands". The precise role of the secretory glands remains to be determined in the context of parasitism and concomitant immunity. However, it

seems likely that the secretory glands have a role in the persistence of *P. tenuis* infection within their deer host. Specific identification of the alpha-Gal modified glycoproteins released from the secretory granules will be necessary to define further the functional role of the secretory glands.

Bibliography

Anderson, R. C. (2000). Nematode parasites of vertebrates : their development and transmission. CABI Pub., Wallingford, Oxon, UK; New York, NY.

Anderson, R. C. (1956). " *Elaphostrongylus odocoilei hobmaier* and *hobmaier*, 1934 in the cranial case of *Odocoileus virginianus borealis miller.*" *Can.J.Zool.,* 34(3), 167-173.

Bedford, R.O. (2010). Molecular conservation of a novel glycan used by parasitic nematodes in immune evasion. Honours Thesis. University of New Brunswick, Fredericton, New Brunswick, Canada, 53 pp.

Bird, A. F. (1971). The structure of nematodes. Academic Press, New York.

Bird, A. F. (1968). "Changes Associated with Parasitism in Nematodes. III. Ultrastructure of the Egg Shell, Larval Cuticle, and Contents of the Subventral Esophageal Glands in *Meloidogyne javanica*, with Some Observations on Hatching." *J.Parasitol.,* 54(3), 475-489.

Brunianská M, Fagerholm HP, and Moravec F. (2007). "Structure of the pharynx in the adult nematode *Anguillicoloides crassus* (Nematoda: Rhabditida)." *J.Parasitol.,* 93(5), 1017-28.

Burgess TL, and Kelly RB. (1987). "Constitutive and regulated secretion of proteins." *Annu.Rev.Cell Biol.,* 3 243-93.

Comai L. (2005). "The advantages and disadvantages of being polyploid." *Nat. Rev.Genet.,* 6(11), 836-46.

Commonwealth Institute of Helminthology., Anderson, R. C., Chabaud, A., and Willmott, S. (1974). *CIH keys to the nematode parasites of vertebrates.* Commonwealth Agricultural Bureaux, Farnham Royal.

Damian RT. (1997). "Parasite immune evasion and exploitation: reflections and projections." *Parasitology,* 115 169-75.

Damian, R. T. (1964). "Molecular Mimicry: Antigen Sharing by Parasite and Host and Its Consequences." *Am.Nat.,* 98(900), 129-149.

Duffy MS, Greaves TA, and Burt MD. (2004). "Establishment of adult *Parelaphostrongylus tenuis,* patent infections, and acquired immunity after experimental infection of white-tailed deer (*Odocoileus virginianus*) and red deer (*Cervus elaphus elaphus).*" *J.Parasitol.,* 90(2), 245-54.

Duffy, M. S., Morris, H. R., Dell, A., Appleton, J. A., and Haslam, S. M. (2006). "Protein glycosylation in *Parelaphostrongylus tenuis*-first description of the Galα1-3Gal sequence in a nematode." *Glycobiology,* 16(9), 854-862.

Duffy, M. S. (2000). "Life history studies of *Parelaphostrongylus tenius* and *Elaphostrongylus cervi* with investigations into the potential for reliable antemortem immunodiagnosis". University of New Brunswick, Fredericton, N.B.

Flemming, A. J., Shen, Z., Cunha, A., Emmons, S. W., and Leroi, A. M. (2000). "Somatic Polyploidization and Cellular Proliferation Drive Body Size Evolution in Nematodes." *Proc.Natl.Acad.Sci.U.S.A.,* 97(10), 5285-5290.

Galili U, Shohet SB, Kobrin E, Stults CL, and Macher BA. (1988). "Man, apes, and Old World monkeys differ from other mammals in the expression of alpha-galactosyl epitopes on nucleated cells." *J. Biol. Chem.,* 263(33), 17755-62.

Hewezi, T., Howe, P., Maier, T. R., Hussey, R. S., Mitchum, M. G., Davis, E. L., and Baum, T. J. (2008). "Cellulose Binding Protein from the Parasitic Nematode *Heterodera schachtii* Interacts with *Arabidopsis* Pectin Methylesterase: Cooperative Cell Wall Modification during Parasitism." *Plant Cell,* 20(11), 3080-3093.

Hewitson, J. P., Grainger, J. R., and Maizels, R. M. (2009). "Helminth immunoregulation: The role of parasite secreted proteins in modulating host immunity." *Mol. & Biochem. Parasitol.,* 167(1), 1-11.

Huber, M. D., and Gerace, L. (2007). "The Size-Wise Nucleus: Nuclear Volume Control in Eukaryotes." *J.Cell Biol.,* 179(4), 583-584.

Hussey, R. S., Davis, E. L., and Baum, T. J. (2002). "Secrets in secretions: genes that control nematode parasitism of plants." *Braz. J. Plant Physiol.,* 14(3).

Laemmli UK. (1970). "Cleavage of structural proteins during the assembly of the head of bacteriophage T4." *Nature,* 227(5259), 680-5.

Lee DL. (1970). "The fine structure of the excretory system in adult *Nippostrongylus brasiliensis* (Nematoda) and a suggested function for the 'excretory glands'." *Tissue Cell,* 2(2), 225-31.

McLaren DJ. (1974). "The anterior glands of adult *Necator americanus* (Nematoda: Strongyloidea). I. Ultrastructural studies." *Int.J.Parasitol.,* 4(1), 25-37.

McLaren DJ, Burt JS, and Ogilvie BM. (1974). "The anterior glands of adult Necator americanus (Nematoda: Strongyloidea). II. Cytochemical and functional studies." *Int.J.Parasitol.,* 4(1), 39-46.

Nelson FK, Albert PS, and Riddle DL. (1983). "Fine structure of the *Caenorhabditis elegans* secretory-excretory system." *J.Ultrastruct.Res.,* 82(2), 156-71.

Nelson FK, and Riddle DL. (1984). "Functional study of the *Caenorhabditis elegans* secretory-excretory system using laser microsurgery." *J.Exp.Zool.,* 231(1), 45-56.

Rideout, E.G.W. (2012). Localization of glycosylated reproductive proteins from *Parelaphostrongylus tenuis* with a potential role in immune evasion. Honours Thesis. University of New Brunswick, Fredericton, New Brunswick, Canada, 47 pp.

Reynolds, E. S. (1963). " The use of lead citrate at high pH as an electron-opaque stain in electron microscopy." *J. Cell Biol.,* 17(1), 208-212.

Schallig HD, van Leeuwen MA, Verstrepen BE, and Cornelissen AW. (1997). "Molecular characterization and expression of two putative protective excretory secretory proteins of *Haemonchus contortus*." *Mol.Biochem.Parasitol.,* 88(1-2), 1-2.

Severinghaus, C. W. (1949). "Tooth Development and Wear as Criteria of Age in White-Tailed Deer." *J. Wildl. Manage,* 13(2), 195-216.

Terrazas LI, Walsh KL, Piskorska D, McGuire E, and Harn DA Jr. (2001). "The schistosome oligosaccharide lacto-N-neotetraose expands Gr1(+) cells that secrete anti-inflammatory cytokines and inhibit proliferation of naive CD4(+) cells: a potential mechanism for immune polarization in helminth infections." *J. Immunol.,* 167(9), 5294-303.

van Die I., and Cummings R.D. (2010). "Glycan gimmickry by parasitic helminths: A strategy for modulating the host immune response?" *Glycobiology,* 20(1), 2-12.

van Stijn CM, van den Broek M, Vervelde L, Alvarez RA, Cummings RD, Tefsen B, and van Die I. (2010). "Vaccination-induced IgG response to Galalpha1-3GalNAc glycan epitopes in lambs protected against *Haemonchus contortus* challenge infection." *Int.J.Parasitol.,* 40(2), 215-22.

Waddell, A. H. (1968). "The excretory system of the kidney worm *Stephanurus dentatus* (Nematoda)." *Parasitology,* 58(04).

Chapter 3 : Identification of Alpha-Gal-Modified Excreted/Secreted Proteins From Adult *Parelaphostrongylus tenuis*

3.1 Introduction

Helminth is a term that describes parasitic organisms that are either in the Phylum Nematoda or Platyhelminthes. Helminth parasites cause substantial socioeconomic costs due to their impact on the health of humans, companion animals and the health and production of domestic livestock species and agriculture crop species (van Stijn *et al.*, 2010; Hotez *et al.*, 2008). Efforts to control parasitic helminth infections in livestock have led to substantial expenditures (van Stijn *et al.*, 2010) and have resulted in an increase of anthelminthic-resistance in some parasites. The emergence of anthelmintic resistant parasites (Newton, 1999) carries as yet undefined socioeconomic costs for contemporary agriculture in our immediate future. Efforts to control parasitic helminth infections of humans living in non-developed countries are inadequate (Hotez, *et al.*, 2010). Furthermore, identification of candidate vaccine antigens with high efficacy has proven to be very difficult (Diemert *et al.*, 2012). Limited success has been observed using protein-based vaccines, and typically only when using native proteins. Recombinant versions of candidate vaccine-antigens tend not to confer protection (Hein and Harrison, 2005). The high immunogenicity of glycan moieties and their role in mediating parasitism at the host-parasite interface has led to a shift in focus to these molecules as targets for therapeutic intervention (Harn *et al.*, 2009).

Most pathogens are eliminated from an animal host following onset of acquired immunity. Quite unlike most infectious disease agents, a distinctive feature of helminth parasites is their persistence as chronic infections without elimination by host immune responses (van Die and Cummings, 2010). Concomitant immunity is a type of acquired immunity that describes persistence of chronic infection by adult helminth parasites, while retaining conspecific anti-larval capabilities (Smithers and Terry, 1969). One can envision the evolution of concomitant immunity to prevent parasite overcrowding to ensure host and parasite survival. One important example of concomitant immunity is that which takes place during schistosome infection. It had long been thought that larval stages were eradicated from the host during secondary infections due to activation of host memory cells specific to larval antigens. However, important foundation work showing that adult worms alone could induce anti-larval immunity was ignored for years. Interestingly, monkeys showed resistance to challenge infections by larval stages following transplant of adult schistosomes, although the immune system had never been exposed to larvae (Smithers and Terry, 1967). Immunity was clearly not attributed to larval-specific antigens. It remains unknown what mechanisms are employed by adult parasites to evade immune responses that are capable of killing alternate life-stages with conserved antigens.

While concomitant immunity still remains poorly understood, it is obvious that adult helminth parasites must employ stage-restricted molecules that both facilitate immune evasion and promote chronic infection. *Parelaphostrongylus tenuis* is a parasite that induces concomitant immunity and can survive in the central nervous system for the

entire life of its deer host (Duffy *et al.*, 2004). Interestingly, investigations of glycans from *P. tenuis* revealed that they produce a terminal disaccharide (Galα1-3Gal; alpha-Gal) that is restricted to the adult parasite life-stage, but also found commonly in their deer host (Duffy *et al.*, 2006). A role for parasite-derived alpha-Gal at the host-parasite interface has yet to be determined. However, it is known that parasites secrete host-like glycans that interact with innate immune cells to modulate immune responses and promote chronic infection (van Die and Cummings, 2010). As an example, Galβ1-3Gal is a terminal disaccharide of *Leishmania* parasites that promotes the binding of surface proteins on macrophages to mediate infection (Pelletier *et al.*, 2003). These findings suggest that parasite-derived alpha-Gal could be similarly poised to bind host cells and modulate immune responses.

Investigations of helminth-induced modulation of host immune responses have focused on the excretory/secretory (E/S) products to identify the secretome of parasites that infect animals and humans (Hewitson *et al.*, 2011). While cellular interactions that promote chronicity of parasite infection remain largely unclear, recent work has provided some insight on a role for eosinophils (Gebreselassie *et al.*, 2012). Transition from a T_H2 response to a modified T_H2 response is characteristic of helminth infection (Fallon and Mangan, 2007). This modified T_H2 response promotes parasite survival with reduced pathology to the host. E/S proteins with host-like terminal glycans such as alpha-Gal (Duffy *et al.*, 2006) are of special interest because glycans are found abundantly at the host-parasite interface and can modulate immune responses (van Die and Cummings, 2010). Identification of E/S products with an immunomodulatory role

provides insight into host-parasite co-evolution and they represent potential candidate vaccine antigens (Maizels *et al.*, 2012). Accordingly, this current study has focused on the identification of the specific E/S glycoproteins modified with alpha-Gal given their potential role in host immune modulation via promotion of a modified T_H2 environment. Peptides analyzed by LC-MS/MS were compared to conceptual protein translations of an adult *P. tenuis* transcriptome, which was enriched for transcripts from secretory glands.

3.2 Materials and Methods

The current study sequenced alpha-Gal-modified E/S proteins via nano LC-MS/MS. This approach identified multiple candidate *P. tenuis* transcripts encoding the sequenced peptides, as described below.

3.2.1 Generation of a Transcriptome From Secretory Glands of Adult *P. tenuis*

Given the end goal of specific identification of alpha-Gal-modified E/S proteins, and given the fact that the genome of *P. tenuis* has yet to be sequenced, we generated a *P. tenuis* transcriptome enriched for transcripts synthesized in secretory glands.

3.2.1.1 Purification of RNA Enriched for Transcripts From Secretory Glands

Intact adult *P. tenuis* were placed in 1X sterile PBS on ice and were cut immediately posterior to the excretory gland with a scalpel while viewed under a dissecting microscope. The anterior ends representing ~1% of total worm length were stored in PBS at -80°C and later disrupted with a Kontes Pellet Pestle Cordless Motor (Fisher Scientific). Anterior ends from 37 adult *P. tenuis* were used for purification of the secretory gland-enriched RNA. RNA was purified using the RNeasy Micro Kit (Qiagen, Toronto, Ontario, Canada) and was sent to the Genome Quebec Innovation Centre (Montreal, PQ, Canada) for cDNA synthesis.

3.2.1.2 cDNA Synthesis

Four μg of total RNA, with an RNA integrity number of 8.3/10, was used to generate the cDNA (TruSeq RNA Sample Kit Preparation Guide Version 1; Illumina, San Diego, California, USA). Fragmentation time was shortened to 7 minutes at 94°C to generate RNA fragments (~155 bases (120-225 bases). First strand cDNA was generated using reverse transcriptase and second strand cDNA was generated using DNA polymerase I and RNase H. RNA Adapter Index 1 was used to ligate adapters to cDNA fragments.

3.2.1.3 Sequencing

Illumina paired-end sequencing of the cDNA fragments was performed following the manufacturer's instructions. Briefly, the cDNA was diluted to a concentration of 9 pM and was loaded onto one lane of the flow cell of the Illumina GAIIx sequencer. Clonal clusters were amplified using a cBot (TruSeq PE Cluster kit v3-cBot-HS; Illumina, San Diego, California). Two reads of 100 bases and one 7-base index read were completed for 100 cycles, generating 228,924,109 reads using the TruSeq SBS Kit v3-HS (Illumina, San Diego, California). The image analysis and base calling were completed using HiSeq Control Software (v1.4.8; Illumina, San Diego, California) and the fastq files were created with CASAVA (v1.8.2; Illumina, San Diego, California).

3.2.1.4 Transcript *de novo* Assembly

Adapter fragments were removed and raw reads were trimmed if Phred quality scores

were below 20 (FASTX Toolkit). Subsequently, any trimmed reads that were less than 30 base pairs were removed. Raw reads were assembled *de novo* using Velvet (European Bioinformatics Institute; v1.2.01) followed by OASES (European Bioinformatics Institute; v0.2.04). Assembly parameters were set at a k-mer value of 57 bp and a read category of short paired.

3.2.2 Two-Dimensional Gel Electrophoresis and Western Blot

Isoelectric focusing, SDS-PAGE and excision of alpha-Gal-modified proteins were performed at the Cornell University Life Sciences Core Laboratories Center's Proteomics and Mass Spectrometry Facility.

3.2.2.1 Isoelectric Focusing

Excreted/secreted products from adult female *P. tenuis* were concentrated using a vacuum concentrator (Eppendorf Vacufuge Concentrator, Fisher Scientific, Ottawa, Ontario, Canada) and resuspended in 150 µl of lysis buffer (7M Urea, 2M Thiourea, 2% (w/v) CHAPS) to a final concentration of 6.5 µg/µl. First dimensional separation by isoelectric focusing was completed in a Multiphor II Electrophoresis System (GE Healthcare, Pittsburgh, PA, USA) by adding E/S proteins to a 13-cm non-linear, pH 3-10 Immobiline DryStrip gel IPG Strip (GE Healthcare, Pittsburgh, PA, USA). Running conditions were set at 20°C, with a maximum current of 2mA and maximum power of 5 W. Focusing times and voltage for each step was as follows: 300V for 1 minute;

linear ramp from 300-3500 V over 1.5 hours; constant 3500 V for 6 hours.

3.2.2.2 SDS-PAGE

IPG Strips were removed from the instrument and equilibrated for 15 minutes with SDS equilibration buffer with dithiothreitol (6M urea, 75mM Tris-HCl pH 8.8, 29% glycerol, 2% SDS, 0.002% bromophenol blue, 1% dithiothreitol). The buffer was removed and IPG Strips were equilibrated for 15 minutes with SDS equilibration buffer with iodoacetamide (6M urea, 75mM Tris-HCl pH 8.8, 29% glycerol, 2% SDS, 0.002% bromophenol blue, 2.5% iodoacetamide). The strips were applied to 12% tris-glycine homogenous gels and melted agarose was used to seal the strip in place on the gel. Gels were inserted into the SE 600 Ruby System (GE Healthcare, Pittsburgh, PA, USA), and 12 ul of PageRuler Plus Prestained Protein Ladder (10-250 kDa, Thermo Scientific, USA) was loaded. Electrophoresis was performed at a constant current of 15 mA/gel for 15 minutes, followed by an increase in current to 32 mA/gel for 5 hours. Electrophoresis was stopped once the dye front was approximately 1 mm from the bottom of the gels. One gel was removed, fixed with 40/10 methanol/acetic acid (v/v) in water for 1 hour, stained with Novex Colloidal Coomassie Blue (Invitrogen, Carlsbad, CA, USA) overnight, destained with 8% acetic acid for 5 minutes followed by water for 5 hours and was scanned with a Typhoon 9410 Laser Scanner (Amersham Biosciences). Proteins from the other gel were transferred to PVDF (BioRad Trans-Blot SD Semi-dry Transfer Cell) dried overnight, and shipped to the University of New Brunswick.

3.2.2.3 Two Dimensional Western Blot and Selection of Alpha-Gal-Modified Proteins

The PVDF membrane was stained with Ponceau S (0.2% Ponceau S, 3% trichloro acetic acid, 3% sulfosalicylic acid) to detect protein transfer. The membrane was then washed in tris-buffered saline (TBS; 0.05 M Tris Base, 0.13 M NaCl, pH 7.6) to remove excess Ponceau S and was left to dry overnight. The membrane was placed in 100% methanol for 1 minute before being placed in TBS for 1 hour for rehydration. The membrane was blocked in a 5% bovine serum albumin (BSA; Sigma-Aldrich, Oakville, Ontario, Canada) in TBS for 1 hour, followed by 3X 15-minute washes with TBS. The membrane was then probed with a 1:5 dilution of anti-alpha-Gal antibody (M86; Cedarlane Laboratories, Burlington, ON) in 5% BSA in TBS at 4°C overnight. The membrane was placed on an ADAMS Nutator (ClayAdams, Parsippany, New Jersey, USA) for 1 hour at room temperature before it was washed 3x 15 minutes with 0.05% Tween® 20 in TBS. The PVDF membrane was then incubated in a solution containing 5% skim milk (Nestle, North York, Ontario, Canada), 5% normal goat serum (NGS) (Cedarlane Laboratories, Burlington, Ontario, Canada), and a 1:1000 dilution of horseradish peroxidase (HRP)-conjugated goat anti-mouse IgM antibody (Cedarlane Laboratories, Burlington, ON) dilution in TBS. After one hour, the wash protocol described above was repeated. Pierce ECL substrate (Fisher Scientific, Ottawa, ONT) was placed on the membrane in a dark room and film was exposed (Thermo Scientific CL-XPosure Film; Fisher Scientific, Ottawa, Ontario, Canada). Autoradiographs were developed according to manufacturer's recommendations. Spots that were

immunoreactive in autoradiographs were aligned with protein spots in the corresponding Coomassie-stained 2D gel and were excised for nano LC-MS/MS.

3.2.3 Peptide Identification

The nano LC-MS/MS and MS/MS data analysis were performed at the Cornell University Life Sciences Core Laboratories Center's Proteomics and Mass Spectrometry Facility.

3.2.3.1 Nano LC-MS/MS

Protein spots from SDS-PAGE were subjected to in-gel trypsin digestion and subsequent extraction (Rosenfeld J et al. 1992). The tryptic digest was reconstituted in 10 µL of 2% acetonitrile (ACN) with 0.5% formic acid (FA) for nano LC-ESI-MS/MS analysis using a LTQ-Orbitrap Velos mass spectrometer (Thermo-Fisher Scientific, San Jose, CA) equipped with a "CorConneX" nano ion source device (CorSolutions LLC, Ithaca, NY). The Orbitrap Velos is interfaced with an UltiMate3000 RSLCnano system (Thermo-Dionex, Sunnyvale, CA). The gel-extracted peptides (5-10 µL) were injected onto a PepMap C18 trap column (5 µm, 300 µm × 5 mm, Dionex) at 20 µL/minute flow rate for on-line desalting. Peptides were separated on a PepMap C18 RP nano column (3 µm, 75 µm x 15 cm, Dionex) installed in the CorConneX device with a 10-µm spray emitter (New Objective, Woburn, MA) mounted in front of Orbitrap orifice. Peptides were eluted in a 60 min gradient of 5% to 40% ACN in 0.1% formic acid at 300

nL/minute, followed by 3-minute ramping to 95% ACN-0.1% FA and a 5-minute holding at 95% ACN-0.1%FA. The column was re-equilibrated with 2% ACN-0.1% FA for 20 minutes prior to the next run. The Orbitrap Velos is operated in positive ion mode with nano spray voltage set at 1.5 kV and source temperature at 275°C. Either internal calibration using the background ion signal at m/z 445.120025 as a lock mass or external calibration for FT mass analyzer is performed. The instrument is operated in parallel data-dependent acquisition (DDA) mode using FT mass analyzer for one survey MS scan for precursor ions followed by MS/MS scans of the 7 most intense peaks with multiple charged ions above a threshold ion count of 10000 in the LTQ mass analyzer. MS survey scans at a resolution of 60,000 (fwhm at m/z 400), for the mass range of m/z 375-1400. Dynamic exclusion parameters were set at repeat count 1 with a 25 second repeat duration, exclusion list size of 500, 45 second exclusion duration, and ±10 ppm exclusion mass width. Collision induced dissociation (CID) parameters were set at the following values: isolation width 2.0 m/z, normalized collision energy 35%, activation Q at 0.25, and activation time 10 ms. All data are acquired under Xcalibur 2.1 operation software (Thermo-Fisher Scientific, San Jose, CA).

3.2.3.2 Data Analysis

All MS and MS/MS raw spectra were processed using Proteome Discoverer 1.2 (PD1.2, Thermo) and the spectra from each DDA file were output as an MGF file for subsequent database search using in-house license Mascot Deamon (version 2.3.02, Matrix Science, Boston, MA). Conceptual protein translations of the *P. tenuis* transcriptome sequences

(182,400 sequences) were used for comparison to identified peptides (nano LC-MS/MS) with one missed cleavage site by trypsin allowed per peptide. The peptide tolerance was set to 10 ppm and MS/MS tolerance was set to 0.8 Da. A fixed carbamidomethyl modification of cysteine, variable modifications on methionine oxidation and deamination of asparagine and glutamine were set. All matches were above a 99.9% confidence interval (CI) with significant scores defined by MASCOT probability analysis (www.matrixscience.com/help/scoring_help.htm#PBM) for protein identifications.

3.2.4 Identifying *P. tenuis* Proteins Corresponding to Sequenced Peptides

To assess whether the peptides identified by LC-MS/MS could have originated from contaminating proteins from the deer host, each peptide was first compared to the NCBI non-redundant protein database (NCBI, Bethesda, Maryland, USA) using BLASTp. All peptides had highest identity with known nematode proteins, indicating that contamination of *P. tenuis* E/S proteins by deer host products was unlikely.
The LC-MS/MS data analysis described above (section 3.1.3.2) identified 16 transcripts from the *P. tenuis* transcriptome that encoded one or more of the LC-MS/MS peptides. However, closer examination of these transcripts revealed that they contained numerous frameshifts, and so did not contain continuous open reading frames encoding full-length proteins.

To generate *P.tenuis* transcripts encoding continuous open reading frames,

transcriptome assembly was performed a second time using the previously generated Illumina data. To avoid the incorrect assembly of transcripts observed in the first assembly, the re-assembly was performed using Trinity software (release 2012-10-05; Grabherr et al., 2011) by Dr. Chris Jackson of the University of New Brunswick. Trinity has been reported to assemble transcripts more accurately than alternative assembly software, such as Velvet/Oases.

Prior to transcriptome assembly using Trinity the raw (untrimmed) paired-end Illumina data was first trimmed according to specified sequence quality parameters, using the program Trimmomatic in paired end more (version 0.22; Lohse *et al.*, 2012). For each 100 nucleotide Illumina read, Trimmomatic removed nucleotides from either read end if their Phred quality score was below 3. Subsequently, each read was scanned using a sliding window of four nucleotides, and reads were trimmed if the average Phred quality score within the sliding window fell below 30. Following trimming, reads less than 36 nucleotides long were discarded. The final Trimmomatic output produced two fields containing matching forwards and reverse paired-end reads, and a third file containing orphan reads (reads for which the corresponding paired-end read was discarded during the trimming process). Quality-trimmed Illumina data were assembled using Trinity (release 2012-10-05; Grabherr et al., 2011), and a file of putative *P. tenuis* transcripts in FASTA format was generated.

To identify Trinity transcripts that corresponded to the initially identified Velvet/Oases assembled transcripts (putatively encoding the peptides identified by MS), the

Velvet/Oases transcripts were used as queries against a BLAST database of Trinity transcripts, using tBLASTX. For each Velvet/Oases-assembled transcript, this approach identified at least one highly similar transcript from the Trinity-assembled transcripts, and conceptual protein translations of these latter transcripts also contained the peptides identified by LC-MS/MS, with 100% identity. In comparison to the Velvet/Oases assembled transcripts, the corresponding Trinity assembled transcripts did not contain frameshifts, and the majority contained full open reading frames encoding a full-length protein (as predicted by alignment with homologues from other nematodes).

Finally, conceptual protein translations of the identified Trinity transcripts were then searched for N-glycosylation sites (NetNGlyc 1.0 Server), signal peptide cleavage sites (SignalP 4.0 Server) and were assessed for non-classical protein secretion (SecretomeP 2.0 Server).

3.3 Results

3.3.1 Transcriptome Assembly

A transcriptome enriched for secretory glands of adult *P. tenuis* was produced using Illimina sequencing. The 228,924,109 transcriptome reads generated 239,847 transcripts following *de novo* assembly using Velvet (v1.2.01) and OASES (v0.2.04). Conceptual transcripts had a mean sequence length of 858 bp (± 1204; 100-28491). Frame shifts in many assembled sequences resulted in reassembly using Trinity software (SourceForge; version: r2012-10-05). Conceptual transcripts had a mean sequence length of 1081 bp (± 1382; 201-21,906). Substantially larger conceptual transcripts with fewer frameshifts led to longer open reading frames and greater reliability. The Trinity-derived assembly was used for all subsequent analyses.

3.3.2 Selection of Alpha-Gal-Modified Excreted/Secreted Proteins for MS/MS Peptide Identification

Alpha-Gal-modified E/S proteins were selected for MS/MS peptide identification to help infer function of this glycan during parasitism. 2,679 μg of excreted/secreted (E/S) proteins were collected from 58 adult female *P. tenuis* maintained *in vitro*. Two-dimensional Polyacrylamide Gel Electrophoresis (2D-PAGE) separation revealed a diverse array of E/S proteins (Figure 3.1). Alpha-Gal-modified proteins were detected using a monoclonal anti-alpha-Gal antibody in an immunoblot of a 2D gel. These proteins had apparent molecular masses of 40-50 kDa (Figure 3.2). Five alpha-Gal

modified proteins were chosen for tandem mass spectrometry (MS/MS) analysis (Figure 3.3). One spot that did not contain alpha-Gal-modified proteins was selected as a negative control for MS/MS peptide analysis (Figure 3.3).

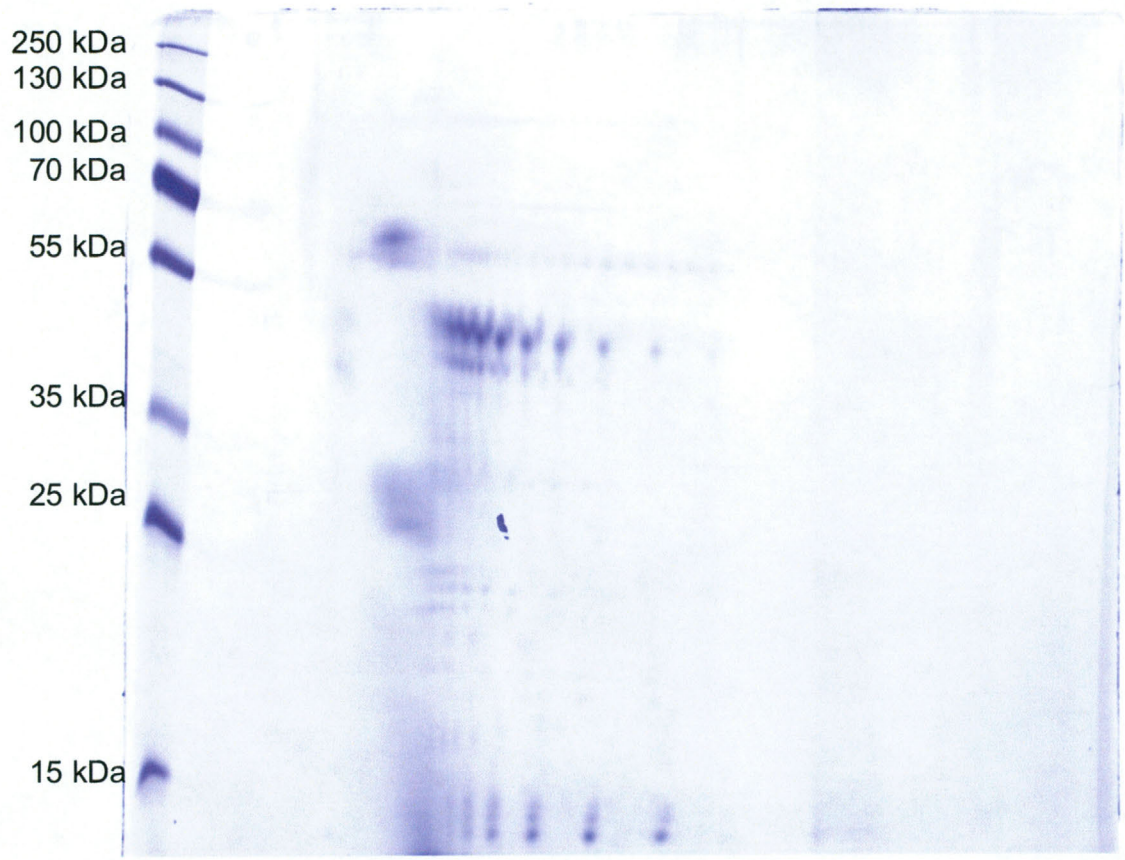


Figure 3.1 The Two-Dimensional Polyacrylamide Gel profile of E/S proteins from adult female *P. tenuis*. Proteins were separated on a 12% homogenous tris-glycine gel with an IPG strip with a pH range of 3-10NL. The gel was stained with Coomassie Brilliant Blue.

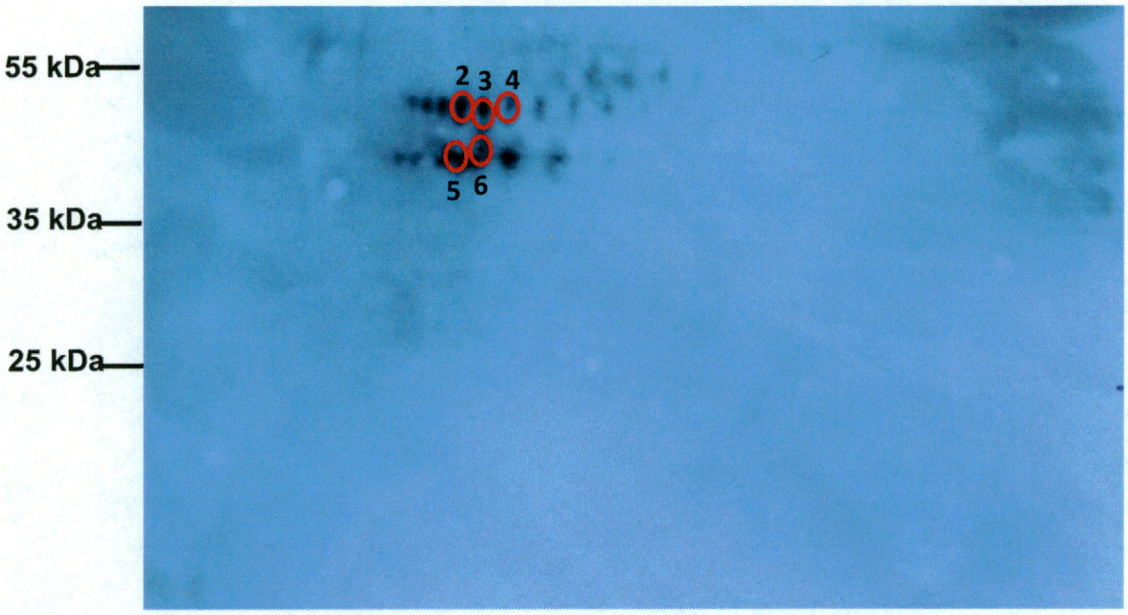


Figure 3.2 Immunoblot detection of alpha-Gal on 40-50 kDa E/S proteins from adult female *P. tenuis* in a 2D SDS-PAGE blot. Spots 2-6 correspond with those in Figure 3.3 selected for MS/MS sequencing.

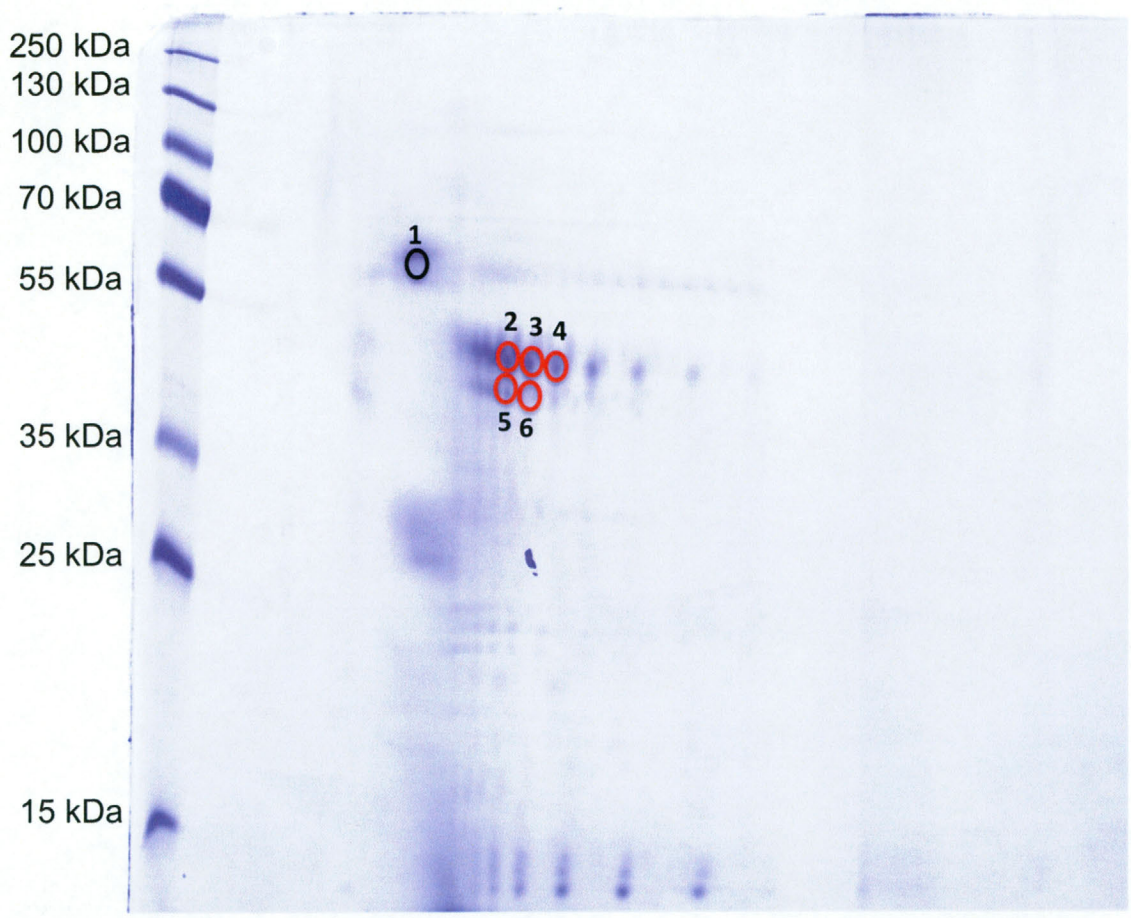


Figure 3.3 Adult female *P. tenuis* E/S proteins were selected for MS/MS sequencing. Spots 2-6 were alpha-Gal-modified, whereas spot 1 was selected as a negative control (See Figure 3.2).

3.3.3 nano LC-MS/MS

Peptide analysis of the six excised spots was completed using nano LC-MS/MS. The MS total ion current (TIC) chromatograms are found in Appendix 1. The MS/MS ion search data was used to search the custom *P. tenuis* transcriptome database using BLAST. All peptides had 100% amino acid identity to coverage against *P.tenuis* open reading frames generated from the conceptually-derived transcriptome database from

adult *P. tenuis*. In all, 17 proteins (including 4 pairs of paralogues) were identified from the selected spots. Figures 3.4-3.20 indicate amino acid composition of the 16 proteins that were represented in alpha-Gal-modified spots. The 17 *P. tenuis* proteins containing identified peptides from MS/MS analysis had homology with known nematode proteins in the public database (Table 3.1). Predicted signal peptide cleavage sites, prediction of non-classical protein secretion, and predicted N-glycosylation sites are also indicated. Table 3.2 summarizes these findings, in addition to other protein characteristics (predicted molecular weight, spot localization), and the fact that some peptides were found in multiple spots. Alignments of *P. tenuis* proteins with sequences of highest similarity in the public database are found in Appendix 2.

MPITKIHARQIYDSRGNPTVEVDLYTDKGVFRAAVPSGASTGVHEALELRDKDKAVHHGKGVLKA
VANINDKIAPALIAKNFCVTQQRDIDQFMLALDGTENKSNLGANAILGVSLAVAKAGAVHKGMPL
YKYIAELAGVSKVILPVPAFNVINGGSHAGNKLAMQEFMILPIGASSFSEAMRMGSEVYHHLKSE
IKKRYGLDATAVGDEGGFAPNIQDNKEGLDLLKTAIQLAGYTGKISIGMDVAASEFFKEGKYDLD
FKNPNSDPSKWLTGEKLAELYQTFIKEYPVVSIEDAFDQDDWDNWGKFKAATNIQLVGDDLTVTN
PKRIRQAIEKKSCNCLLLKVNQIGTVTESIEAAKLSRSNGWGVMVSHRSGETEDTFIADLVVGLA
TGQIKTGAPCRSERLAKYNQLLRIEEELGKDAIYAGADFRNPKV

Figure 3.4 Pt-ENO-1. *P. tenuis* Enolase from the TIM phosphate binding superfamily. Blue amino acids are from peptides found exclusively in spot 2; red amino acids are from peptides found in spot 2 and 3; and green amino acids are from peptides found in spots 2, 3 and 4. A predicted N-glycosylation site is located on the asparagine in the box (amino acid 102). No signal peptide cleavage site was predicted.

MTKTTDPANEQLEQYKKATPRTTVLTTSTGAPISNKTNVLTVGPRGPMLMQDVVYMDEMAHFDRE
RIPERVVHAKGAGAHGYFEVTHNITKYCRAEIFSSIGKQTPCFVRFSTVGGESGSADTVRDPRGF
AIKFYTEEGNWDLVGNNTPIFFIRDPIQFPNFIHTQKRNPQTHLKDANMMWDFWGLRPESTHQVM
FLMSDRGTPDGYRFMNGYGSHTFKLVNSDGKAVYCKFHLKPKEVRNLTAAEAGRLAGEDPDYAIR
DLYNAIERGDYPQWTFFIQVMTFEQAERWPMNPFDVTKVWPHGEFPLIPVGKLILNKNPKNYFAE
VEQSAFCPAHVVPGIEFSPDKMLQGRLFSYTDTHFYRLGTNYNQLPINCPYRARAHNTQRDGTAT
FDNQGNAPNYFPNSFNGGMECPRAVESRWSAAGDVERHESINDDNFDQPREFWTKVLNNAERERL
VENIFHTMKDCLPHIQDRAIDNFRKVHSDFGGRLRQMVDAYNAQKGCRPRI

Figure 3.5 Pt-CTL-2. *P. tenuis* Catalase from the catalase-like superfamily. Brown amino acids are from peptides found only in spot 4; red amino acids are from a peptide found only in spot 6; black amino acids are from peptides found in both spots 3 and 4; blue amino acids are from peptides found in spots 2, 3 and 4; green amino acids are from peptides found in spots 2, 3, 4 and 5; orange amino acids are from peptides found in spots 2, 3, 4 and 6; and blue amino acids are from peptides found in spots 2, 3, 4, 5 and 6. A predicted N-glycosylation site is located on three asparagines in the boxes (amino acids 35, 88, 241). No signal peptide cleavage site was predicted.

MALEELRLGGNADKRKHGGIDGKRSKAYTDIEEKENMEVNNEVLELSSNPKANGDVVAVCSSDLE
EPFLVENPNRFVIFPLNHHDIWDFYKRAVASFWTVEEVDLAKDMSDWEKMNDNERFFISRVLAFF
AASDGIVNENLVERFSKEVQVPEARFFYGFQIAVENIHSEMYSKLIETYIRDESERHILFNAIFE
FPCIAKKAQWALEWIADHKAPFAERLIAFAAVEGIFFSGSFAAIFWLKKRGLMPGLTHSNELISR
DEGLHRDFACLMYSHIVNKLPQERIHRIIKDAVVIEQEFLTESLPVDMIGMNCRLMSQYIEFVAD
LLLIELGCEKLYDVKNPFDFMENISIDGKTNFFEKKVSEYQRTGVMAAEDDRQFQLNADF

Figure 3.6 Pt-RNR-2. *P. tenuis* Ribonucleotide Reductase from the ferritin-like superfamily. Red amino acids are from peptides found in spot 6. A predicted N-glycosylation site is located on the asparagine (amino acid 348) in the box. No signal peptide cleavage site was predicted.

MCDDEVAALVVDNGSGMCKAGFAGDDAPRAVFPSIVGRPRHQGVMVGMGQKDSYVGDEAQSKRGI
LTLKYPIEHGIVTNWDDMEKIWHHTFYNELRVAPEEHPVLLTEAPLNPKANREKMTQIMFETFNT
PAMYVAIQAVLSLYASGRTTGVVLDSGDGVTHTVPIYEGYALPHAILRLDLAGRDLTDYLMKILT
ERGYSFTTTAERGIVRDIKEKLCYVALDFEQEMATAASSSSLEKSYELPDGQVITVGNERFRCPE
AMFQPSFLGMESAGIHETSYNSIMKCDIDIRKDLYANTVLSGGTTMYPGIADRMQKEITALAPST
MKIKIIAPPERKYSVWIGGSILASLSTFQQMWISKQEYDESGPSIVHRKCF

Figure 3.7 Pt-Act-3. *P. tenuis* Actin from the NBD sugar-kinase HSP70 actin superfamily. Green amino acids are from a peptide found only in spot 2; red amino acids are from a peptide found only in spot 3; orange amino acids are from a peptide found in both spot 2 and 3; and, blue amino acids are from peptides found in spots 2, 3 and 4. A predicted N-glycosylation site is located on the asparagine in the box (amino acid 13). No signal peptide cleavage site was predicted.

MSGKKRRNIEPTAEDLSAVEFESSEEVEVIPTFDSMGLREPLLRGIYSYGFEKPSAIQQRAIKPI
LKGRDVIAQAQSGTGKTATFSISVLQSIDMDLRECQALILSPTRELAVQIQKVVLALGDYMNVQC
HACIGGTNIGEDIRKLDYGQHVVSGTPGRVFDMIRRRNLRTRSIKLLVLDEADEMLNKGFKEQLY
DIYRYLPPGAQVVLLSATLPHEILEMTSKFMTDPIRILVKRDELTLEGIKQFFVAVDCEEWKFDT
LVDLYDTLTITQAVLFCNTRRKVDWLAEKMKEANFTVSSMHGDMEQKEREQIMKDFRAGNSRVLI
STDVWARGLDVPQVSLVINYDLPNNRELYIHRIGRSGRFGRKGVAINFVKHDDVRILRDIEQYYS
TQIDEMPMNIADMI

Figure 3.8 Pt-EIF-4A-III. *P. tenuis* Eukaryotic Initiation Factor from the P-loop NTPase superfamily. Red amino acids are from a peptide found in spots 5 and 6. A predicted N-glycosylation site is located on the asparagine in the box (amino acid 294). No signal peptide cleavage site was predicted.

MTDANTRNKYVNNGGSAGSVAVDADGLIEGNYDQVVPSFDEMNLKENLLRGIYAFGFEKPSAIQQ
RAIVPCCTQRDVIAQAQSGTGKTATFSISILQRIDENNSCVQALVMAPTRELAQQIQKVMSALGD
YMKVKVHACIGGTSIRDDQRKLESGVHVVVGTPGRVNDMINREILQTDSIKMFVLDEADEMLSRG
FKDQIYEVFKRMPQDVQVVLLSATMPADVLDVTQCFMRDPIRILVKKEELTLEGIRQFYVNVQKD
EYKFDTLCDLYNVINITQSVIFCNTRRRVEQLSDQMTAQKFTVSCLHGDMEQMERNVIMREFRSG
SSRVLITTDLLARGIDVQQVSLVINYDLPSNRENYIHRIGRSGRFGRKGVAINFITENDVRQLKD
IEAFYNTVIEEMPMSIADLL

Figure 3.9 Pt-EIF-4A. *P. tenuis* Eukaryotic Initiation Factor from the P-loop NTPase superfamily. Red amino acids are from a peptide found in spots 5 and 6. Predicted N-glycosylation sites are located on the asparagines in the boxes (amino acids 102, 175). No signal peptide cleavage site was predicted.

MRFLLILVGVCFAVHQSVD|LLPLKPHNEHVFRFEGNVHFGIPVSSENSVTRIRAMAHVQTLDDRT
TILKLKDVRIATDENERSDNKKSIDDLKARTISSKHLEILEMPVEFVYKNGMVDDLHFAEKEQAW
SANIKRSVLNMLHINLQKVGRIDETSMDGALVSRENDFFTVNERTIEGDCEVAYMILKRKDDTTE
ITKSVDFEKCSRRPEAKYNFRHRSECRDCKMADNFEPSTVYNYVIEKDGLKKVEVVSFYTVTFER
QPKMKSEVRATLVLEDVRKIKEKFESVKGKIESLIYSNEMEKDIERFYMHGDDTEVLPFEHIKEK
INAAHRNIEEIREQKENNYENTLLMHRLVSILRMCSLHELGVVHSEVYTKGDERLMAIMEHALAI
AGTKNTITHLLRHVEKENVKTHRIVSLLKSIQEMPYPSSKIVEELLRFSDTEIVKRSPVVHQTTW
LAIGSVMHGVVGETMDERLIKENHRGLKQKYLNVLLKQFEKADKIYEKVLALKSLANAGIDLSVY
ELEKIILNKHEELPIRMEAIDALRLLKDSMPRKVRSILMPVYKNRLHHPELRMAALVRIMHTLPQ
QSVVAQIISTMERDSNQQVAAFTYDLLKSFVGSTHTCYKKLANDIRPLLSITRNQRNTRTLTSTY
KFMPLFRENLLSGVNFELGTMFGKSSVWPKEIMMSLDSVFSGMWNKNLFQLGLSQQNIEKIIEKL
INKLMKLEQNSQSVVRGRRIKESLTLLKDIAKKLDIRPRINDDKTPYAMLYLRYKEMDYAVLPID
EKIIDDLLEKYIDNGRIERRELDRLFNRDPEFQLHSMTFLHETIRHLPSTLGLCLTLKDVQPFIA
HAEGEFTIETISSGLRIRLNTSPTLASTQLSQMRLWNPLFEHGVKTERFVEARLPINFDAEVLYK
NQIELKYTINVPSEEKTLLRVWSHPVTFFRMMCGPKYFSGLEQKSVVIPKWRSAAKEYEKTINIW
GIKAVLRGNMVSNWDRRDIPVGYYDWEIVMRPSQDIPRKLRFHLTTDRCEKVRLDSIDSTHLLDQ
KFDIEPTKYEKFEERKRRDHLNKFTRDIERSEGYKHHLNLR**VEAVESNVER**YGNAKVVTVCEKGL
RFCKMTVEGSFSPSEGQRRDWKIFTTMQLLLPKMAKSLMELKNQAHREIQGSVHSKWGADEVNEL
NVKFQIEQSKEQKEWTRLADKEYKGLASYDLLRQSSLLNQIKIVADYDLTPFTKNLVHRVYDYIK
LYTFWQSKFTPNNGEQGKLFLKMSVDPISRSLLNVHLETPQERVEVKNFVIPQLYLPSIARRSLR
EIRDELVKEQVCEVRSTKVRTFDDLVFRAPITNCYSVIAKDCSEEPRFAVLLKKIEKNAEEKELK
IINERQEVIKVRMDDNRLRIFVDDQEIGRDRVQDYDIEKIEDNMVRVKLEDLEVRFDGYDTKVYM
GKHISQRQCGLCGHFDEDKDNEFHTSKNEYTDDVEEFHKSYLLTDECEVEKEFSFDKKDYAVEMD
EERRDDWTNAYDDENTSDDWKDSKEDVLKTTHIMEFPHRVCFSLEPVRKCRKNEKKEDVVEKKVR
FTCLPRSSYETRQFLHKARTSVLDLSDYPVSFVENIQVPTACAVY

Figure 3.10 Pt-VIT-2. *P. tenuis* vitellogenin from the domain of unknown function superfamily. Red amino acids are from a peptide found in spots 2 and 3. No N-glycosylation sites were predicted. A vertical line between amino acids 19 and 20 indicates the predicted signal peptide cleavage site.

MAEVGGSYK**DSLSQALKDELREIAEKIVADGKGILAADESTGTIGK**RLDSISLENNENNRRKYRQ
LLFTTPHLSHISGVILYEETYNQSTDSGEKFVDLLNK**QGIVPGIK**LDLGVVPLAGTIGEGTTQGL
DNLAQRAAAFKKGGCGFAWRCVLTIGPH**TPSHLGMLENANVLARYATICQSVGLVPIVEPEVLCD**
GDHDLDRAQK**VTEQVLAFVYK**ALADHHVYLEGTLLKPNMVTPGQSCSKKASHEEIGLATVTALRR
GVPAAVPGITFLSGGQSELDATANLHAINMVK**LLKPWKLTFSYGRALQASVLKAWQGKDENVEAA**
QKVLLHRAKANGMAALGKYEGEDAAGAAAESLFIEKHAY

Figure 3.11 Pt-ALDO-2. *P. tenuis* Fructose-1, 6-bisphosphate Aldolase from the TIM phosphate-binding superfamily. Green amino acids are from a peptide found in spot 5; blue amino acids are those from peptides in spots 5 and 6; and red amino acids are those from a peptide identified in spots 2, 3, 4, 5 and 6. No N-glycosylation sites were predicted. No signal peptide cleavage site was predicted.

MKVLLLFAIAYAFA|DDSKDRSSEESKEKNYRKYIGERDYKLPFKTRVSEAFVVGQTIHAV
GTLSENPTRIDFNFHKGAAKDADLPLHFSIRFDEGIFSGKVVYNTFKDGNWSDNEQRISN
PFKAGKEFDLRVRILENKFQVFANRIEVGVFEQRQPLDGIDHVSIRGDLVKLRLFHYGGR
IFPNPYMAVAELKPGKRLDISALPTGKRVNVNLYRENKEYALQVSIRFNEGAIVRNAMNN
NVWGKEEREGDMPISKGEVFDLTIINEEFSFQIFFNGKRFAAFSHRGSPTDIKTLEIDGD
VEIHTVTINDAPGL

Figure 3.12 Pt-Galectin-5. *P. tenuis* Galectin from the GLECT superfamily. Red amino acids are those from peptides in spots 5 and 6 and blue amino acids are those from a peptide identified only in spot 5. A predicted N-glycosylation site is located on the asparagine in the box (amino acid 110). A vertical line between amino acids 14 and 15 indicates the predicted signal peptide cleavage site.

MVHYKLLYFDGRGRAECARQLFALADQQYEDVRMSKEQFASIKPKLPFGQMPVLEVDGRQ
LAQSQAINRYLAKTFGFAGKDPFEEAVIDSLVDQYTDYRNDIKPFFYVALGFAPGDLDKL
KKETFMPAREKFLGFLTKFLKKNASSGFLVGSSLTWVDVLIADHVSDFSKRVPEFFDGFP
EVKAHMEKVRSNPKLKNWIDKRPETSF

Figure 3.13 Pt-cGST-1. *P. tenuis* Glutathione-S-transferase from the Thioredoxin-like superfamily and the GST-C family superfamily. Red amino acids are those from a peptide found in spots 2, 5 and 6. No N-glycosylation sites were predicted. No signal peptide cleavage site was predicted.

MVHYKLTYFDGRGLAECARQLFALADQQYEDVRLTKEQFAPIKDKMPFGQMPVLEVDGKQ
LAQSQAINRYLAKTFGFAGKDAFESAVIDSLADQYMDYRAEIKPYFYALLGFMPGDVDKL
KKETMMPAREKFLGIVTKFLKNAASTGYLVGNSLTWVDVLIAEHVSDISKKVPDYLDGYP
EVKAHMEKVHSNPKIKKWIDSRPQTAF

Figure 3.14 Pt-GST-2. *P. tenuis* Glutathione-S-transferase from the Thioredoxin-like superfamily and the GST-C family superfamily. Red amino acids are those from a peptide found in spots 2, 5 and 6. No N-glycosylation sites were predicted. No signal peptide cleavage site was predicted.

MSNNGETNSQLGGTVVAFDYIKFIVGNAKQAAFWYCVNFGFEPFAYRGLETGSRIVAQHA
VKQNKIVFIFESALLPGNKELGDHLVRHGDGVKDVCFEVDDVVSILEHAKKAGAVVVKDV
TEESDEHGSIKYATVRTYGDTVHTLLEKKNYHGFFLPGFKPHPQSKSLFQSLPKAGLNLI
DHCVGNQPDLQMTPAVEWYEKVLGFHRFWSVDDSVIHTEYSALRSIVVTNKSETIKMPVN
EPAMGRKAVSQIQEFVDYYGGAGVQHIALNTNNIISAIEALRARGVEFLTIPDSYYDNLR
ARLKQSATKVKEDMNHLQKLRILVDFDENGYLLQIFSKPCTDRPTLFIEIIQRHNHQGFG
AGNFKALFESLELEQNQRGNLFYKDVVEGGRKLQL

Figure 3.15 Pt-HPD-1. *P. tenuis* 4-hydroxyphenylpyruvate dioxygenase from the Glo EDI_BRP-like superfamily. Red amino acids are those from peptides found in both spots 5 and 6. The black underlined amino acids represent a peptide from spots 5 and 6 that differs only at the first amino acid (a leucine was identified by mass spectrometry instead of the isoleucine shown here). A predicted N-glycosylation site is located on the asparagine in the box (amino acid 230). No signal peptide cleavage site was predicted.

MSNNGETNSQLGGTVVAFDYIKFIVGNAKQAAFWYCVNFGFEPFAYRGLETGSRIVAQHA
VKQNKIVFIFESALLPGNKELGDHLVRHGDGVKDVCFEVDDVVSILEHAKKAGAVVVKDV
TEESDEHGSIKYATVRTYGDTVHTLLEKKNYHGFFLPGFKPHPQSKSLFQSLPKAGLNLI
DHCVGNQPDLQMTPAVEWYEKVLGFHRFWSVDDSVIHTEYSALRSIVVTNKSETIKMPVN
EPAMGRKAVSQIQEFVDYYGGAGVQHIALNTNNIISAIEALRARGVEFLTIPDSYYDNLR
ARLKQSATKVGYITLSA

Figure 3.16 Pt-HPD-1a. *P. tenuis* 4-hydroxyphenylpyruvate dioxygenase from the Glo EDI_BRP-like superfamily. Red amino acids are those from peptides found in spots 5 and 6. The black underlined amino acids represent a peptide from spots 5 and 6 that differs only at the first amino acid (a leucine was identified by mass spectrometry instead of the isoleucine shown here). A predicted N-glycosylation site is located on the asparagine in the box (amino acid 230). No signal peptide cleavage site was predicted.

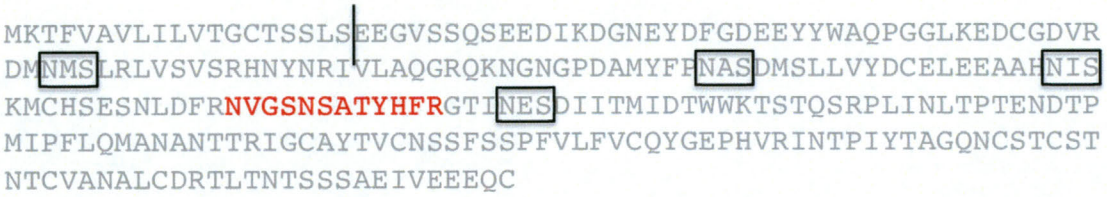


Figure 3.17 Pt-ASP-16a. *P. tenuis* Venom Allergen/Ancylostoma Secreted Protein from the SCP superfamily. Red amino acids are those from a peptide found in spots 2, 5 and 6. Predicted N-glycosylation sites are located on the asparagines in the boxes (amino acids 63, 99, 118, 148). A vertical line between amino acids 19 and 20 indicates the predicted signal peptide cleavage site.

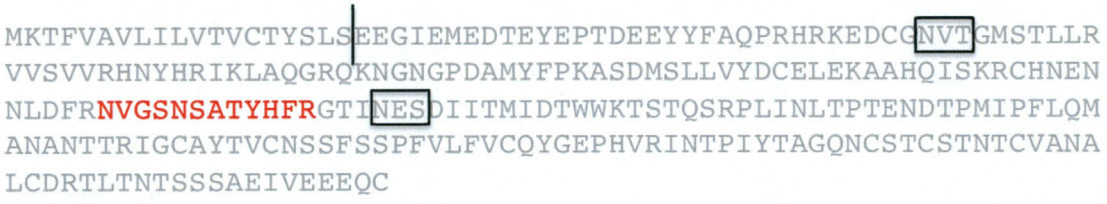


Figure 3.18 Pt-ASP-16b. *P. tenuis* Venom Allergen/Ancylostoma Secreted Protein from the SCP superfamily. Red amino acids are those from a peptide found in spots 2, 5 and 6. Predicted N-glycosylation sites are located on the asparagines in the boxes (amino acids 51, 141). A vertical line between amino acids 19 and 20 indicates the predicted signal peptide cleavage site.

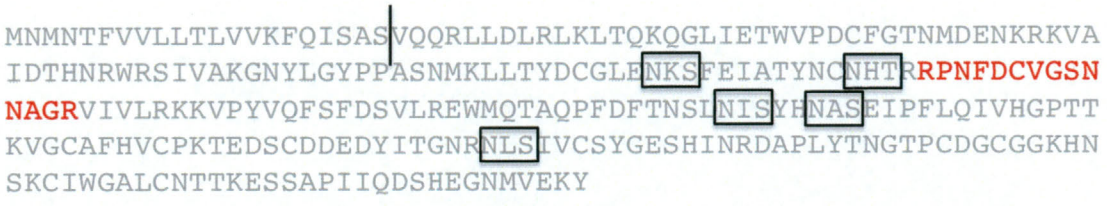


Figure 3.19 Pt-ASP. *P. tenuis* Ancylostoma Secreted Protein from the SCP superfamily. Red amino acids are those from a peptide found in spot 2. Predicted N-glycosylation sites are located on the asparagines in the boxes (amino acids 96, 107, 160, 165, 207). A vertical line between amino acids 19 and 20 indicates the predicted signal peptide cleavage site.

MVQLFLLITTYVFVVLDA|SMCPDRDNTDEMRELYLKYHNDARSRLAKGKERDLNRQLGPAK
NIYKLSWSCELEKIAKELAQGCGYDFTRYRSYGQNRETFFGSYGVSTFDVKKHIKQALDKW
WGKVKNSYVNQDNKYDPSLFEFSNMAHYKNTELGCAHVICPDHSFSKLQVLCVYKRLGYMG
GSIMWRNGKYCRVGSDCTIFPNSRCENGLCVRPKEQPDSGASQICGSNGVMTDAVRNAFLD
MHNFYRSVVATGRAVDKIDRQAPKAAAMPKLKYSCELEQSATNHAGFCQFSHSQGNNVGEN
LYTVYTPGFDKRVIAEMATEGWFEELEDYGVGRANILTQQLFNRPGQIGHYTQLVWQGTRY
VGCGIRDCHSSTLVVCQYKNAGNRFGNKIYEIGQPCSKCAADEQCTPTEGLCIGRA

Figure 3.20 Pt-ASP_ANCCA. *P. tenuis* Ancylostoma Secreted Protein from the SCP superfamily. Green amino acids are from a peptide found in spot 4; blue amino acids are those from peptides found in Spots 2 and 4; and red amino acids are from peptides found in Spot 2, 3 and 4. No N-glycosylation sites were predicted. A vertical line between amino acids 18 and 19 indicates the predicted signal peptide cleavage site.

Table 3.1 Adult *P. tenuis* Excreted/Secreted Proteins Identified from Tandem Mass Spectrometry Analysis

	Protein of Highest Identity by BLAST analysis			
***P. tenuis* Protein Name**	Homologue Identity	Species	Accession #	E-Value
Pt-ENO-1	Enolase	*Haemonchus contortus*	ADK47524.1	0.0
Pt-CTL-2	Catalase	*Haemonchus contortus*	AAT28330.1	0.0
Pt-RNR-2	Ribonucleotide reductase	*Caenorhabditis brenneri*	EGT45534.1	0.0
Pt-Act-3	Actin	*Caenorhabditis elegans*	NP_505817.1	0.0
Pt-EIF-4A-III	Eukaryotic initiation factor	*Loa loa*	EFO21014.2	0.0
Pt-EIF-4A	Eukaryotic initiation factor	*Ascaris suum*	ADY42814	0.0
Pt-VIT-2	Vitellogenin	*Caenorhabditis elegans*	NP_508868	0.0
Pt-ALDO-2	Fructose-1,6-bisphosphate aldolase	*Caenorhabditis remanei*	XP_003110723.1	0.0
Pt-Galectin-5	Galectin	*Angiostrongylus cantonensis*	AEK98127	0.0
Pt-cGST-1	Cytosolic glutathione-S-transferase	*Oesophagostomum dentatum*	ACA30414	2e-105
Pt-GST-2	Glutathione-S-transferase	*Heligmosomoides polygyrus*	1TW9_A	1e-105
Pt-HPD-1	4-hydroxyphenylpyruvate dioxygenase	*Caenorhabditis briggsae*	XP_002642363.1	0.0
Pt-HPD-1a	4-hydroxyphenylpyruvate dioxygenase	*Caenorhabditis briggsae*	XP_002642363.1	2e-174
Pt-ASP-16a	Venom allergen/Ancylostoma secreted protein	*Heligmosomoides polygyrus bakeri*	AEP82932.1	4e-16
Pt-ASP-16b	Venom allergen/Ancylostoma secreted protein	*Heligmosomoides polygyrus bakeri*	AEP82932.1	3e-17
Pt-ASP	Ancylostoma secreted protein	*Ascaris suum*	ADY48180.1	3e-09
Pt-ASP_ANCCA	Ancylostoma secreted protein	*Ancylostoma caninum*	Q16937.1	3e-109

Table 3.2 Protein Composition of Alpha-Gal-Modified Spots Identified from 2D Gels. Summary of Predicted Molecular Mass, Extracellular Secretion and N-Glycosylation.

Protein ID	Peptides Found in Spot(s)	Predicted MW (kD)	SignalP	SecretomeP**	Predicted N glycosylation site
Pt-ENO-1	2, 3, 4	47.18	No	No (0.480)	102
Pt-CTL-2	2, 3, 4, 5, 6	58.08	No	No (0.380)	35, 88, 241
Pt-RNR-2	6	44.56	No	Yes (0.589)	348
Pt-Act-3	2, 3, 4	41.8	No	No (0.497)	13
Pt-EIF-4A-III	5, 6	46.15	No	Yes (0.652)	294
Pt-EIF-4A	5, 6	46.31	No	Yes (0.573)	102, 175
Pt-VIT-2	2, 3	175.29	Yes	No (0.332)	-
Pt-ALDO-2	2, 3, 4, 5, 6	39.06	No	No (0.364)	-
Pt-Galectin-5	5, 6	35.87	Yes	No* (0.801)	110
Pt-cGST-1	2, 5, 6	23.81	No	No (0.376)	-
Pt-GST-2	2, 5, 6	23.55	No	No (0.351)	-
Pt-HPD-1	5, 6	44.44	No	No (0.466)	230
Pt-HPD-1a	5, 6	35.2	No	No (0.444)	230
Pt-ASP-16a	2, 5, 6	29.72	Yes	No* (0.792)	63, 99, 118, 148
Pt-ASP-16b	2, 5, 6	29.37	Yes	No* (0.773)	51, 141
Pt-ASP	2	30.65	Yes	No* (0.565)	96, 107, 160, 165, 207
Pt-ASP_ANCCA	2, 3, 4	47.76	Yes	No* (0.520)	

* Warning signal from SecretomeP indicated that the protein had a signal sequence predicted by SignalP.

** A SecretomeP score over 0.9 is indicative of a predicted non-classically secreted protein.

A total of 17 excreted/secreted proteins were identified as candidates for modification by alpha-Gal from the 5 spots selected for MS/MS. It is possible that this number is lower because four paralogue pairs (Pt-EIF-4A-III/Pt-EIF-4A, Pt-cGST-1/Pt-GST-2, Pt-ASP-16a/Pt-ASP-16b and Pt-HPD-1/Pt-HPD-1a) were identified from the transcriptome but could not be distinguished specifically due to localization of the MS/MS peptides identified by MS/MS only in conserved regions. Accordingly, the minimum number of candidate proteins modified with alpha-Gal is 13. Secreted proteins modified with alpha-Gal should possess at least one N-glycosylation site and either a signal peptide sequence or meet SecretomeP characteristics. Absence of either glycosylation or secretion eliminated the protein as a potential alpha-Gal modified secreted protein and these were not discussed in-depth. Peptides found in both control spot 1 and spots modified by alpha-Gal were eliminated as potential alpha-Gal-modified proteins (vitellogenin and catalase). Several proteins were found in multiple spots (Table 3.2.), creating a trail or 'stutter' phenomenon. The shift in pI could be explained by isoforms with different phosphorylation states, or in the case of the paralogues, changes in amino acid composition. Predicted molecular weights of several proteins (Table 3.2) were less than their apparent molecular weight according to the 2D gel. However, the predicted N-glycosylation sites could contribute to up to 2.6 kDa per glycan (Duffy *et al.*, 2006).

3.4 Discussion

The alpha-Gal epitope is abundant on mammalian glycolipids and glycoproteins (Macher and Galili, 2008). It exists as millions of copies per cell in all mammals with the exception of Old World primates. The most likely explanation for the loss of this epitope in Old World primates was selection to avoid viral infection. Absence of this glycan might have eliminated the possibility of cell recognition by viruses that used alpha-Gal as a receptor (Bishop and Gagneux, 2007). Like most mammals, deer have alpha-Gal in abundance on most of their cells. Deer alpha-Gal is predominately present on the cell surface as glycoproteins and glycolipids, and likely will not have the same potential for cellular interaction as soluble parasite-derived alpha-Gal-modified proteins. Although alpha-Gal is known to modify laminin (Gabrielli *et al.*, 1991) and thyroglobulin (Thall and Galili, 1990), the only circulating host proteins modified by alpha-Gal are immunoglobulins (IgA, IgG: (Arkestal *et al.*, 2011; Thall and Galili, 1990)) and fibrinogen (Thall and Galili, 1990). Besides a conventional role in blood clot formation, soluble fibrinogen modulates neutrophil activation and survival (Fernández *et al.*, 2005) and soluble IgA and IgG bind Fc receptors on most innate immune cells to promote effector function (Otten and van Egmond, 2004; Looney, 1993). In all cases, soluble alpha-Gal-modified mammalian proteins are involved in regulation of innate immune cells via glycan-ligand interactions. The function of secreted parasite-derived alpha-Gal-modified gylcoproteins is unknown currently but a role in immunoregulation seems obvious based on alpha-Gal distribution on circulating host proteins. Known interactions of alpha-Gal with receptors on immune effector cells

suggest that alpha-Gal on E/S proteins from adult *P. tenuis* are poised to have a role in immune modulation. It is of interest to identify the parasite proteins modified by alpha-Gal to help infer their specific function during parasitism.

To fully understand the potential role of helminth secreted proteins and the alpha-Gal epitope during immunomodulation, a basic description of the vertebrate immune response is required. The innate immune response is comprised of cells and molecules that evolved to eliminate pathogens in a non-specific manner immediately upon contact. This is in contrast to the adaptive immune response that is characterized by specificity and memory that develops over time to target pathogens in a specific manner (Medzhitov and Janeway, 1997). Host T cell responses to intracellular pathogens differ from T cell responses to extracellular helminths. A T helper 1 (T_H1) type of response is associated with intracellular pathogens, whereas a T helper 2 (T_H2) type of response is characteristic of extracellular helminth infection (Maizels *et al.*, 2004). Upon infection, host antigen presenting cells (APCs) identify pathogen-associated molecular patterns (PAMPs) via pattern recognition receptors (PRPs) and activate naïve T cells to become either T_H1 or T_H2 cells. The helminth-induced polarization of T cells to T_H2 is similar to the type of response that is elicited against innocuous antigens called allergens. However, unlike allergens, helminths induce a special type of response termed a modified T_H2 response. Specifically, helminths induce T regulatory (T_{REG}) cell activation that downregulates immune responses by suppressing inflammation and pathology. A modified T_H2 environment supports chronic helminth infection (van Die and Cummings, 2010) because inflammation can be detrimental to the host without

regulation (Maizels, 2009). T_H2 responses to parasitic helminths are characterized by marked increases in circulating immunoglobulin E (IgE) and innate cells called eosinophils. Eosinophils are granulocytes that can damage helminth parasites by releasing enzymes and oxidizing agents. These cells are effective at killing invading larval helminths (Meeusen, 2000). However, this usually occurs only during challenge infections because opsonization of parasites by IgE is required for eosinophil effector function via antibody dependent cell-mediated cytoxicity (ADCC). Antibody generation requires several weeks following infection and helminths will have already developed to life stages capable of maintaining chronic infection in spite of abundant parasite-specific IgE (MacDonald *et al.*, 2002). The mechanisms underlying this ability of adult helminths to persist as chronic infections remain poorly understood. However, the interaction with alpha-Gal and a β-galactoside binding protein, galectin-3 (Gal-3), may provide some insight.

Alpha-Gal is a terminal disaccharide (galactose-alpha 1,3-galactose) that binds Gal-3 (Jin R *et al.*, 2006). This finding is of particular interest to this current study because Gal-3 is an adhesion molecule on eosinophils that binds to vascular cell adhesion molecule 1 (VCAM-1; (Truong *et al.*, 1993). Binding of Gal-3 to VCAM-1 enables eosinophil rolling and adhesion and leads to extravasation and inflammation at the site of infection. Eosinophil recruitment to the site of parasitic helminth infection, and subsequent interaction with helminth-bound IgE, is required for ADCC to occur. Eosinophil rolling and adhesion was inhibited by galactose-containing glycans that blocked Gal-3 (Rao *et al.*, 2007). Galactose is also a known competitive inhibitor of

Gal-3-mediated activation of ADCC by eosinophils (Truong *et al.*, 1993). Two potential mechanisms for modulation of eosinophils can be envisioned during *P. tenuis* infections due to the secretion of soluble alpha-Gal-modified proteins by adult parasites. First, inhibition of eosinophil binding to VCAM-1 on endothelial cells due to interactions between Gal-3 and parasite-derived alpha-Gal represents a mechanism for inhibition of eosinophil rolling and adhesion. This would result in impaired eosinophil extravasation and recruitment to the site of infection due to competitive inhibition. Secondly, parasite-derived alpha-Gal could block IgE binding that is required for eosinophil effector function. The binding of the IgE protein moiety to Fcε receptors and the IgE carbohydrate moiety to Gal-3 on eosinophils are both essential for ADCC (Liang and Ganley-Leal, 2009; Truong, *et al.*, 1993). Using similar logic as described above, binding of soluble alpha-Gal-modified *P. tenuis* E/S proteins to Gal-3 on eosinophils would inhibit binding of IgE and thereby prevent ADCC. This would be effective in blocking ADCC against adult parasites and promoting chronic infections because alpha-Gal synthesis is stage-restricted and unique to the adult stage of development. The absence of alpha-Gal in larval stages is compatible with the susceptibility of infective larvae to the concomitant immunity that prevents establishment of challenge infections (Duffy *et al.*, 2004).

Recruitment of host eosinophils is a hallmark of chronic helminth infection, in spite of the fact that eosinophils do not kill adult helminths (Meeusen, 2000). This begs the question, "what is the role of eosinophils during chronic helminth infection?". Eosinophil recruitment is reduced during modified T_H2 responses (Maizels and

Yazdanbakhsh, 2003) but eosinophils are still found at the site of helminth infection (Fallon and Mangan, 2007). Originally presumed detrimental to parasitic helminths, eosinophils have been shown to regulate inducible nitric oxide synthase-producing neutrophils in support of immunoregulation and homeostasis (Gebreselassie *et al.*, 2012). Furthermore, eosinophils are known to secrete IL-4, the cytokine required for activation of alternatively activated macrophages (AAMs) (Gebreselassie *et al.*, 2012), the cells that induce and maintain a modified T_H2 environment in support of chronic helminth infection. Induction of a modified T_H2 response alleviates issues caused by autoimmune pathologies associated with infection, and creates an environment conducive for parasite survival (Jacobsen *et al.*, 2007). If parasitic helminths require eosinophils for polarization of a T_H2 response, they must also have the ability to regulate these cells that have the ability to degranulate and destroy the worm. The documented interaction of alpha-Gal with Gal-3 suggests that soluble parasite-derived alpha-Gal could down-regulate eosinophil recruitment and block the degranulation of those cells that do arrive at the site of infection. Importantly, degranulation is not required for eosinophil-mediated induction of T_H2 responses (Gebreselassie *et al.*, 2012). Accordingly, the effector functions of eosinophils would be restricted to cytokine secretion for activation of AAMs.

Roles for eosinophil regulation have been proposed via interaction of soluble parasite-derived alpha-Gal with host Gal-3. Interestingly, extravasation of neutrophils, another leukocyte, is dependent on oligomerization of Gal-3 on the surface of neutrophils (Sato *et al.*, 2002). Monocyte migration is similarly reliant upon Gal-3 (Polli *et al.*,

2013). Gal-3 forms pentamers when binding to multivalent carbohydrates (Yang *et al.*, 2008), so it is tempting to speculate that soluble parasite-derived alpha-Gal could block rolling and adhesion of neutrophils and monocytes, in addition to eosinophils. The N-terminal domain of Gal-3 is extremely flexible, and is necessary for pentimerization (Newlaczyl and Yu, 2011). One or more carbohydrate recognition domain (CRD) of pentameric Gal-3 would bind cell surface carbohydrates on leukocytes (eosinophils, neutrophils, monocytes), leaving the other CRDs available for ligand interaction and extravasation. *Parelaphostrongylus tenuis* glycoproteins modified with multiple alpha-Gal epitopes (i.e. Pt-ASPs) should effectively block interaction with VCAMs and thereby block extravasation. These same proteins could inhibit the stabilized binding of IgE to eosinophils that arrive at the site of infection to block ADCC. An overview of ADCC is found in Figure 3.21 and the proposed model is shown in Figure 3.22 and 3.23.

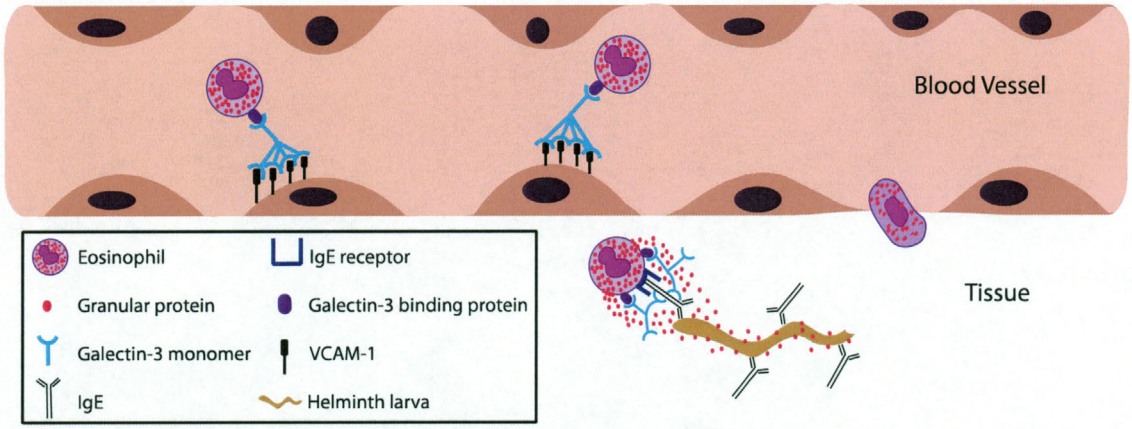


Figure 3.21 Mechanism of eosinophil-mediated killing of parasitic helminth larvae via antibody-dependent cell-mediated cytotoxicity (ADCC). Galectin-3 on eosinophils is required for attachment to vascular cell adhesion molecule 1 (VCAM-1) to enable extravasation to the site of infection. Galectin-3 also provides stabilization for binding of Immunoglobulin E (IgE) to Fcε receptors on eosinophils in the tissue, a process required for degranulation and subsequent killing of the parasitic helminth via ADCC.

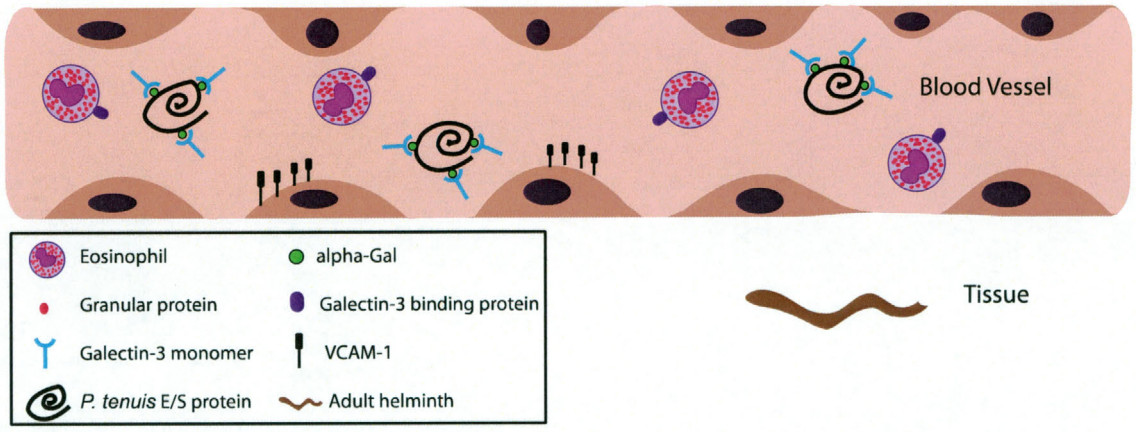


Figure 3.22 Proposed model for inhibition of eosinophil extravasation to site of infection by parasite alpha-Gal. Soluble alpha-Gal-modified E/S proteins released from adult *P. tenuis* bind to host galectin-3 before it is expressed on the surface of circulating eosinophils. This interaction inhibits pentamerization and simultaneous binding of galectin-3 to VCAM-1 on host endothelial cells. Eosinophils will not extravasate to site of infection in host tissue, enabling persistence of *P. tenuis* infection.

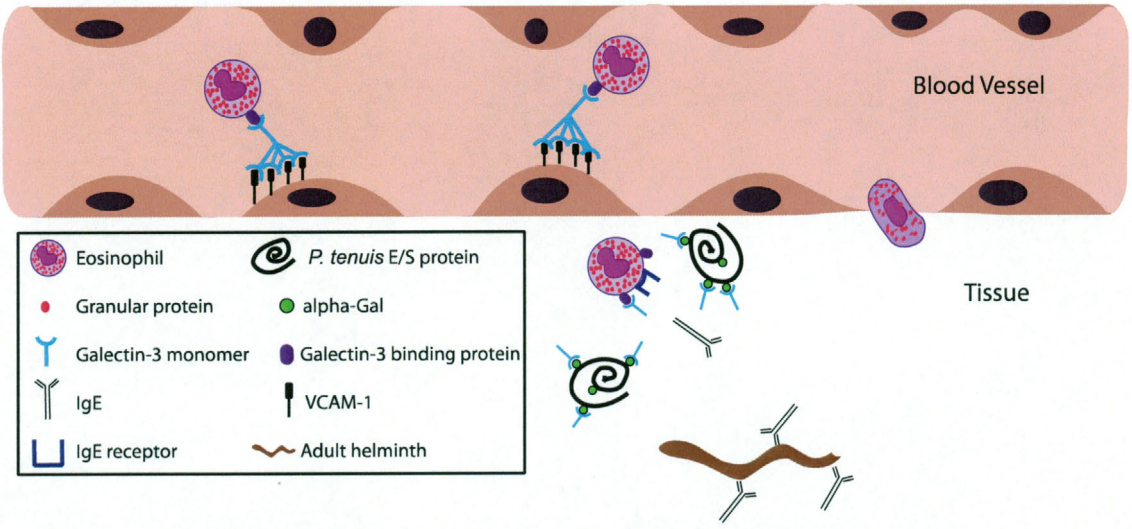


Figure 3.23 Proposed model for blocking ADCC via alpha-Gal mediated inhibition of the interaction between Immunoglobulin E (IgE) and Fcε receptors on eosinophils. Should eosinophils arrive at the site of P. *tenuis* infection, soluble alpha-Gal-modified E/S proteins released from adult P. *tenuis* will bind to host galectin-3. This inhibits the interaction between galectin-3 and the Fc portion of IgE. The binding of galectin-3 to the galectin-3 binding protein on the surface of the eosinophils would also be inhibited. The lack of the stabilizing interaction of IgE with the Fcε receptor will result in blocking of degranulation and promotion of parasitic helminth survival.

3.4.1 Adult *P. tenuis* E/S Proteins Identified by Mass Spectrometry Analysis

3.4.1.1. Proteins with Predicted N-glycosylation Sites and Signal Peptide

Four *P. tenuis* proteins identified by MS/MS from alpha-Gal-modified protein spots (Pt-ASP-16a, Pt-ASP-16b, Pt-ASP and Pt-Galectin-5) have at least one N-glycosylation site and an N-terminal signal sequence. Accordingly, these proteins are good candidates for being alpha-Gal-modified secreted proteins.

Venom Allergen-Like/Ancylostoma Secreted Protein

Three *P. tenuis* Venom Allergen-Like (VAL)/Ancylostoma Secreted Protein (ASP) orthologues with predicted N-glycosylation sites were identified from alpha-Gal-modified protein spots. Pt-ASP-16a, Pt-ASP-16b and Pt-ASP had 28-32% identity with parasitic nematode sequences in GenBank. Although often having relatively low identity overall, the nematode ASPs are cysteine-rich secretory proteins (CRISPs) (Zhan *et al.*, 2003) that are members of the SCP (sperm coat protein) family. The *P. tenuis* ASPs identified in this study had at least 10 cysteine residues and contained an SCP domain. Interestingly, many helminth ASP orthologues proteins have been localized to secretory glands of parasitic nematodes. These include Ov-ASP-1, a protein localized to granules in the glandular oesophagus of *Onchocerca volvulus* third-stage larve (MacDonald *et al.*, 2004), two VAL transcripts (*Hg-vap-1* and *Hg-vap-2*) that localized to subvental oesophageal gland cells from *Heterodera glycines* second-stage juveniles (Gao *et al.*, 2001) and ASP-2 from *A. caninum*, a protein localized to the glandular oesophagus of third-stage larvae (Bethony *et al.*, 2005).

In addition to VAL/ASPs, the SCP family includes plant pathogenesis-related proteins (PRPs), mammalian CRISPs, and venom allergen proteins (Hewitson *et al.*, 2011). Plant PRPs were first identified in the 1970s (Cantacessi *et al.*, 2009). The absence of PRPs in healthy plant tissue and their upregulation during infection by pathogens led to discovery of antimicrobial activity (O'Rourke *et al.*, 2006) and other defense-related functions (Van Loon *et al.*, 2006). Other PRP orthologues still have unknown function. SCPs from vertebrates and invertebrates have sequence conservation that suggests a common evolutionary origin. Accordingly, these proteins might have a role in the basic physiology of organisms in addition to a role in defense (Cantacessi *et al.*, 2009).

The widespread distribution of SCPs across many eukaryotic organisms led to phylogenetic analysis of sequence data to provide more consistency with nomenclature when referring to these proteins (Cantacessi *et al.*, 2009). One would presume that nematode proteins would be more closely related to those from other invertebrates. However, the phylogenetic analysis revealed that nematode proteins were more similar to sequences from vertebrates (Cantacessi *et al.*, 2009), the animals that serve as their hosts. The function of this gene family still remains to be determined (Maizels *et al.*, 2012). However, their secretion with E/S products implies a role in parasitism of vertebrates. Original identification of ASPs was from the hookworm *Ancylostoma caninum,* as the dominant protein in E/S products from infective larvae (Hawdon *et al.*, 1996). ASPs are common in E/S products (Hewitson *et al.*, 2011) and up to 12% of E/S proteins from some nematodes are ASPs (Yatsuda *et al.*, 2003). ASP function in

nematodes remains poorly characterized in general. However, an ASP from *A. caninum* blocks adhesion of activated neutrophils to endothelial cells and also blocks release of H_2O_2 (Moyle *et al.*, 1994), a reactive oxygen species that can damage helminth parasites. It has been termed a neutrophil inhibitory factor (NIF). This is not the only neutrophil regulatory molecule released by helminths, so it is likely that the importance of modulating neutrophils in helminth infections remains to be discovered (Cadman and Lawrence, 2010). The phylogenetic distribution of alpha-Gal in nematodes remains to be determined. However, given the proposed role for *P. tenuis* alpha-Gal in modulating eosinophil recruitment and degranulation, it is tempting to speculate that alpha-Gal, or perhaps another glycan, might modify NIF to modulate via Gal-3 and a similar mechanism. NIF contains 7 predicted N-linked glycosylation sites (Moyle *et al.*, 1994) and Gal-3 binds numerous β-galactosides in addition to alpha-Gal(Hirabayashi *et al.*, 2002). The *P. tenuis* ASPs seem to be likely candidates for modification by alpha-Gal. While definitive information regarding function is lacking, the abundance of VAL/ASPs in nematode E/S products released at the host-parasite interface is compatible with a role in ensuring persistence of infection within their host.

Galectin

Parelaphostrongylus tenuis galectin (Pt-Galectin-5) had an identity of 94% with a galectin from *Angiostrongylus cantonensis,* a parasitic nematode of humans. Galectins are proteins with sugar-binding properties, with an affinity for N-acetyl lactosamines (Morassutti and Graeff-Teixeira, 2012). Galectins have high sequence similarity across the animal kingdom (Cooper and Barondes, 1999), and have been identified in many

parasitic nematodes, including *Haemonchus contortus* (Turner *et al.*, 2008), *Dirofilaria immitis* (Pou-Barreto *et al.*, 2008), *Brugia malayi* (Bennuru *et al.*, 2009) and *Trichostrongylus colubriformis* (Greenhalgh *et al.*, 1999). The core sequence of ~130 amino acids is highly conserved amongst all galectins. The CRD is found between amino acids 30 and 90 (Cooper and Barondes, 1999). All galectins are classified in one of three groups: prototype galectins contain one CRD; tandem-repeat galectins have two CRDs that are linked; and, a chimera type of galectin has one CRD and a non-lectin domain that has proline and glycine rich short stretches. Pt-Galectin-5 is compatible with the prototype galectins (Rabinovich and Toscano, 2009).

Mammalian galectins do not have classical signal sequences. However, they are localized in the extracellular environment in addition to being in the cytoplasm and nucleus (Yang *et al.*, 2008). Accordingly, mammalian galectins are secreted independent of the classical secretion pathway that involves the endoplasmic reticulum and golgi apparatus (Menon and Hughes, 1999). Interestingly, *Onchocerca volvulus* (Joseph *et al.*, 2000), *Angiostongylus cantonensis* (Liu *et al.*, 2013) and the Pt-Galectin-5 possess classical signal peptide sequences. Extracellular galectins interact with cells via glycoprotein receptors, resulting in cell adhesion, clustering and endocytosis (Liu and Rabinovich, 2010). It has been proposed that nematode galectins could function similar to host galectins, with involvement in immune modulation via cell recruitment and regulation of apoptosis (Young and Meeusen, 2004). Among many functions, several galectins have been linked to eosinophil recruitment (Turner *et al.*, 2008). Eosinophilia is an immunological event that is a consistent feature of helminth infection

(Yazdanbakhsh, 1996). Galectins are of great interest in research because increasing evidence suggests that eosinophils may promote persistence of helminth infection (Gebreselassie *et al.*, 2012).

Mammalian galectin-5 is currently known only from rats but it shows high sequence similarity with the C-domain of galectin-9 (Wu *et al.*, 2006) that is involved in eosinophil migration in mammals (Turner *et al.*, 2008). Given that the C-terminal CRD of galectin-9 acts as an eosinophil chemoattractant (Sato *et al.*, 2002), it seems likely that Pt-Galectin-5 could recruit eosinophils to the site of infection to promote and maintain a modified T_H2 response via AAM activation (Gebreselassie *et al.*, 2012).

To summarize, evidence from orthologues suggests that the *P. tenuis* ASPs and the galectins likely function to modulate host immune responses. If the Pt-ASPs function similar to that of the NIF, this would prevent damage to the parasite via ADCC. Galectins are present at the host-parasite interface in both parasitic and host forms. *Pt*-Galectin-5 may be responsible for the recruitment of eosinophils for activation of AAMs (Gebreselassie *et al.*, 2012) to promote both host and parasite survival.

3.4.1.2 Multiple Proteins from Alpha-Gal-modified Spots from *P. tenuis* E/S Extracts Lacked a Conventional Secretory Signal but did Have Predicted N-Glycosylation Sites.

Classical protein secretion is defined by the use of the endoplasmic reticulum (ER) to Golgi membrane pathway. This process requires that proteins have an N-terminal signal sequence. However, proteins lacking a signal peptide can also be secreted. This non-classical or leaderless protein secretion is common to all eukaryotes and does not require transit through the ER and golgi (Bendtsen *et al.*, 2004). Regardless, the possibility exists that parasite glands specialized for secretion might release proteins through novel mechanisms besides the classical or non-classical secretion pathways. Most of the MS/MS identified *P. tenuis* E/S proteins are found commonly in E/S products from other nematodes and so this gives insight into the composition of the *P. tenuis* secretome.

Eight proteins identified in this study had an N-glycosylation site but lacked an N-terminal signal sequence. However, they are still of interest due to their presence in E/S products and the possibility that they are secreted by a non-conventional secretion pathway (Nickel and Seedorf, 2008). Regardless of their mechanism of secretion, many of these proteins are components of the secretome of other parasitic helminths and should be discussed thoroughly. These proteins include Pt-ENO-1, Pt-CTL-2, Pt-RNR-2, Pt-Act-3, Pt-EIF-4A-III, Pt-EIF-4A, Pt-HPD-1 and Pt-HPD-1a.

Enolase

Parelaphostrongylus tenuis enolase (Pt-ENO-1) had an identity of 92% with enolase from *Haemonchus contortus*, a gastrointenstinal nematode of small ruminants. Enolase (2-phospho-D-glycerate hydrolase) is an enzyme that catalyzes conversion of 2-phosphogylcerate to phosphoenolpyruvate during glycolysis (Lebioda *et al.*, 1989). Not only is enolase a glycolytic enzyme, it functions as a heat shock protein, binds cytoskeletal structures and has plasminogen binding properties (Pancholi, 2001). Interestingly, enolase from the tegument of *Schistosoma bovis* may have a role in preventing blood clotting around adult parasites (Ramajo-Hernandez *et al.*, 2007). Pt-ENO-1 was collected from E/S products despite absence of a signal peptide. Enolases have been documented from other parasitic nematode enolases, including *Haemonchus contortus* (Han *et al.*, 2012).

Catalase

Parelaphostrongylus tenuis catalase (Pt-CTL-2) had an identity of 81% with a catalase from *Haemonchus contortus*. Catalase is active during metabolic processes in addition to a protective role within a host due to its ability to convert hydrogen peroxide into water and oxygen. Host hydrogen peroxide is produced by activated leukocytes to damage parasite membranes and molecules. The activity of parasitic catalase serves to mitigate the toxic effects of the activated host reactive oxygen species (Kotze and McClure, 2001). Pt-CTL-2 was collected from E/S products despite absence of a signal peptide. It is unlikely to represent a byproduct of worm degradation given the stringent

culturing protocols that were followed. Further investigation of catalase as a secreted product is required. Catalase is not found abundantly in helminths in spite of apparent benefits as a secreted antioxidant enzyme for protection against reactive oxygen species (Dzik, 2006).

Ribonucleotide Reductase

Parelaphostrongylus tenuis ribonucleotide reductase (Pt-RNR-2) had an identity of 74% with ribonucleotide reductase from *Caenorhabditis brenneri,* a free-living nematode. Ribonucleotide reductase is a member of the ferritin-like superfamily and is found in all eukaryotes and prokaryotes. It catalyzes the conversion of ribonucleotides to deoxyribonucleotides (Nordlund and Reichard, 2006). Ribonucleotide reductase was identified in E/S products of another parasitic nematode, *Heligmosomoides polygyrus*, but no explanation for its presence in ES products was given (Hewitson *et al.*, 2011), nor does my data shed any light on this finding.

Actin

Parelaphostrongylus tenuis actin (Pt-Act-3) had an identity of 100% with actin from *Caenorhabditis elegans,* a free-living nematode. Actin, a cytoskeletal protein found in all eukaryotic cells, is also found in an extracellular form that may be secreted in a regulated fashion (Lind and Smith, 1991). Like enolase, it was found that actin can bind plasminogen, and may have a role in preventing blood clot formation around adult *Schistosoma bovis* (Ramajo-Hernandez *et al.*, 2007). Actin is found commonly in E/S products from a number of helminths (Sotillo *et al.*, 2008) so the possibility exists that

actin is secreted via a non-classical secretion pathway.

Eukaryotic Initiation Factor

Two eukaryotic initiation factor (EIF) proteins were identified. *Parelaphostrongylus tenuis* Pt-EIF-4A-III had an identity of 90% with EIF-4A-III from *Loa loa*, a parasitic filarial nematode of humans, and Pt-EIF-4A had an identity of 80% with EIF-4A from *Ascaris suum*. EIF is responsible for the first step in initiation of cap-dependent translation in eukaryotes, the recruitment of the capped (7-methyl-guanosine) mRNA to the ribosome (Wallace *et al.*, 2010). Very little information is available regarding nematode eukaryotic initiation factor, especially in papers investigating secretomes of parasitic nematodes.

Hydroxyphenylpyruvate dioxygenase

Two *Parelaphostrongylus tenuis* hydroxyphenylpyruvate dioxegenase (HPPD) proteins were identified. Pt-HPD-1 and Pt-HPD-1a had identities of 77% and 76% respectively with a HPPD from *Caenorhabditis briggsae*. One peptide identified by mass spectrometry did not align perfectly with the conceptually-translated amino acid sequence from the transcriptome. The peptide from mass spectrometry results contained a leucine (L), whereas the translated transcript had an isoleucine (I) in its place. The mass spectrometer data cannot be used to distinguish between these isomers since they have the same mass. Accordingly, the translated amino acid sequence with an isoleucine at amino acid 66 is considered more reliable. HPPD will catalyze the conversion of 4-hydroxyphenylpyruvate to 2,5-dihydroxyphenylacetate, a reaction that

has a role in a numerous functions, including tyrosine catabolism in mammals (Moran, 2005). A literature search did not provide any evidence that nematode HPPD may have additional functions beyond its role in aerobic metabolism.

3.4.1.3 Proteins with No Predicted N-glycosylation Site

The absence of an N-glycosylation site excluded five proteins (Pt-GST-2, Pt-cGST-1, Pt-ALDO-2, Pt-VIT-2 and Pt-ASP_ANCCA) as possible alpha-Gal-modified proteins. However, their presence in *P. tenuis* E/S products provided an opportunity to gain additional insight into proteins of significance during host-parasite interactions. Accordingly, a brief description of each of these proteins is provided.

Venom Allergen-Like (VAL)/Anycolostoma Secreted Protein (ASP)

Parelaphostrongylus tenuis Ancylostoma secreted protein (Pt-ASP_ANCCA) had an identity of 42% with an ASP from *Ancylostoma caninum*. While this particular ASP does not have an N-glycosylation site, three *P.tenuis* ASPs did. Accordingly, a description of ASP proteins was provided earlier (Section 3.3.1.1.).

Fructose-1, 6-bisphosphate aldolase

Parelaphostrongylus tenuis fructose-1, 6-bisphosphate (FBP) aldolase (Pt-ALDO-2) had an identity of 87% with FBP aldolase from *Caenorhabditis remanei,* a free-living nematode. FBP aldolase is a glycolytic enzyme that catalyzes the cleavage of FBP to glyceradehyde-3-phosphate and dihydroxyacetone phosphate (DHAP) (Inoue *et al.*,

1997), and is of particular interest because of its various functions. Because of its essential role in glycolysis, FBP aldolase is considered a primary vaccine candidate for *Schistosoma mansoni*, a human parasitic helminth that has a high rate of metabolic activity (Marques *et al.*, 2008). Aldolase also has actin binding properties, which may enable binding to host cytoskeleton (Jewett and Sibley, 2003). Studies have also shown that FBP aldolase may have a role in decreasing granuloma formation, a hallmark of some helminth infections (Marques *et al.*, 2008). Aldolase of the fungus *Candida albicans* has been shown to bind human plasminogen (Crowe *et al.*, 2003), so it is possible that parasitic nematode aldolase may share this function, similar to parasitic nematode enolase and actin. The lack of a signal peptide sequence in *P.tenuis* FBP aldolase is consistent with other secreted FBP aldolases found on bacterial cell surfaces (Tunio *et al.*, 2010), so a mechanism for unconventional protein secretion is supported.

Glutathione-S-transferase

Two glutathione-S-transferase proteins were identified. *Parelaphostrongylus tenuis* cytosolic glutathione-S-transferase (Pt-cGST-1) had an identity of 71% with a GST from *Oesophagostomum dentatum*, a parasitic nematode of swine. Another *P. tenuis* GST, Pt-GST-2 had an identity of 68% with a GST from *Heligmosomoides polygyrus*, a parasitic nematode of mice. GSTs are responsible for conjugation of glutathione to a variety of substrates (Hayes *et al.*, 2005) and interestingly have been considered as top vaccine candidates against parasitic helminths. While GSTs have been found in free-living nematodes, and are obviously involved in metabolic function, they may also have a role at the host-parasite interface (Joachim and Ruttkowski, 2008). A GST of

Ancylostoma caninum, a blood feeding hookworm, is suggested to have a role in heme detoxification or transport following feeding. Researchers have dedicated efforts to target this feeding pathway to search for candidates for vaccine development (Zhan *et al.*, 2005)

Vitellogenin

Parelaphostrongylus tenuis vitellogenin (Pt-VIT-2) had an identity of 39% with vitellogenin from *Caenorhabditis elegans,* a free-living nematode. Vitellogenin is an egg yolk protein (Spieth *et al.*, 1985) that has been found in E/S products of *Heligmosomoides polygyrus* (Hewitson *et al.*, 2011). While this protein is normally considered a somatic protein, it is very likely that is released with intrauterine contents into the media *in vitro*. A literature review provided no other potential explanation for release of vitellogenin with E/S products.

3.4.2 Rationale for Galectin-5 and ASPs as Alpha-Gal-Modified E/S Proteins

In summary, *P. tenuis* Galectin-5 and one or more of the ASPs were the only proteins that contained both N-glycosylation sites and signal peptide sequences. However, in addition to binding to epitopes of the *P. tenuis* Galectin-5 (spots 5 & 6) and one or more of the ASPs (Spots 2, 5 & 6), the anti-alpha-Gal antibody also bound to epitopes found in proteins in both spots 3 and 4. This result highlights that proteins other than the galectin-5 and ASPs are modified by alpha-Gal. Accordingly, further explanation must be provided as to why proteins in spots 3 and 4 are also positive for alpha-Gal.

The anti-alpha-Gal antibody could be binding to catalase (found in spots 2, 3, 4, 5 & 6), actin (found in spots 2, 3 & 4) and/or enolase (found in spots 2, 3 & 4) given that all three proteins have predicted N-glycosylation sites. This would provide an explanation for the positive binding in spots 3 and 4. It is unlikely, however, that catalase is an alpha-Gal-modified immunomodulatory protein since there is substantial evidence to suggest that it has a role in detoxification of reactive oxygen species (Kotze and McClure 2001). Similarly, actin and enolase can bind plasminogen and may prevent blood clot formation (Ramajo-Hernandez et al. 2007), however no immunomodulatory function is known. Interestingly, enolase from alpha-Gal knockout pigs has been shown to cross-react with natural occurring polyclonal anti-alpha-Gal antibody (Burlak, 2012). The possibility exists that the anti-alpha-Gal monoclonal antibody used in this experiment could have cross-reacted with *P. tenuis* enolase, and thus provides a possible explanation for the positive reactivity in spots 2, 3 and 4. However, given that none of these proteins is secreted, based on absence of SignalP or SecretomeP signatures, other glycosylated proteins from spots 5 and 6 must be considered candidates for alpha-Gal modification in addition to galectin-5 and the ASPs. This does cast some doubt on the earlier suggestion that galectin-5 and the ASPs are the most likely candidates for modification with alpha-Gal. If enolase, catalase and actin are candidates for modification with alpha-Gal in spots 3 and 4, then Pt-HPD-1, Pt-HPD-1a, Pt-EIF-4A-III and Pt-EIF-4A are candidates for modification with alpha-Gal in spots 5 and 6, in addition to galectin-5 and the ASPs, because they are also glycosylated but lack secretory signatures. However, neither the HPPDs nor EIFs are known to function

extracellularly or in an immunomodulatory capacity (Moran, 2005, Wallace *et al.*, 2010). Furthermore, both galectin-5 and ASPs are known to have immunomodulatory potential and so they remain as likely candidates for modification with alpha-Gal.

With the current results, it is impossible to distinguish between alpha-Gal on galectin-5 versus it being on one or more of the ASPs. While many ASPs still have unknown function, it is known that an ASP called NIF can inhibit neutrophil recruitment (Moyle M et al. 1994), presumably using a manner similar to that proposed in the model for alpha-Gal-mediated eosinophil impairment (Figures 3.21 and 3.22). It seems reasonable to expect that *P. tenuis* ASPs may also have immunomodulatory function. Perhaps just as significant is the possible role of galectin-5 as an eosinophil chemoattractant (Sato et al. 2002; Wu AM et al. 2006), suggesting that *P. tenuis* galectin-5 could also have immunomodulatory function. While it might seem counter-intuitive that a parasite recruits immune effector cells that have the capacity to kill them, there is increasing evidence that eosinophils might be the source of cytokines that promote the modified T_H2 environment that leads to immune regulation and parasite survival (Gebreselasie et al., 2012). The proposed models for immunomodulation of eosinophils using alpha-Gal via pentamerization of Gal-3 suggest that *P. tenuis* ASPs, with their multiple N-glycosylation sites, are the obvious candidates for modification with alpha-Gal (versus Galectin-5, which only has 1 N-glycosylation site). While it remains possible that one or more of enolase, catalase, actin, HPDs, and EIFs are modified with alpha-Gal, there are no obvious indications regarding how these proteins would interact with host molecules in any capacity.

Bibliography

Arkestal, K., Sibanda, E., Thors, C., Troye-Blomberg, M., Mduluza, T., Valenta, R., Gronlund, H., and van Hage, M. (2011). "Impaired allergy diagnostics among parasite-infected patients caused by IgE antibodies to the carbohydrate epitope galactose-α1,3-galactose." *J.Allergy Clin.Immunol.,* 127(4), 1024-1028.

Bennuru S, Semnani R, Meng Z, Ribeiro JM, Veenstra TD, and Nutman TB. (2009). "*Brugia malayi* excreted/secreted proteins at the host/parasite interface: stage- and gender-specific proteomic profiling." *PLoS Negl. Trop. Dis.,* 3(4).

Bethony J, Loukas A, Smout M, Brooker S, Mendez S, Plieskatt J, Goud G, Bottazzi ME, Zhan B, Wang Y, Williamson A, Lustigman S, Correa-Oliveira R, Xiao S, and Hotez PJ. (2005). "Antibodies against a secreted protein from hookworm larvae reduce the intensity of hookworm infection in humans and vaccinated laboratory animals." *FASEB J.* 19(12), 1743-5.

Bishop, J. R., and Gagneux, P. (2007). "Evolution of carbohydrate antigens-microbial forces shaping host glycomes?" *Glycobiology,* 17(5).

Burlak C, Wang ZY, Chihara RK, Lutz AJ, Wang Y, Estrada JL, and Tector AJ. (2012). "Identification of human preformed antibody targets in GTKO pigs." *Xenotransplantation,* 19(2).

Cadman ET, and Lawrence RA. (2010). "Granulocytes: effector cells or immunomodulators in the immune response to helminth infection?" *Parasite Immunol.,* 32(1), 1-19.

Cantacessi C, Campbell BE, Visser A, Geldhof P, Nolan MJ, Nisbet AJ, Matthews JB, Loukas A, Hofmann A, Otranto D, Sternberg PW, and Gasser RB. (2009). "A portrait of the "SCP/TAPS" proteins of eukaryotes--developing a framework for fundamental research and biotechnological outcomes." *Biotechnol.Adv.,* 27(4),.

Cooper DN, and Barondes SH. (1999). "God must love galectins; he made so many of them." *Glycobiology,* 9(10), 979-84.

Crowe JD, Sievwright IK, Auld GC, Moore NR, Gow NA, and Booth NA. (2003). "Candida albicans binds human plasminogen: identification of eight plasminogen-binding proteins." *Mol.Microbiol.,* 47(6), 1637-51.

Diemert DJ, Pinto AG, Freire J, Jariwala A, Santiago H, Hamilton RG, Periago MV, Loukas A, Tribolet L, Mulvenna J, Correa-Oliveira R, Hotez PJ, and Bethony JM. (2012). "Generalized urticaria induced by the Na-ASP-2 hookworm vaccine: implications for the development of vaccines against helminths." *J.Allergy*

Clin.Immunol., 130(1), 169-76.

Duffy MS, Cevasco DK, Zarlenga DS, Sukhumavasi W, and Appleton JA. (2006). "Cathepsin B homologue at the interface between a parasitic nematode and its intermediate host." *Infect.Immun.,* 74(2), 1297-304.

Duffy MS, Greaves TA, and Burt MD. (2004). "Establishment of adult *Parelaphostrongylus tenuis,* patent infections, and acquired immunity after experimental infection of white-tailed deer (*Odocoileus virginianus*) and red deer (*Cervus elaphus elaphus).*" *J.Parasitol.,* 90(2), 245-54.

Duffy, M. S., Morris, H. R., Dell, A., Appleton, J. A., and Haslam, S. M. (2006). "Protein glycosylation in *Parelaphostrongylus tenuis*-first description of the Galα1-3Gal sequence in a nematode." *Glycobiology,* 16(9), 854-862.

Dzik JM. (2006). "Molecules released by helminth parasites involved in host colonization." *Acta Biochim.Pol.,* 53(1), 33-64.

Fallon PG, and Mangan NE. (2007). "Suppression of TH2-type allergic reactions by helminth infection." *Nat. Rev. Immunol.,* 7(3), 220-30.

Fernández GC, Ilarregui JM, Rubel CJ, Toscano MA, Gómez SA, Beigier Bompadre M, Isturiz MA, Rabinovich GA, and Palermo MS. (2005). "Galectin-3 and soluble fibrinogen act in concert to modulate neutrophil activation and survival: involvement of alternative MAPK pathways." *Glycobiology,* 15(5), 519-27.

Gabrielli, A., Candela, M., Ricciatti, A. M., Caniglia, M. L., and Wieslander, J. (1991). "Antibodies to mouse laminin in patients with systemic sclerosis (scleroderma) recognize galactosyl (α1-3)-galactose epitopes." *Clin. Exp. Immunol.,* 86(3).

Gao, B., Allen, R., Maier, T., Davis, E. L., Baum, T. J., and Hussey, R. S. (2001). "Molecular characterisation and expression of two venom allergen-like protein genes in *Heterodera glycines.*" *Int. J. Parasitol.,* 31(14), 1617-1625.

Gebreselassie NG, Moorhead AR, Fabre V, Gagliardo LF, Lee NA, Lee JJ, and Appleton JA. (2012). "Eosinophils preserve parasitic nematode larvae by regulating local immunity." *J. Immunol., (Baltimore, Md.: 1950),* 188(1), 417-25.

Grabherr MG, Haas BJ, Yassour M, Levin JZ, Thompson DA, Amit I, Adiconis X, Fan L, Raychowdhury R, Zeng Q, Chen Z, Mauceli E, Hacohen N, Gnirke A, Rhind N, di Palma F, Birren BW, Nusbaum C, Lindblad-Toh K, Friedman N, and Regev A. (2011). "Full-length transcriptome assembly from RNA-Seq data without a reference genome." *Nat.Biotechnol.,* 29(7), 644-52.

Greenhalgh, C. J., Beckham, S. A., and Newton, S. E. (1999). "Galectins from sheep

gastrointestinal nematode parasites are highly conserved." *Mol. Biochem. Parasitol.,* 98(2), 285-289.

Han, K., Xu, L., Yan, R., Song, X., and Li, X. (2012). "Molecular cloning, expression and characterization of enolase from adult *Haemonchus contortus*." *Res.Vet.Sci.,* 92(2), 259-265.

Harn, D. A., McDonald, J., Atochina, O., and Da'dara, A. A. (2009). "Modulation of host immune responses by helminth glycans." *Immunol.Rev.,* 230(01), 247-257.

Hayes, J. D., Flanagan, J. U., and Jowsey, I. R. (2005). "GLUTATHIONE TRANSFERASES." *Annu. Rev. Pharmacol. Toxicol.,* 45(1).

Hein WR, and Harrison GB. (2005). "Vaccines against veterinary helminths." *Vet.Parasitol.,* 132(3-4), 3-4.

Hewitson, J. P., Harcus, Y., Murray, J., van Agtmaal, M., Filbey, K. J., Grainger, J. R., Bridgett, S., Blaxter, M. L., Ashton, P. D., Ashford, D. A., Curwen, R. S., Wilson, R. A., Dowle, A. A., and Maizels, R. M. (2011). "Proteomic analysis of secretory products from the model gastrointestinal nematode *Heligmosomoides polygyrus* reveals dominance of Venom Allergen-Like (VAL) proteins." *J. Proteomics.,* 74(9), 1573-1594.

Hirabayashi J, Hashidate T, Arata Y, Nishi N, Nakamura T, Hirashima M, Urashima T, Oka T, Futai M, Muller WE, Yagi F, and Kasai K. (2002). "Oligosaccharide specificity of galectins: a search by frontal affinity chromatography." *Biochim.Biophys.Acta,* 1572(2-3), 2-3.

Hotez PJ, Bethony JM, Diemert DJ, Pearson M, and Loukas A. (2010). "Developing vaccines to combat hookworm infection and intestinal schistosomiasis." *Nat. Rev. Microbiol.,* 8(11), 814-26.

Hotez PJ, Brindley PJ, Bethony JM, King CH, Pearce EJ, and Jacobson J. (2008). "Helminth infections: the great neglected tropical diseases." *J.Clin.Invest.,* 118(4), 1311-21.

Inoue, T., Yatsuki, H., Kusakabe, T., Joh, K., Takasaki, Y., Nikoh, N., Miyata, T., and Hori, K. (1997). "*Caenorhabditis elegans* Has Two Isozymic Forms, CE-1 and CE-2, of Fructose-1,6-bisphosphate Aldolase Which Are Encoded by Different Genes." *Arch. Biochem. Biophys.,* 339(1), 226-234.

Jacobsen, E. A., Taranova, A. G., Lee, N. A., and Lee, J. J. (2007). "Eosinophils: Singularly destructive effector cells or purveyors of immunoregulation?" *J.Allergy Clin.Immunol.,* 119(6), 1313-1320.

Jewett TJ, and Sibley LD. (2003). "Aldolase forms a bridge between cell surface

adhesins and the actin cytoskeleton in apicomplexan parasites." *Mol.Cell,* 11(4), 885-94.

Jin R, Greenwald A, Peterson MD, and Waddell TK. (2006). "Human monocytes recognize porcine endothelium via the interaction of galectin 3 and alpha-GAL." *J. Immunol.*, 1289-95.

Joachim A, and Ruttkowski B. (2008). "Cytosolic glutathione S-transferases of *Oesophagostomum dentatum.*" *Parasitology,* 135(10), 1215-23.

Hawdon, J.M., Jones, B. F., Hoffman, D.R., Hotez, P.J. (1996). "Cloning and Characterization of Ancylostoma-secreted Protein." *J.Biol.Chem.,* 271(12), 6672-6678.

Joseph, G. T., Huima, T., Klion, A., and Lustigman, S. (2000). "A novel developmentally regulated galectin of *Onchocerca volvulus.*" *Mol. Biochem. Parasitol.,*106(1), 187-195.

Kotze, A. C., and McClure, S. J. (2001). "*Haemonchus contortus* utilises catalase in defence against exogenous hydrogen peroxide in vitro." *Int. J. Parasitol.,* 31(14), 1563-1571.

Lebioda L, Stec B, and Brewer JM. (1989). "The structure of yeast enolase at 2.25-A resolution. An 8-fold beta + alpha-barrel with a novel beta beta alpha alpha (beta alpha)6 topology." *J. Biol. Chem.,* 264(7), 3685-93.

Liang Y, and Ganley-Leal LM. (2009). "A simple method for measuring human cell-bound IgE levels in whole blood." *J.Immunol.Methods,* 343(2), 134-9.

Lind SE, and Smith CJ. (1991). "Actin accelerates plasmin generation by tissue plasminogen activator." *J. Biol. Chem.,* 266(26), 17673-8.

Liu LH, He HJ, Lv ZY, Wei J, Zeng X, Liang JY, Zheng HQ, Yu XB, Sun X, and Wu ZD. (2013). "The mRNA level of the galectin-10 of *Angiostrongylus cantonensis* induced by reactive oxygen stress." *Parasitol.Res.,* 112(3), 933-43.

Liu, F., and Rabinovich, G. A. (2010). "Annals of the New York Academy of Sciences: Galectins: regulators of acute and chronic inflammation." *Ann.N.Y.Acad.Sci.,* 1183(1), 158-182.

Lohse M, Bolger AM, Nagel A, Fernie AR, Lunn JE, Stitt M, and Usadel B. (2012). "RobiNA: a user-friendly, integrated software solution for RNA-Seq-based transcriptomics." *Nucleic Acids Res.,* 40, 622-7.

Looney RJ. (1993). "Structure and function of human and mouse Fc gamma RII." *Blood Cells,* 19(2), 353-9.

MacDonald AS, Araujo MI, and Pearce EJ. (2002). "Immunology of parasitic helminth infections." *Infect.Immun.,* 70(2), 427-33.

MacDonald, A. J., Tawe, W., Leon, O., Cao, L., Liu, J., Oksov, Y., Abraham, D., and Lustigman, S. (2004). "Ov-ASP-1, the *Onchocerca volvulus* homologue of the activation associated secreted protein family is immunostimulatory and can induce protective anti-larval immunity." *Parasite Immunol.,* 26(1), 53-62.

Macher, B. A., and Galili, U. (2008). "The Galα1,3Galβ1,4GlcNAc-R (α-Gal) epitope: A carbohydrate of unique evolution and clinical relevance." *Biochim. Biophys. Acta.,* 1780(2), 75-88.

Maizels RM, Balic A, Gomez-Escobar N, Nair M, Taylor MD, and Allen JE. (2004). "Helminth parasites--masters of regulation." *Immunol.Rev.,* 201 89-116.

Maizels RM, and Yazdanbakhsh M. (2003). "Immune regulation by helminth parasites: cellular and molecular mechanisms." *Nat. Rev. Immunol.,* 3(9), 733-44.

Maizels, R. M., Hewitson, J. P., Murray, J., Harcus, Y. M., Dayer, B., Filbey, K. J., Grainger, J. R., McSorley, H. J., Reynolds, L. A., Smith, K. A., and Molecular and Cellular Biology of Helminth Parasites VI, Hydra,Greece 2010. (2012). "Immune modulation and modulators in *Heligmosomoides polygyrus* infection." *Exp.Parasitol.,* 132(1), 76-89.

Marques, H. H., Zouain, C. S., Torres, C. B. B., Oliveira, J. S., Alves, J. B., and Goes, A. M. (2008). "Protective effect and granuloma down-modulation promoted by RP44 antigen a fructose 1,6 bisphosphate aldolase of *Schistosoma mansoni*." *Immunobiology,* 213(5), 437-446.

Medzhitov R, and Janeway CA Jr. (1997). "Innate immunity: the virtues of a nonclonal system of recognition." *Cell,* 91(3), 295-8.

Meeusen, E. (2000). "Do Eosinophils have a Role in the Killing of Helminth Parasites?" *Parasitol. Today,* 16(3), 95-101.

Menon, R. P., and Hughes, R. C. (1999). "Determinants in the N-terminal domains of galectin-3 for secretion by a novel pathway circumventing the endoplasmic reticulum-Golgi complex." *Eur. J. Biochem.,* 264(2).

Moran, G. R. (2005). "4-Hydroxyphenylpyruvate dioxygenase." *Arch. Biochem. Biophys.,* 433(1), 117-128.

Morassutti AL, and Graeff-Teixeira C. (2012). "Interface Molecules of *Angiostrongylus cantonensis:* Their Role in Parasite Survival and Modulation of Host Defenses." *Int. J.*

Inflam., 2012.

Moyle M, Foster DL, McGrath DE, Brown SM, Laroche Y, De Meutter J, Stanssens P, Bogowitz CA, Fried VA, Ely JA, and et al. (1994). "A hookworm glycoprotein that inhibits neutrophil function is a ligand of the integrin CD11b/CD18." *J. Biol. Chem.,* 269(13), 10008-15.

Newton, S. (1999). "The Development of Vaccines against Gastrointestinal Nematode Parasites, Particularly *Haemonchus contortus*." *Parasitol. Today,* 15(3), 116-122.

Nickel, W., and Seedorf, M. (2008). "Unconventional Mechanisms of Protein Transport to the Cell Surface of Eukaryotic Cells." *Annu. Rev. Cell Dev. Biol.,* 24(1).

Nordlund, P., and Reichard, P. (2006). "Ribonucleotide Reductases." *Annu.Rev.Biochem.,* 75(1).

O'Rourke, D., Baban, D., Demidova, M., Mott, R., and Hodgkin, J. (2006). "Genomic clusters, putative pathogen recognition molecules, and antimicrobial genes are induced by infection of *C. elegans* with *M. nematophilum*." *Genome Res.,* 16(8).

Otten MA, and van Egmond M. (2004). "The Fc receptor for IgA (FcalphaRI, CD89)." *Immunol.Lett.,* 92(1-2), 1-2.

Pancholi V. (2001). "Multifunctional alpha-enolase: its role in diseases." *Cell. Mol. Life Sci,.* 58(7), 902-20.

Pelletier, I., Hashidate, T., Urashima, T., Nishi, N., Nakamura, T., Futai, M., Arata, Y., Kasai, K., Hirashima, M., Hirabayashi, J., and Sato, S. (2003). "Specific Recognition of *Leishmania major* Poly-beta-galactosyl Epitopes by Galectin-9." *J.Biol.Chem.,* 278(25).

POU-BARRETO, C., QUISPE-RICALDE, M. A., MORCHÓN, R., VÁZQUEZ, C., GENCHI, M., POSTIGO, I., VALLADARES, B., and SIMÓN, F. (2008). "Galectin and aldolase-like molecules are responsible for the specific IgE response in humans exposed to *Dirofilaria immitis*." *Parasite Immunol.,* 30(11-12), 596-602.

Rabinovich, G. A., and Toscano, M. A. (2009). "Turning 'sweet' on immunity: galectin-glycan interactions in immune tolerance and inflammation." *Nat. Rev. Immunol.,* 9(5).

Ramajo-Hernandez, A., Perez-Sanchez, R., Ramajo-Martin, V., and Oleaga, A. (2007). "*Schistosoma bovis*: Plasminogen binding in adults and the identification of plasminogen-binding proteins from the worm tegument." *Exp.Parasitol.,* 115(1), 83-91.

Rao SP, Wang Z, Zuberi RI, Sikora L, Bahaie NS, Zuraw BL, Liu FT, and Sriramarao P. (2007). "Galectin-3 functions as an adhesion molecule to support eosinophil rolling and adhesion under conditions of flow." *J. Immunol.,* 179(11), 7800-7.

Rosenfeld J, Capdevielle J, Guillemot JC, and Ferrara P. (1992). "In-gel digestion of proteins for internal sequence analysis after one- or two-dimensional gel electrophoresis." *Anal.Biochem.,* 203(1), 173-9.

Sato, M., Nishi, N., Shoji, H., Seki, M., Hashidate, T., Jun Hirabayashi, Ken-ichi Kasai, Hata, Y., Suzuki, S., Hirashima, M., and Nakamura, T. (2002). "Functional analysis of the carbohydrate recognition domains and a linker peptide of galectin-9 as to eosinophil chemoattractant activity." *Glycobiology,* 12(3), 191.

Smithers SR, and Terry RJ. (1969). "Immunity in schistosomiasis." *Ann.N.Y.Acad.Sci.,* 160(2), 826-40.

Smithers, S. R., and Terry, R. J. (1967). "Resistance to experimental infection with Schistosoma mansoni in rhesus monkeys induced by the transfer of adult worms." *Trans. R. Soc. Trop. Med. Hyg.,* 61(4), 517-533.

Sotillo, J., Valero, L., Sanchez del Pino, M.M., Fried, B., Esteban, J.G., Marcolla, A., and Toledo, R. (2008). "Identification of antigenic proteins from *Echinostoma caproni* (Trematoda) recognized by mouse immunoglobulins M, A and G using an immunoproteomic approach." *Parasite Immunol.,* 30(5), 271-279.

Spieth J, Denison K, Zucker E, and Blumenthal T. (1985). "The nucleotide sequence of a nematode vitellogenin gene." *Nucleic Acids Res.,* 13(19), 7129-38.

Thall A, and Galili U. (1990). "Distribution of Gal alpha 1-3Gal beta 1-4GlcNAc residues on secreted mammalian glycoproteins (thyroglobulin, fibrinogen, and immunoglobulin G) as measured by a sensitive solid-phase radioimmunoassay." *Biochemistry,* 29(16), 3959-65.

Truong MJ, Gruart V, Liu FT, Prin L, Capron A, and Capron M. (1993). "IgE-binding molecules (Mac-2/epsilon BP) expressed by human eosinophils. Implication in IgE-dependent eosinophil cytotoxicity." *Eur.J.Immunol.,* 23(12), 3230-5.

Tunio SA, Oldfield NJ, Berry A, Ala'Aldeen DA, Wooldridge KG, and Turner DP. (2010). "The moonlighting protein fructose-1, 6-bisphosphate aldolase of *Neisseria meningitidis*: surface localization and role in host cell adhesion." *Mol.Microbiol.,* 76(3), 605-15.

Turner DG, Wildblood LA, Inglis NF, and Jones DG. (2008). "Characterization of a galectin-like activity from the parasitic nematode, *Haemonchus contortus*, which modulates ovine eosinophil migration in vitro." *Vet.Immunol.Immunopathol.,* 122(1-2), 1-2.

van Die I., and Cummings R.D. (2010). "Glycan gimmickry by parasitic helminths: A strategy for modulating the host immune response?" *Glycobiology,* 20(1), 2-12.

Van Loon, L. C., Rep, M., and Pieterse, C. M. J. (2006). "Significance of Inducible Defense-related Proteins in Infected Plants." *Annu.Rev.Phytopathol.,* 44(1).

van Stijn CM, van den Broek M, Vervelde L, Alvarez RA, Cummings RD, Tefsen B, and van Die I. (2010). "Vaccination-induced IgG response to Galalpha1-3GalNAc glycan epitopes in lambs protected against *Haemonchus contortus* challenge infection." *Int.J.Parasitol.,* 40(2), 215-22.

Wallace A, Filbin ME, Veo B, McFarland C, Stepinski J, Jankowska-Anyszka M, Darzynkiewicz E, and Davis RE. (2010). "The nematode eukaryotic translation initiation factor 4E/G complex works with a trans-spliced leader stem-loop to enable efficient translation of trimethylguanosine-capped RNAs." *Mol.Cell.Biol.,* 30(8), 1958-70.

Wu AM, Singh T, Wu JH, Lensch M, André S, and Gabius HJ. (2006). "Interaction profile of galectin-5 with free saccharides and mammalian glycoproteins: probing its fine specificity and the effect of naturally clustered ligand presentation." *Glycobiology,* 16(6), 524-37.

Yang RY, Rabinovich GA, and Liu FT. (2008). "Galectins: structure, function and therapeutic potential." *Expert Rev. Mol. Med.,* 10.

Yatsuda AP, Krijgsveld J, Cornelissen AW, Heck AJ, and de Vries E. (2003). "Comprehensive analysis of the secreted proteins of the parasite *Haemonchus contortus* reveals extensive sequence variation and differential immune recognition." *J. Biol. Chem.,* 278(19), 16941-51.

Yazdanbakhsh, M. (1996). "IgE, eosinophils and mast cells in helminth infections." Ned Tijdschr Klin Chem, 21(4), 213-215.

Young AR, and Meeusen EN. (2004). "Galectins in parasite infection and allergic inflammation." *Glycoconj.J.,* 19(7-9), 7-9.

Zhan B, Liu S, Perally S, Xue J, Fujiwara R, Brophy P, Xiao S, Liu Y, Feng J, Williamson A, Wang Y, Bueno LL, Mendez S, Goud G, Bethony JM, Hawdon JM, Loukas A, Jones K, and Hotez PJ. (2005). "Biochemical characterization and vaccine potential of a heme-binding glutathione transferase from the adult hookworm *Ancylostoma caninum.*" *Infect.Immun.,* 73(10), 6903-11.

Zhan, B., Liu, Y., Badamchian, M., Williamson, A., Feng, J., Loukas, A., Hawdon, J. M., and Hotez, P. J. (2003). "Molecular characterisation of the Ancylostoma-secreted protein family from the adult stage of *Ancylostoma caninum.*" *Int.J.Parasitol.,* 33(9).

Chapter 4 : Implications and Future Prospects

4.1 Alpha-Gal at the Host-Parasite Interface

The current work investigated the secretory system of *Parelaphostrongylus tenuis* and identified glycoproteins that are secreted at the interface of this helminth and its deer host. The decision to focus on alpha-Gal-modified glycoproteins was based on their prior localization to the excretory gland, their unknown function, their presence in excreted/secreted (E/S) extracts from adult worms, and the fact that investigation of E/S proteins is consistent with other helminth research pursuing potential vaccine targets (Hewitson *et al.*, 2009). Knowledge that parasite-derived host-like glycans have been shown to shape host immune responses in support of chronic parasite infections (van Die and Cummings, 2010) was another reason for focusing on alpha-Gal-modified glycoproteins. Recent work has provided insight into helminth-mediated induction of T_H2 responses, a hallmark of helminth infection that enables their chronic survival (Gebreselassie *et al.* 2012). Based on the findings of this current study, a role for alpha-Gal in the modulation of modified T_H2 responses is proposed to help explain persistence and chronicity of helminth infections.

Alpha-Gal is localized to secretory glands of a number of Metastrongyloid nematodes, including *P. andersoni, P. odocoilei, Elaphostrongylus rangiferi,* and *Crenosoma vulpis.* It has been determined recently that *Haemonchus contortus*, a member of the

Trichostrongyloidea family, also has glycoproteins that are modified by alpha-Gal (van Stijn *et al.*, 2010). While the *H. contortus* alpha-Gal has yet to be localized within *H. contortus*, this finding indicates a distribution of alpha-Gal outside of the Metastrongyloid superfamily and suggests that it could be distributed more broadly in other families of parasitic nematodes. Further investigation into the phylogenetic distribution of the alpha-Gal epitope within parasitic nematodes should be explored to identify a model system where the immunoregulatory potential of alpha-Gal-modified proteins could be investigated more effectively.

4.2 Defining the Role for Alpha-Gal in Parasitism

The current work attempts to identify specific *P. tenuis* E/S proteins modified by alpha-Gal. This proved challenging because of complications whereby multiple proteins were represented in each spot on the 2D gel (Chapter 3). Accordingly, it is not possible to identify specifically any single protein that is modified by the alpha-Gal epitope. The lack of predicted N-glycosylation sites on some proteins helped to rule out them out as candidates modified by alpha-Gal but two or more candidate proteins were still represented in each spot. Further analysis is required to confirm the presence of alpha-Gal on specific E/S proteins. While affinity purification of alpha-Gal-modified E/S proteins should be possible using a monoclonal anti-alpha-Gal antibody (i.e., M86), the antibody is both extremely expensive and available in only low concentrations. The researcher that produced this antibody was consulted at the onset of this study and was unable to provide antibody at the concentration necessary for affinity purification (Uri

Galili, personal communication). An alternative approach might be the use of naturally occurring anti-alpha-Gal IgG from human serum. Humans and other Old World primates lost the ability to modify proteins with alpha-Gal due to a mutation in a galactosyltransferase and so humans generate antibodies against this epitope. Up to 1% of circulating IgG is directed at the alpha-Gal epitope (Galili 2005). Pre-adsorption of human serum against deglycosylated *P. tenuis* proteins should enable enrichment of polyclonal antibodies against alpha-Gal that do not cross-react with peptide/protein epitopes. However, acquisition of adult *P. tenuis* E/S proteins is also time and cost-intensive. Somatic extracts are comparatively more attainable and more abundant than are E/S products, albeit likely not as enriched for the secreted ASPs and galectin identified from MS/MS analysis. However, 2D gels/blots of more purified protein preparations would likely facilitate the identification of individual proteins modified by alpha-Gal. Given that the three ASPs and the single galectin identified from E/S products of adult *P. tenuis* are the most promising candidates for modification by alpha-Gal, the use of polyclonal antibodies to purify these specific proteins somatic extracts might prove more feasible. Subsequent assessment of glycosylation of these purified proteins with alpha-Gal could then be performed using the monoclonal antibody.

The ASPs identified in the current study are likely candidates for modification by alpha-Gal. While these proteins are abundant in parasitic nematodes (Yatsuda *et al.*, 2003), their specific function remains unknown. One exception is an ASP from *A. caninum* in dogs. This ASP has been termed NIF based upon its inhibition of neutrophil recruitment during infection (Moyle *et al.*, 1994). Assessment of alpha-Gal in *A. caninum* generally, and on NIF specifically, is of interest. Our model for alpha-Gal function during *P. tenuis*

infection proposes both impaired eosinophil recruitment and effector function (ADCC). Deglycosylation of NIF followed by reassessment of its neutrophil inhibition in the absence of N-linked glycans would seem an obvious experiment. Impaired neutrophil function would help define further a specific role for glycans in immune modulation during helminth infections. The proposed ligand Gal-3 recognizes numerous galactosyl-containing glycans and so epitopes other than alpha-Gal might serve a similar role in immune modulation of innate effector cells. Presence of alpha-Gal could be determined using M86 in Western blots of NIF and *A. caninum* extracts, as well as by immunohistochemistry.

Should alpha-Gal be secreted from other parasitic nematodes with better model systems for empirical assessment (i.e., *H. contortus*), experiments to assess the ability of alpha-Gal to inhibit eosinophil extravasation and/or activation of ADCC could be performed as described previously in studies unrelated to alpha-Gal (Gebreselassie *et al.*, 2012; Truong *et al.,* 1993). Alpha-Gal-modified proteins subjected to PNGase-F for removal of the alpha-Gal epitope would serve as a negative control during these experiments. These experiments would provide incredible insight into the specific role for alpha-Gal at the host-parasite interface.

4.3 Secretory Glands as Unique Organs for Protein Secretion

Many researchers studying helminth E/S proteins have focused on proteins that contained a signal peptide in earlier cDNA-based research projects (Nagaraj *et al.*,

2008). Perhaps surprisingly, many proteins in helminth E/S extracts lack a signal peptide (Hewitson *et al.*, 2009). Many of the *P. tenuis* E/S proteins identified from MS/MS analysis were also found to lack a signal peptide and neither did they possess characteristics compatible with leaderless protein secretion. This begs the question: "how are these proteins secreted?". Based on the anatomy of the glands in the secretory system of *P. tenuis* and other parasitic nematodes, secretory granules dominate the cytoplasm of these large cells. It seems likely that proteins are packaged stringently in secretory granules within the secretory glands and are secreted following an external stimulus via mechanisms that have yet to be discovered. Understanding these molecular interactions might reveal unique targets toward development of new anthelmintic drugs. Ivermectin is an anthelmintic drug used commonly to treat helminth infections. It causes paralysis by blocking glutamate-gated chloride channels (Glendinning *et al.*, 2011). The mechanism of action of ivermectin remains undefined (Moreno *et al.*, 2010). Treatment of filarial nematodes with this drug results in a decreased release of E/S proteins from a poorly-defined ES apparatus (Moreno *et al.*, 2010). The presence of a muscle-layer surrounding the ES vesicle suggests that protein movement from the vesicle to the excretory pore is an active process, and treatment with ivermectin blocks the release of E/S proteins (Moreno *et al.*, 2010). The possible emergence of anthelmintic resistance to ivermectin and its apparent undefined role in blocking protein secretion support more widespread investigation of both the anatomy and regulation of protein secretion from nematode secretory systems.

Bibliography

Galili, U. (2005). "The alpha-gal epitope and the anti-Gal antibody in xenotransplantation and in cancer immunotherapy." *Immunol. Cell Biol.,* 83(6), 674-686.

Gebreselassie NG, Moorhead AR, Fabre V, Gagliardo LF, Lee NA, Lee JJ, and Appleton JA. (2012). "Eosinophils preserve parasitic nematode larvae by regulating local immunity." *J. Immunol.,* 188(1), 417-25.

Glendinning, S. K., Buckingham, S. D., Sattelle, D. B., Wonnacott, S., and Wolstenholme, A. J. (2011). "Glutamate-Gated Chloride Channels of *Haemonchus contortus* Restore Drug Sensitivity to Ivermectin Resistant *Caenorhabditis elegans*." *PLoS ONE,* 6(7).

Hewitson, J. P., Grainger, J. R., and Maizels, R. M. (2009). "Helminth immunoregulation: The role of parasite secreted proteins in modulating host immunity." *Mol. Biochem. Parasitol.,* 167(1), 1-11.

Moreno Y, Nabhan JF, Solomon J, Mackenzie CD, and Geary TG. (2010). "Ivermectin disrupts the function of the excretory-secretory apparatus in microfilariae of *Brugia malayi*." *Proc. Natl. Acad. Sci. U.S.A.,* 107(46), 20120-5.

Nagaraj SH, Gasser RB, and Ranganathan S. (2008). "Needles in the EST haystack: large-scale identification and analysis of excretory-secretory (ES) proteins in parasitic nematodes using expressed sequence tags (ESTs)." *PLoS Negl. Trop. Dis.,* 2(9).

Truong MJ, Gruart V, Liu FT, Prin L, Capron A, and Capron M. (1993). "IgE-binding molecules (Mac-2/epsilon BP) expressed by human eosinophils. Implication in IgE-dependent eosinophil cytotoxicity." *Eur.J.Immunol.,* 23(12), 3230-5.

van Die I., and Cummings R.D. (2010). "Glycan gimmickry by parasitic helminths: A strategy for modulating the host immune response?" *Glycobiology,* 20(1), 2-12.

van Stijn CM, van den Broek M, Vervelde L, Alvarez RA, Cummings RD, Tefsen B, and van Die I. (2010). "Vaccination-induced IgG response to Galalpha1-3GalNAc glycan epitopes in lambs protected against *Haemonchus contortus* challenge infection." *Int.J.Parasitol.,* 40(2), 215-22.

Appendix 1

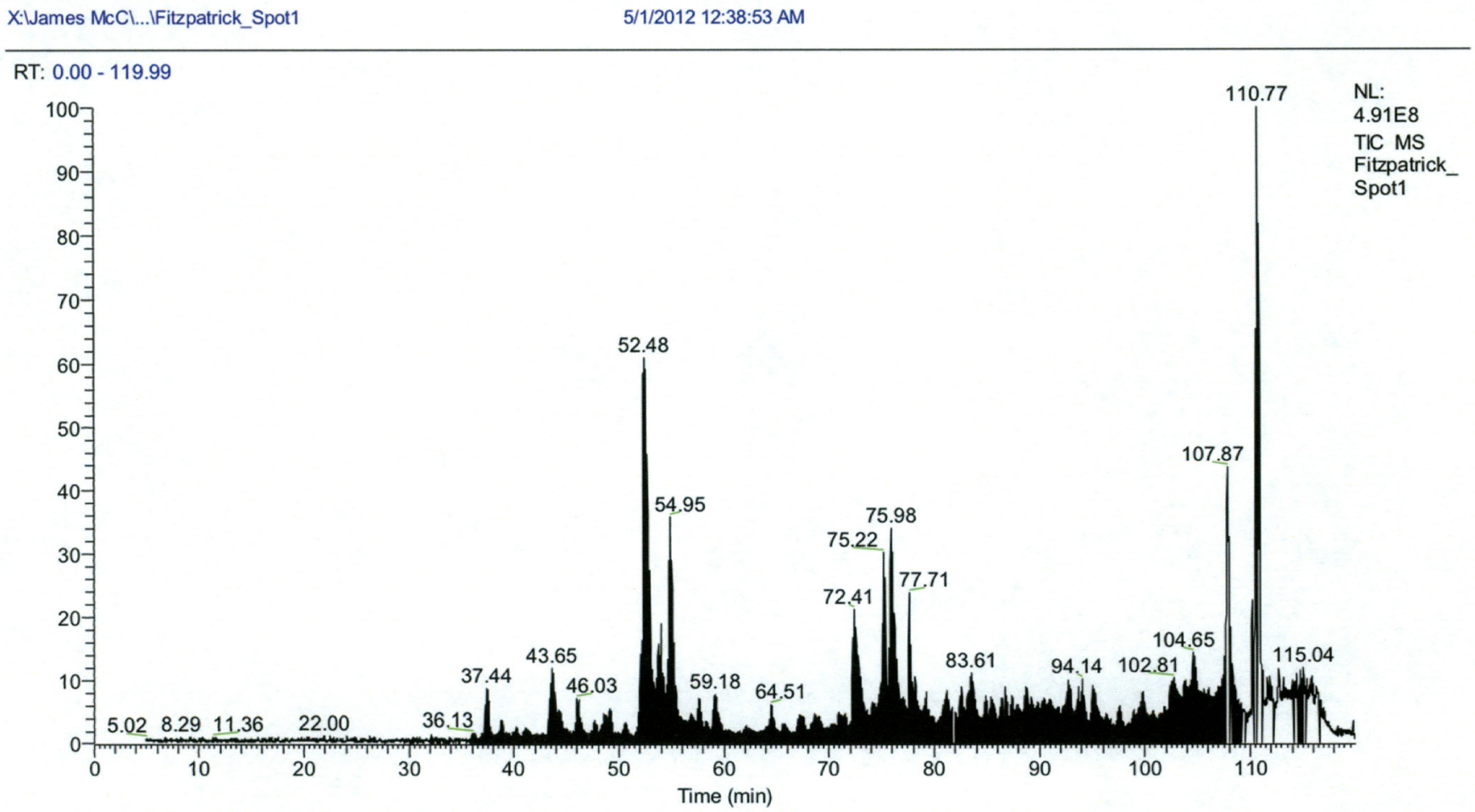


Figure A1-1 LC-MS/MS total ion current (TIC) chromatogram for Spot 1.

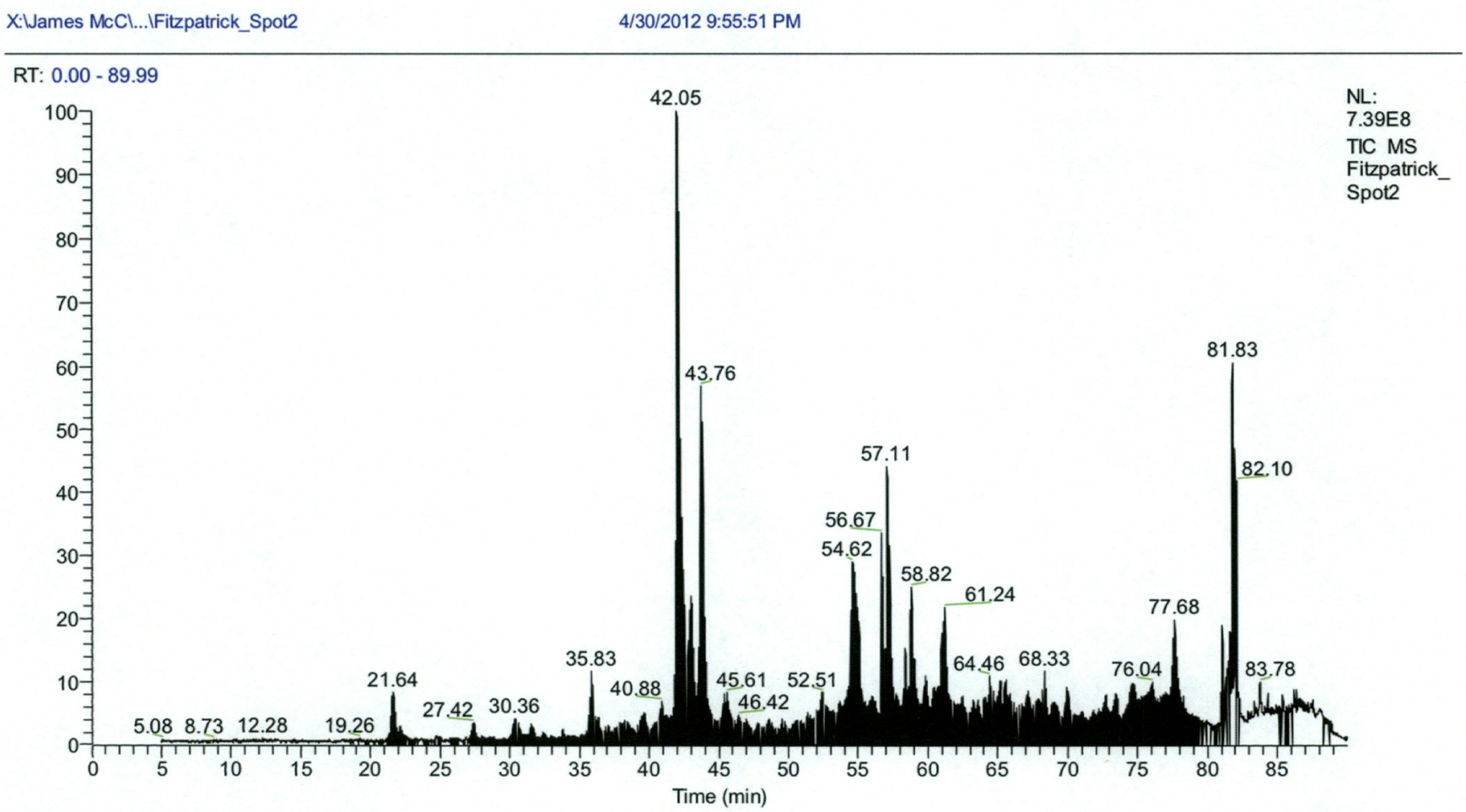


Figure A1-2 LC-MS/MS total ion current (TIC) chromatogram for Spot 2.

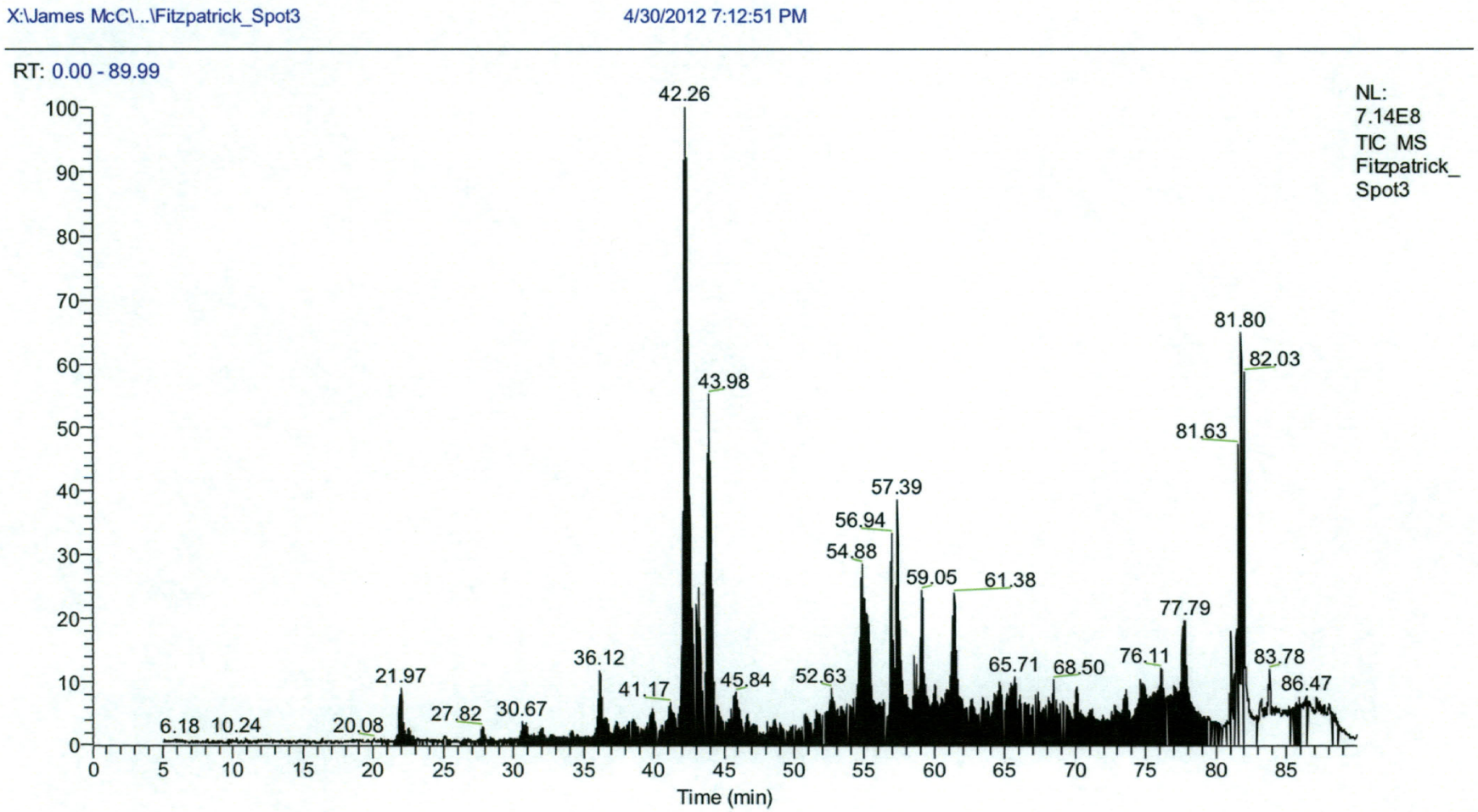


Figure A1-3 LC-MS/MS total ion current (TIC) chromatogram for Spot 3.

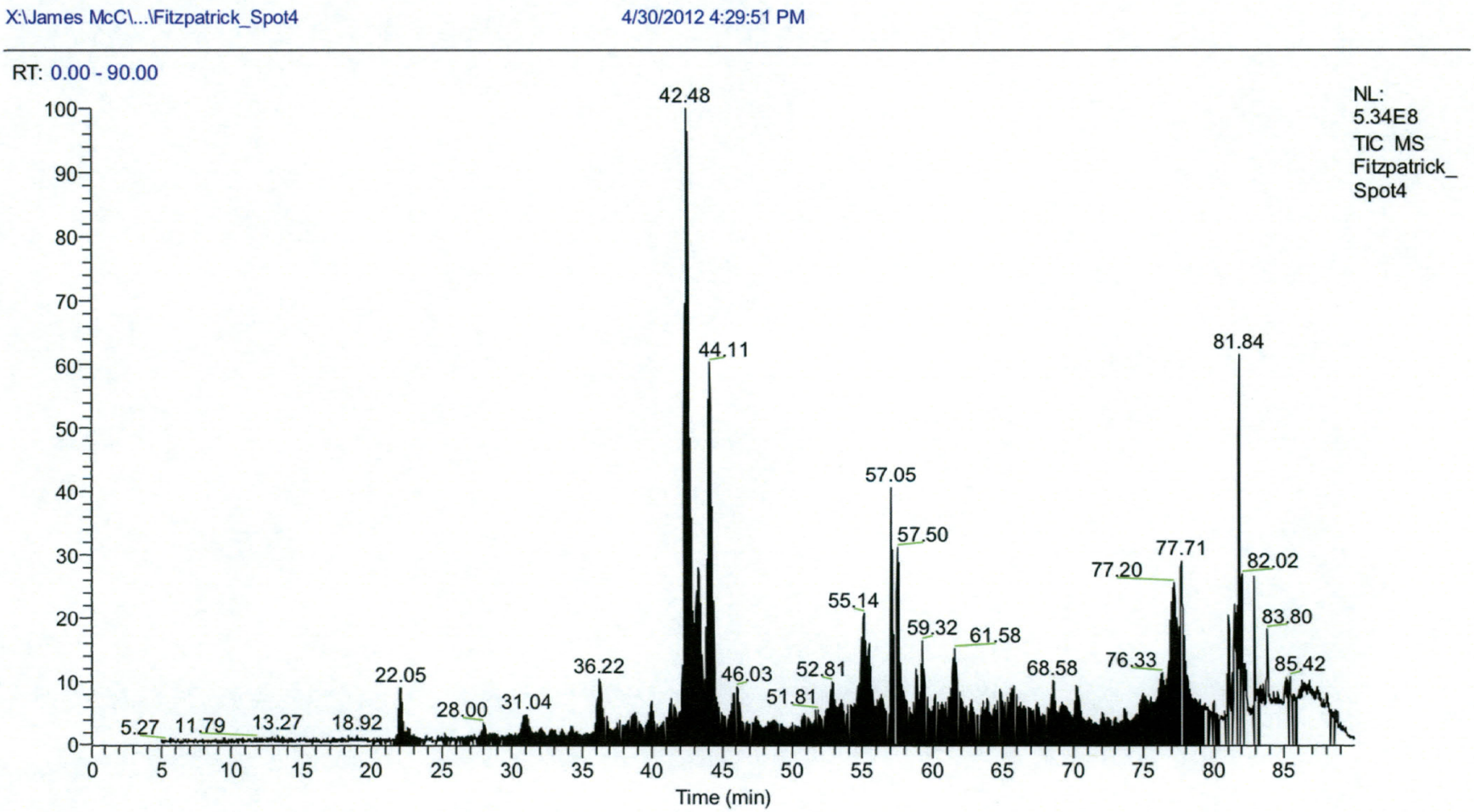


Figure A1-4 LC-MS/MS total ion current (TIC) chromatogram for Spot 4.

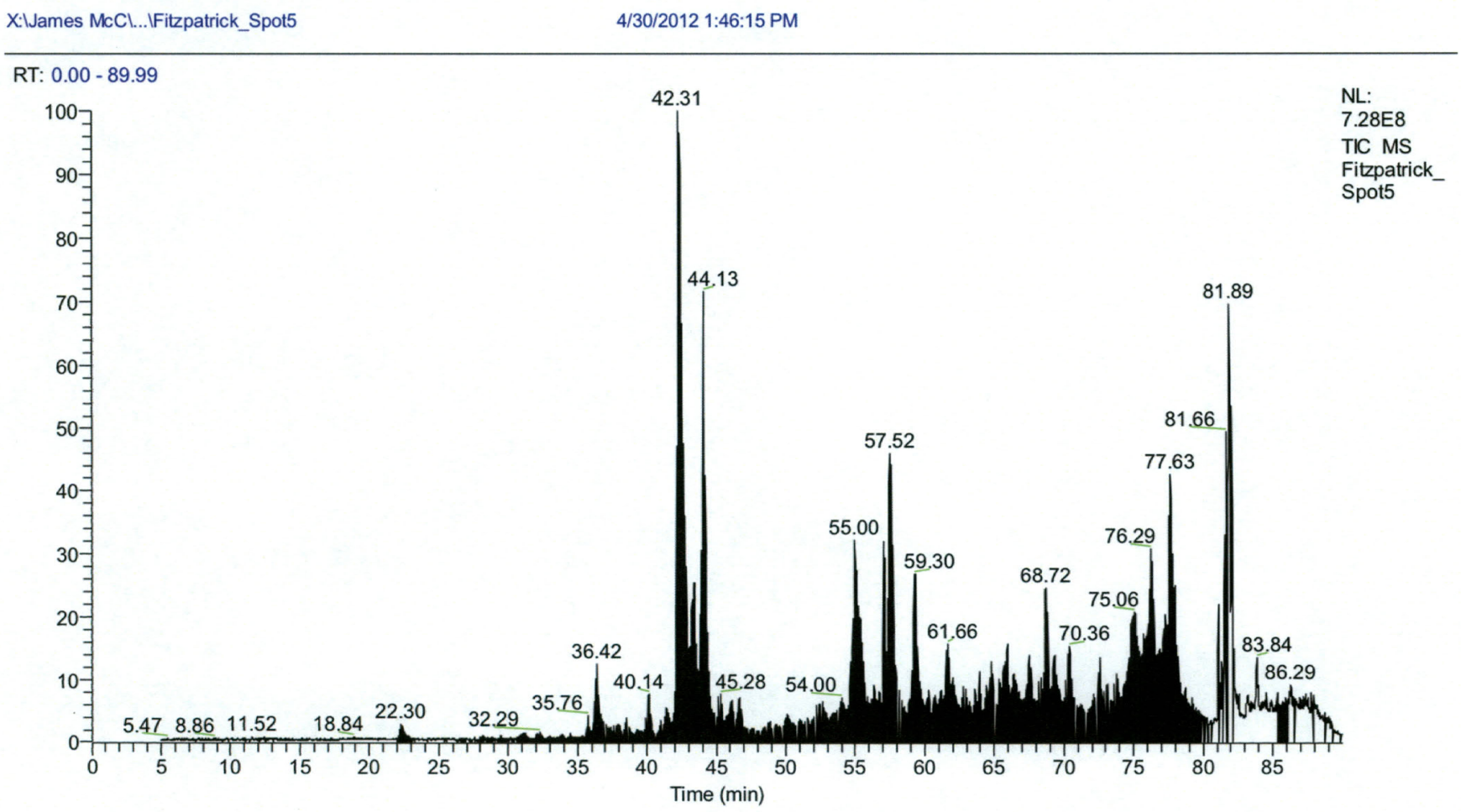


Figure A1-5 LC-MS/MS total ion current (TIC) chromatogram for Spot 5.

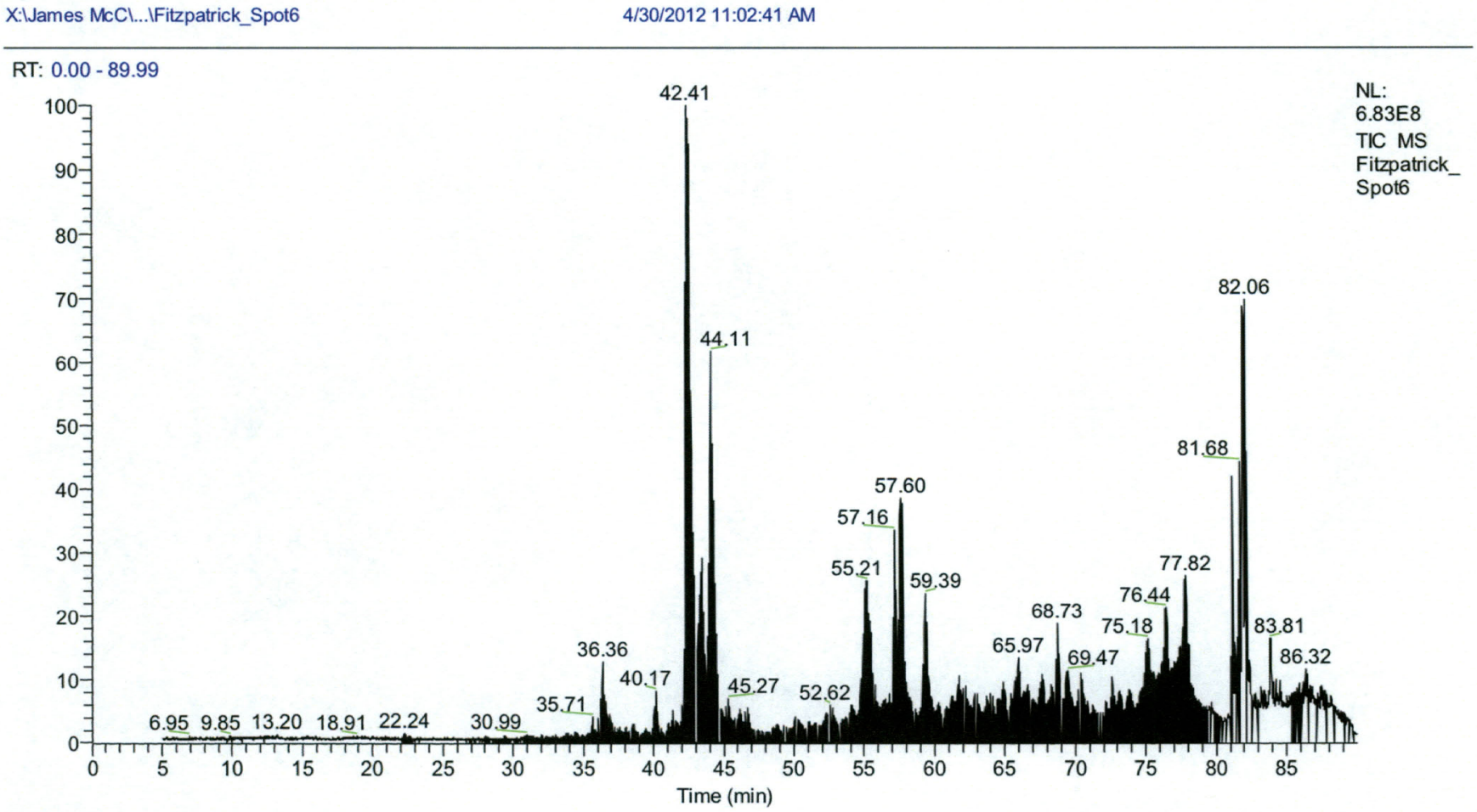


Figure A1-6 LC-MS/MS total ion current (TIC) chromatogram for Spot 6.

Appendix 2

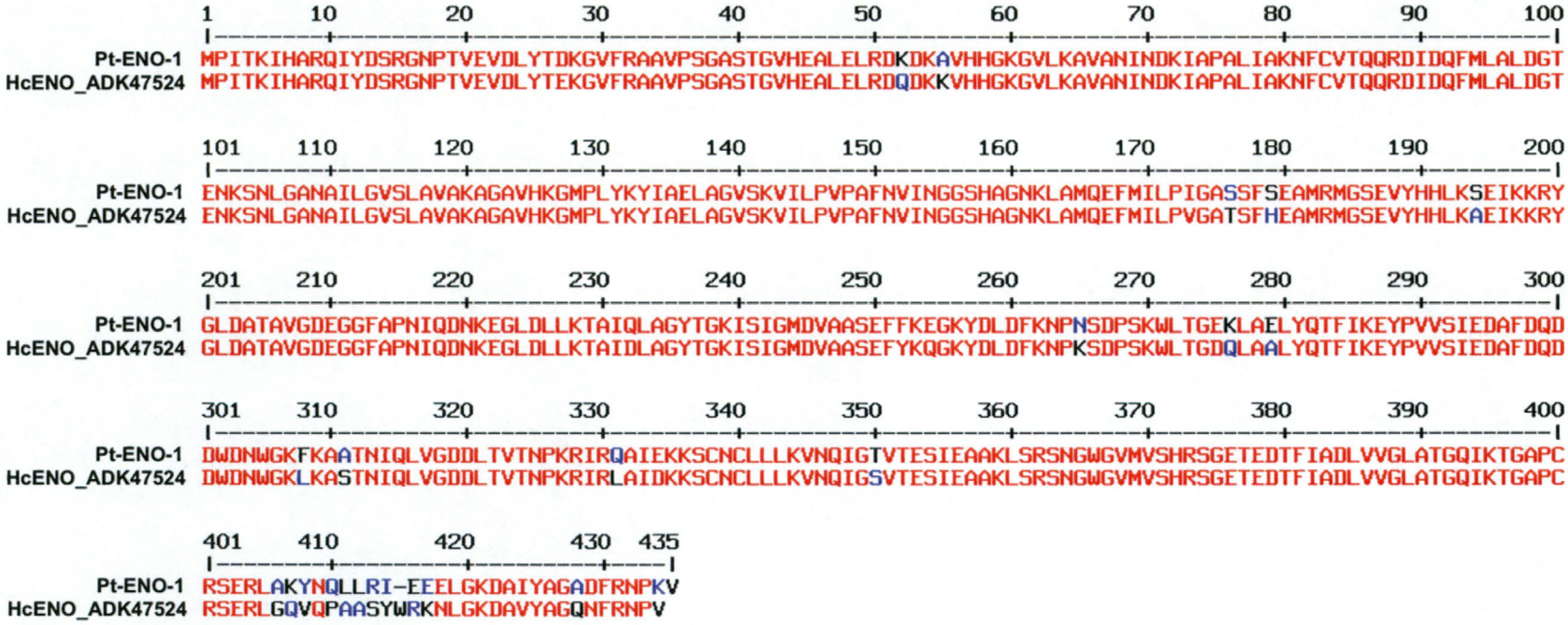


Figure A2-1 *P. tenuis* enolase has 92% identity with enolase of *Haemonchus contortus*. Alignment of Pt-ENO-1 with *H. contortus* enolase (ADK47524.1) was performed using the BLASTp program from NCBI. The amino acids displayed are in standard single-letter code and identical residues are in red.

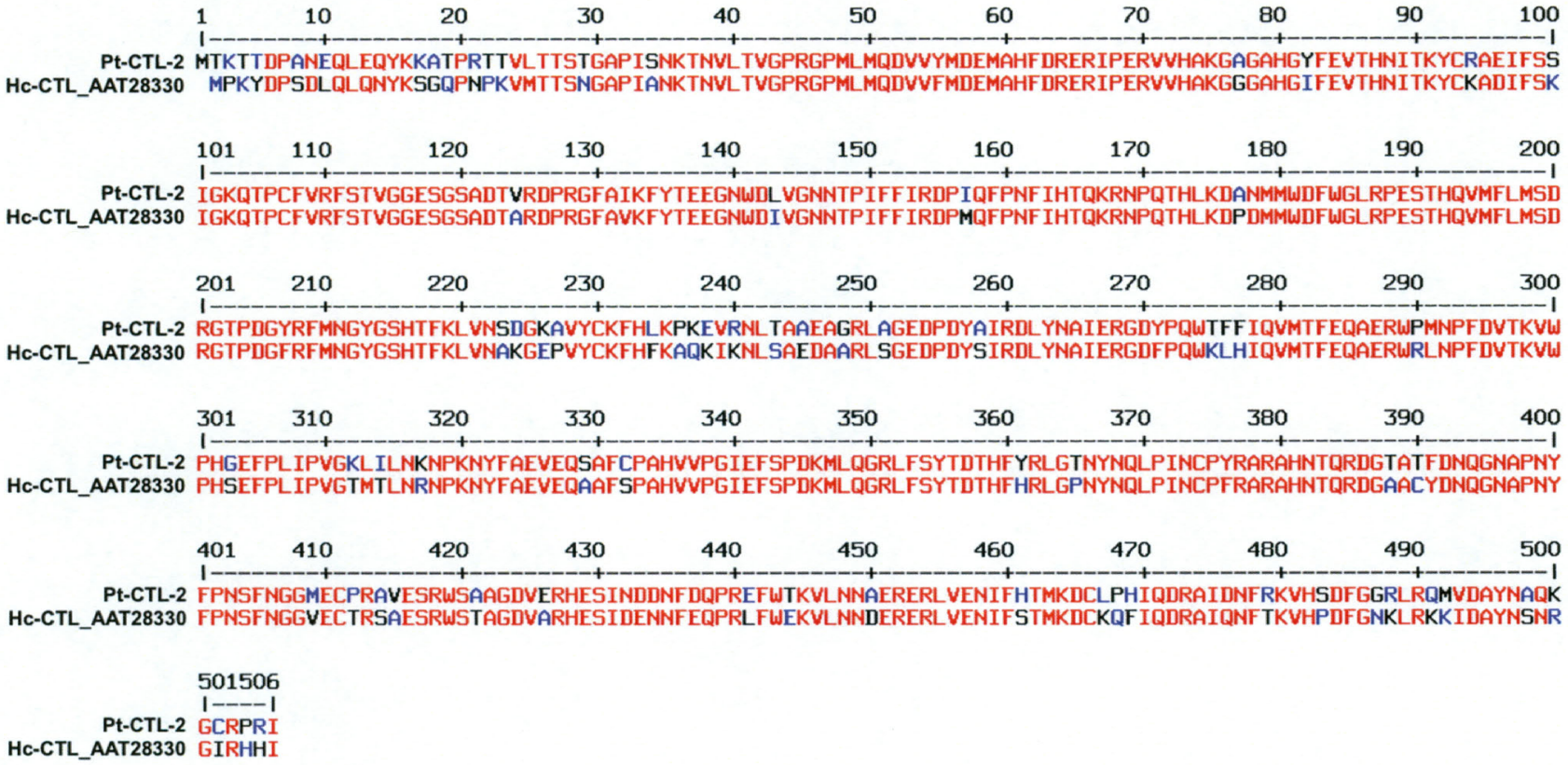


Figure A2-2 *P. tenuis* catalase has 81% identity with catalase of Haemonchus contortus. Alignment of Pt-CTL-2 with H. contortus catalase (AAT28330.1) was performed using the BLASTp program from NCBI. The amino acids displayed are in standard single-letter code and identical residues are in red.

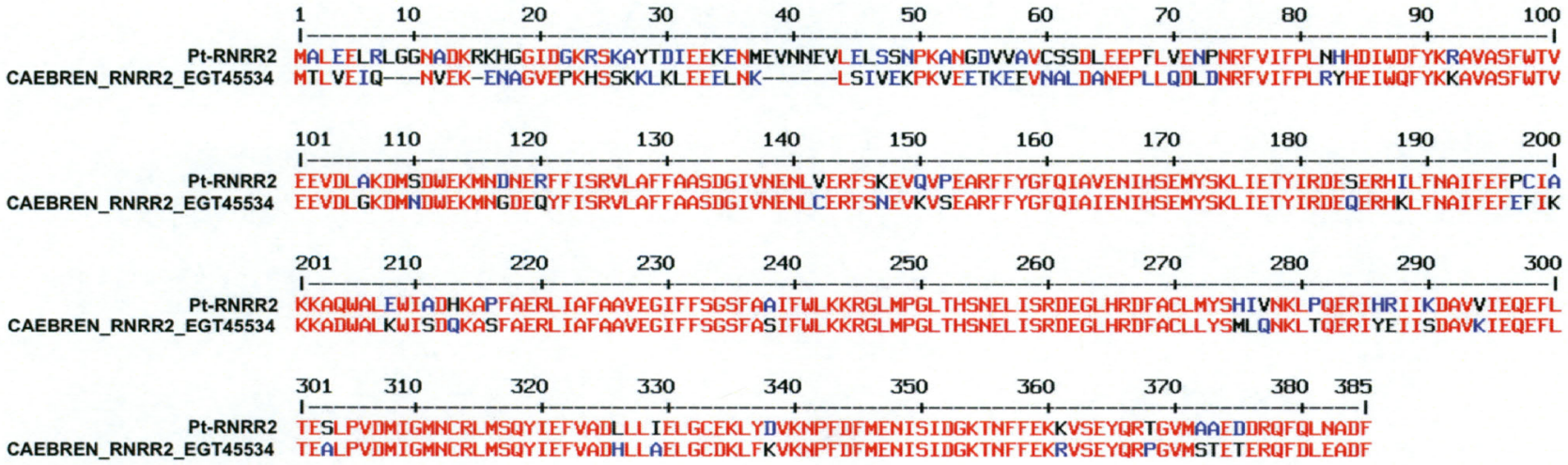


Figure A2-3 *P. tenuis* ribonucleotide reductase has 74% identity with ribonucleotide reductase of *Caenorhabditis brenneri*. Alignment of Pt-RNRR2 with *C. brenneri* ribonucleotide reductase (EGT45534.1) was performed using the BLASTp program from NCBI. The amino acids displayed are in standard single-letter code and identical residues are in red.

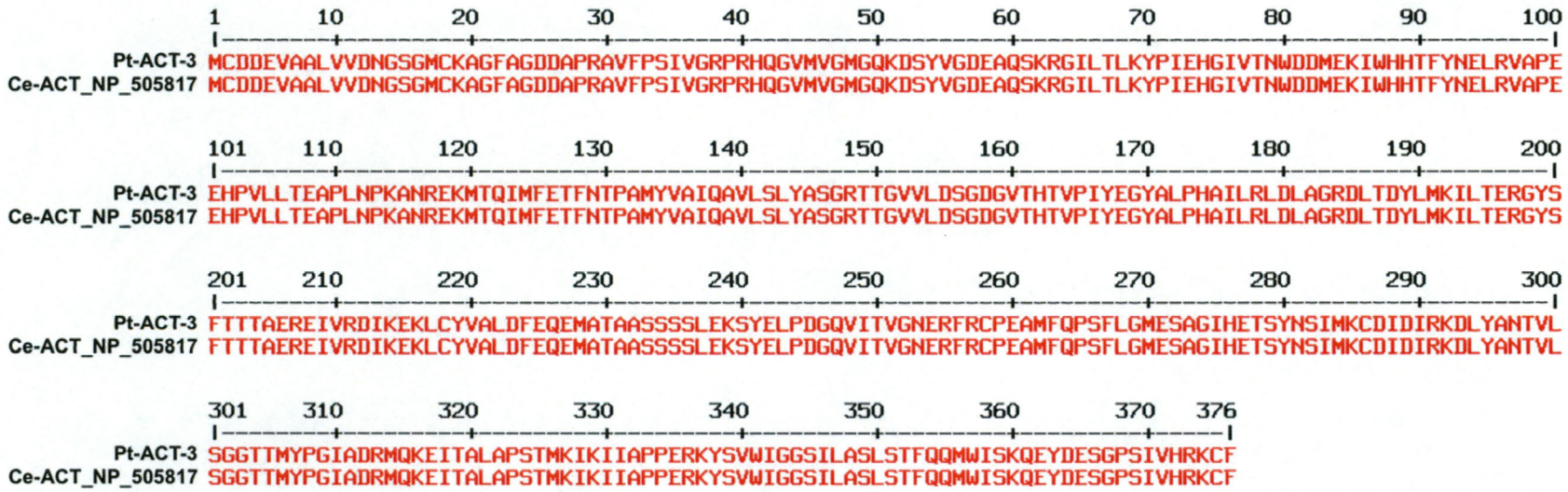


Figure A2-4 *P. tenuis* actin has 100% identity with actin of *Caenorhabditis elegans*. Alignment of Pt-ACT-3 with *C. elegans* actin (NP_505817.1) was performed using the BLASTp program from NCBI. The amino acids displayed are in standard single-letter code and identical residues are in red

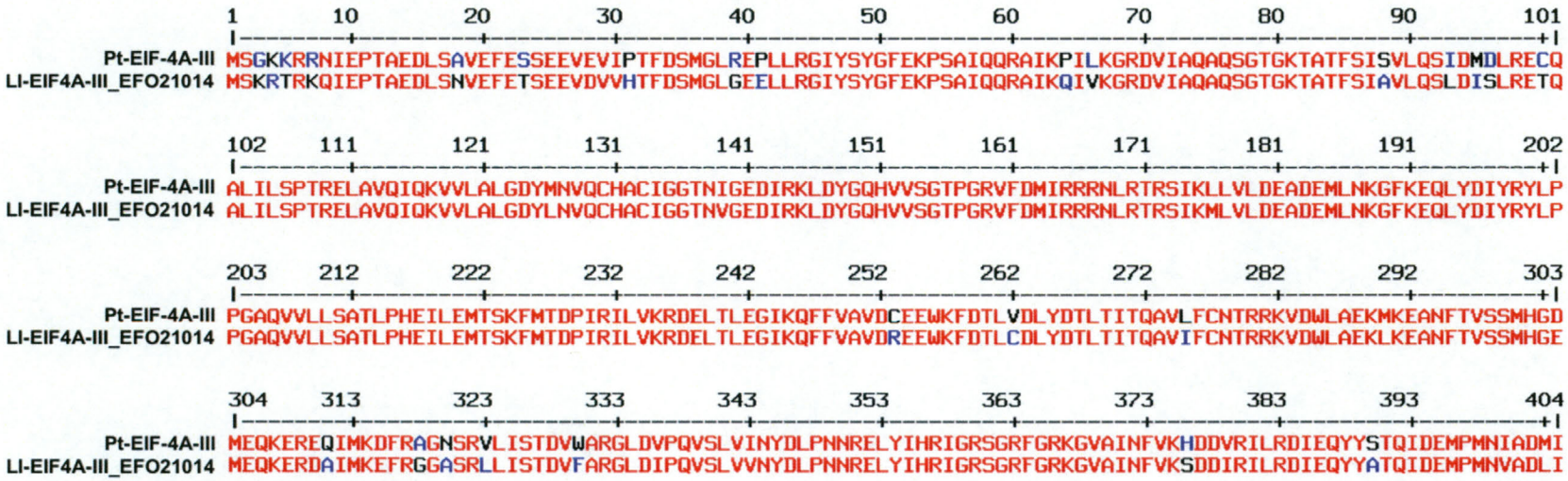


Figure A2-5 *P. tenuis* eukaryotic initiation factor has 90% identity with eukaryotic initiation factor of *Loa loa*. Alignment of Pt-EIF-4A-III with *Loa loa* eukaryotic initiation factor (EFO21014.2) was performed using the BLASTp program from NCBI. The amino acids displayed are in standard single-letter code and identical residues are in red.

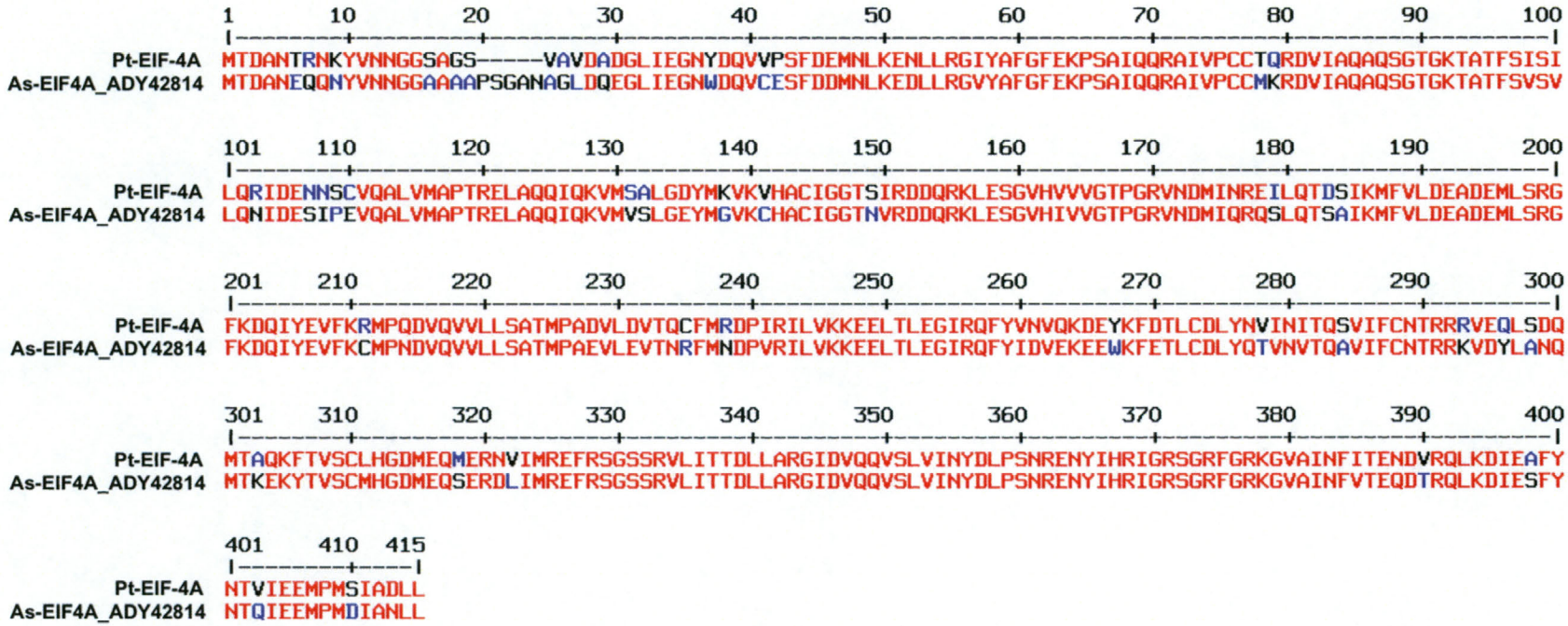


Figure A2-6 *P. tenuis* eukaryotic initiation factor has 90% identity with eukaryotic initiation factor of *Ascaris suum*. Alignment of Pt-EIF-4A with *A. suum* eukaryotic initiation factor (ADY42814) was performed using the BLASTp program from NCBI and graphic developed using the MultAlin sequence alignment program. The amino acids displayed are in standard single-letter code and identical residues are in red.

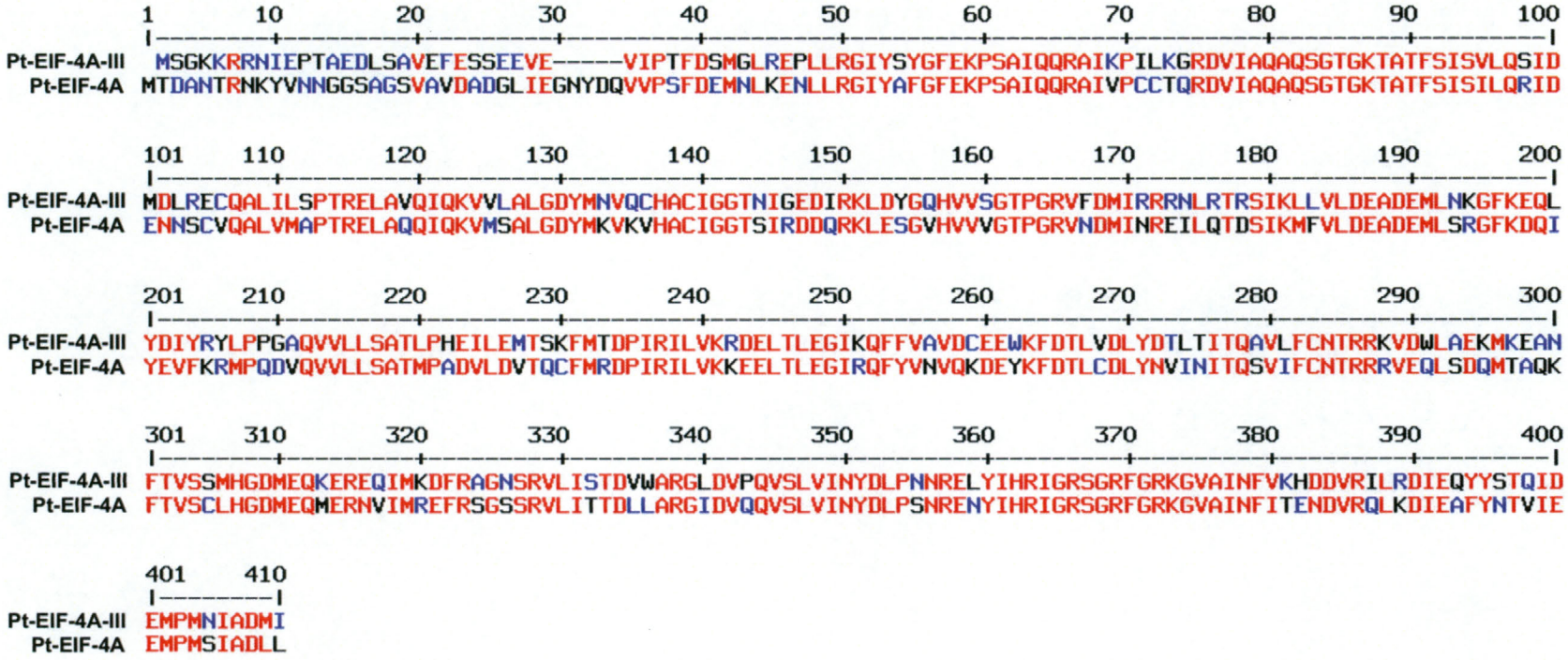


Figure A2-7 *P. tenuis* eukaryotic initiation factor paralogues have 69% identity with each other. The alignment graphic of Pt-EIF-4A with Pt-EIF-4A-III was developed using the MultAlin sequence alignment program. The amino acids displayed are in standard single-letter code and identical residues are in red.

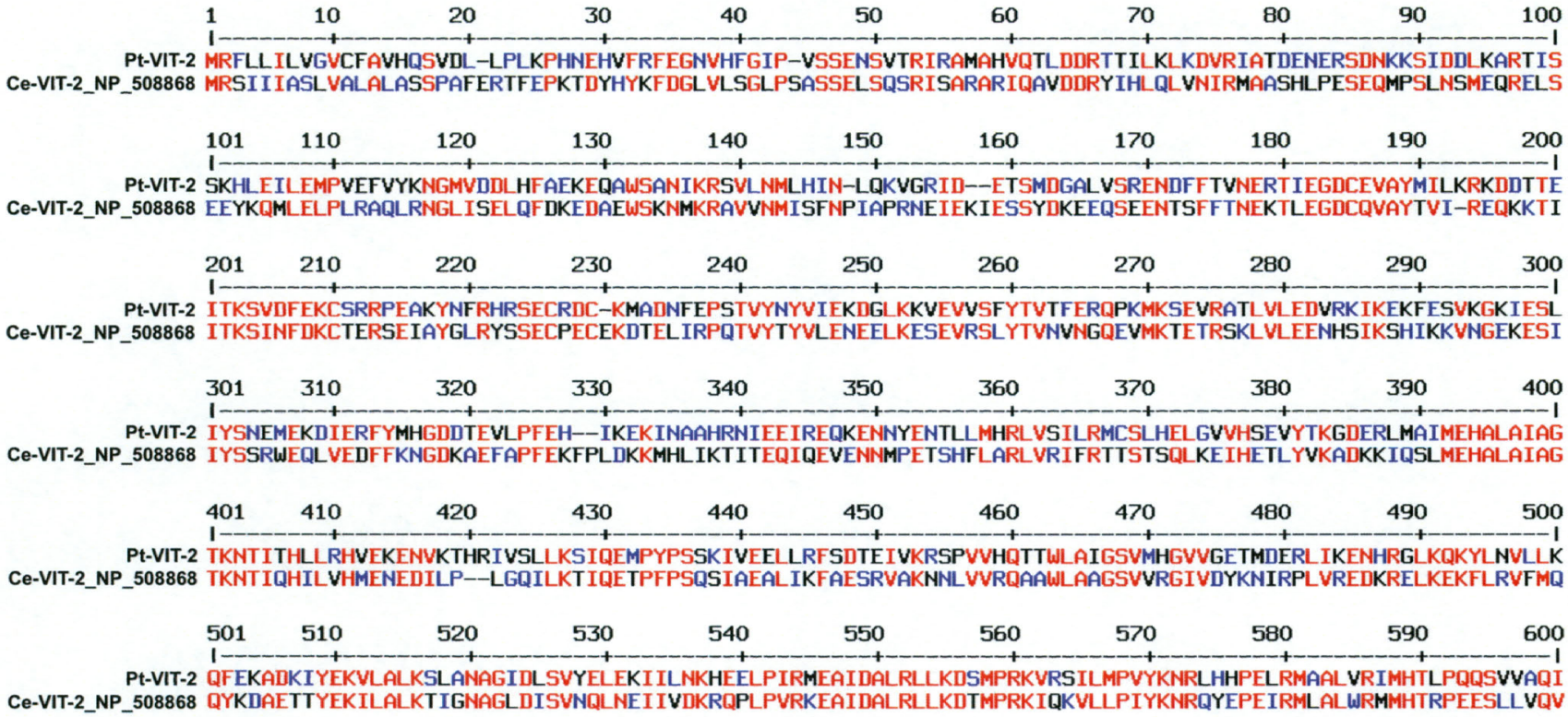


Figure A2-8 *P. tenuis* vitellogenin has 39% identity with vitellogenin of *Caenorhabditis elegans*. Alignment of Pt-VIT-2 with *C. elegans* vitellogenin (NP_508868) was performed using the BLASTp program from NCBI. The amino acids are displayed in standard single-letter code and identical residues are in red.

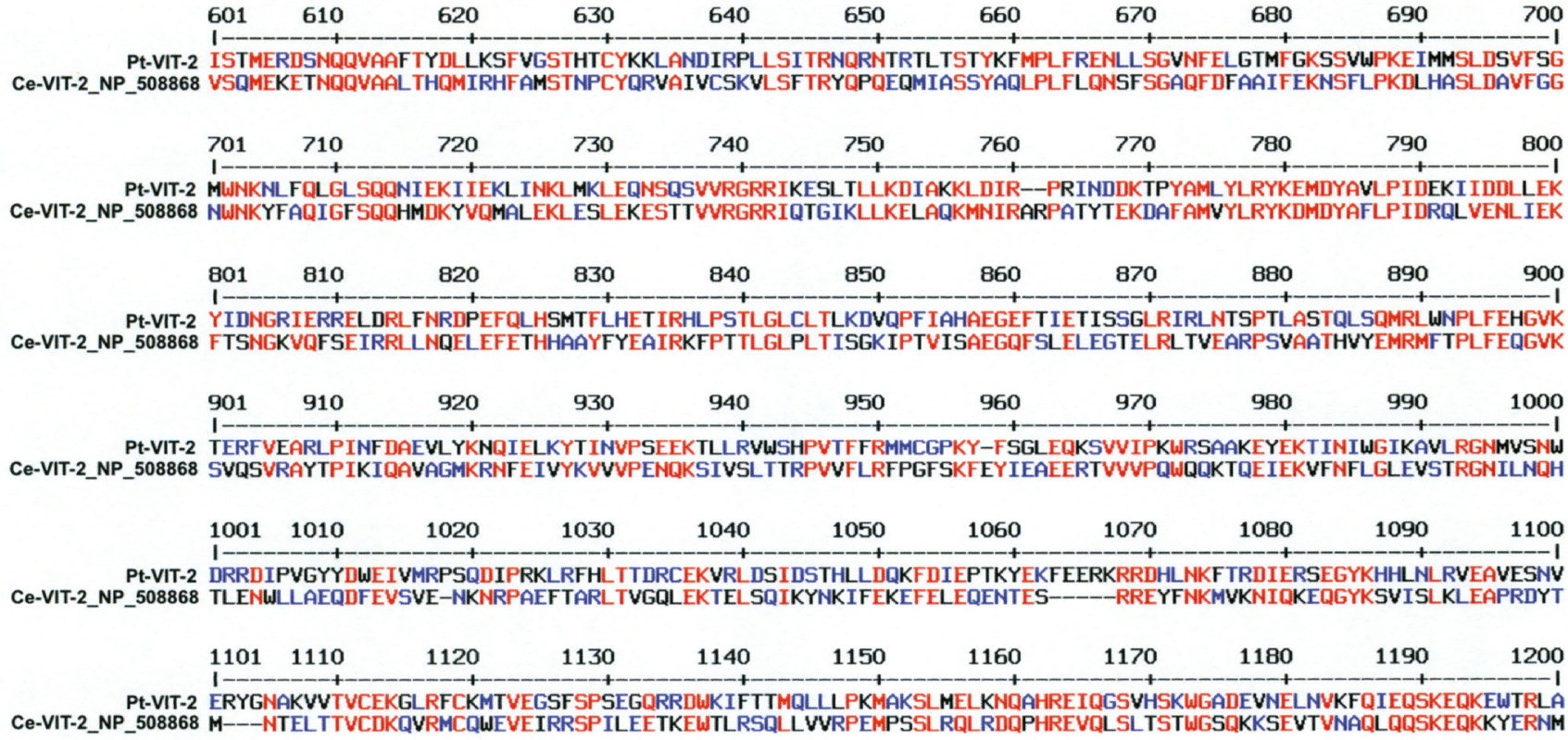


Figure A2-9 *P. tenuis* vitellogenin has 39% identity with vitellogenin of *Caenorhabditis elegans*. Alignment of Pt-VIT-2 with *C. elegans* vitellogenin (NP_508868) was performed using the BLASTp program from NCBI. The amino acids are displayed in standard single-letter code and identical residues are in red. (con'd)

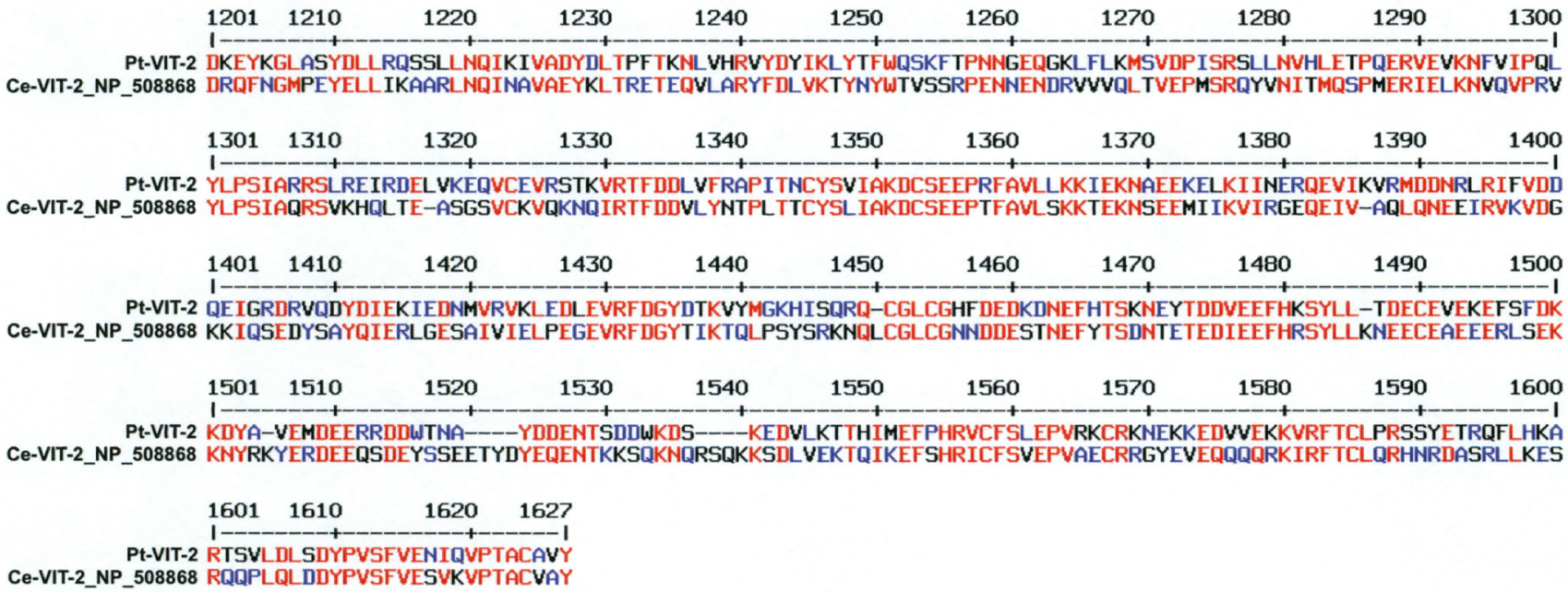


Figure A2-10 *P. tenuis* vitellogenin has 39% identity with vitellogenin of *Caenorhabditis elegans*. Alignment of Pt-VIT-2 with *C. elegans* vitellogenin (NP_508868) was performed using the BLASTp program from NCBI. The amino acids are displayed in standard single-letter code and identical residues are in red. (con'd)

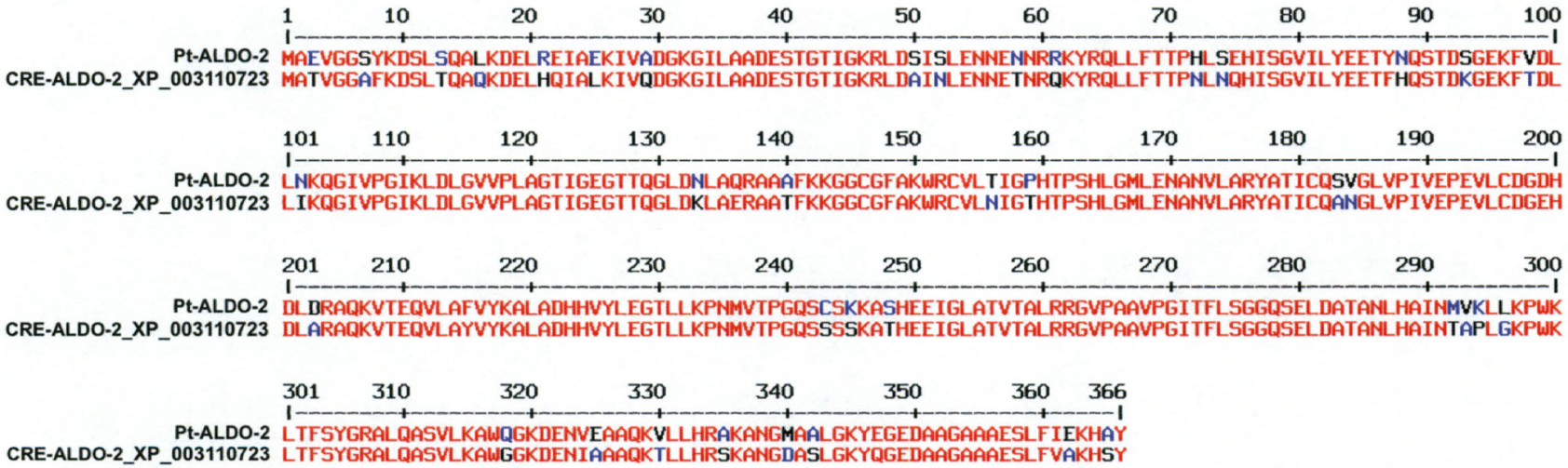


Figure A2-11 *P. tenuis* fructose-1,6-bisphosphate (FBP) aldolase has 87% identity with FBP aldolase of *Caenorhabditis remanei*. Alignment of Pt-ALDO-2 with *C. remanei* FBP aldolase (XP_003110723.1) was performed using the BLASTp program from NCBI. The amino acids are displayed in standard single-letter code and identical residues are in red.

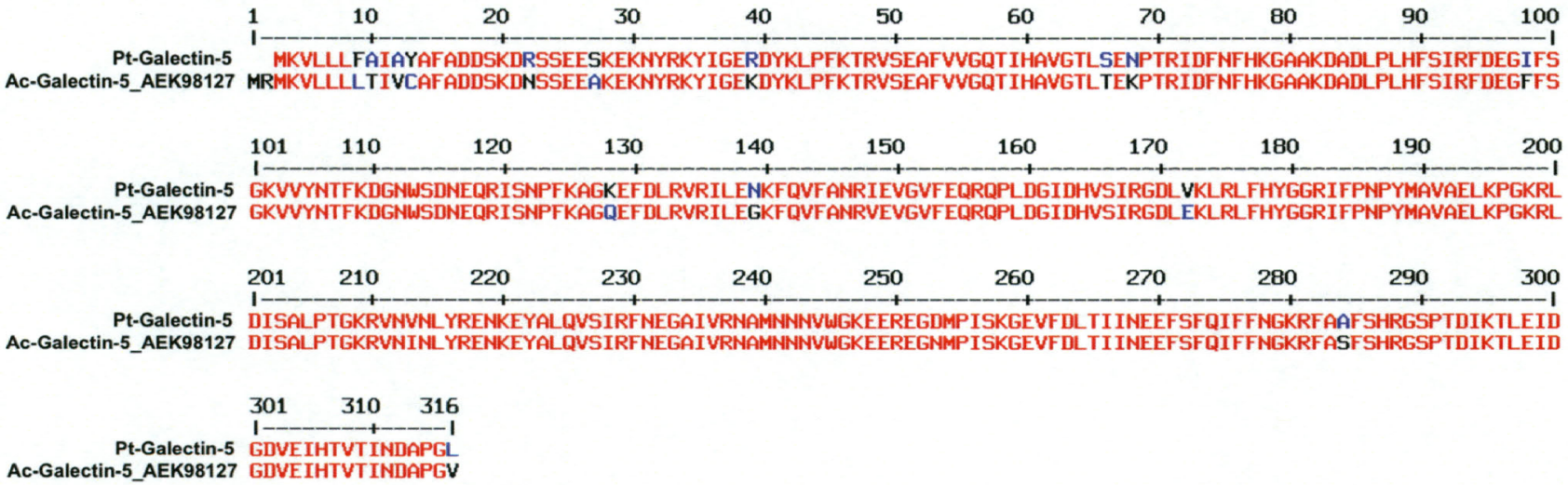


Figure A2-12 *P. tenuis* galectin has 94% identity with galectin of *Angiostrongylus cantonensis*. Alignment of Pt-Galectin-5 with *A. cantonensis* galectin (AEK98127) was performed using the BLASTp program from NCBI. The amino acids are displayed in standard single-letter code and identical residues are in red.

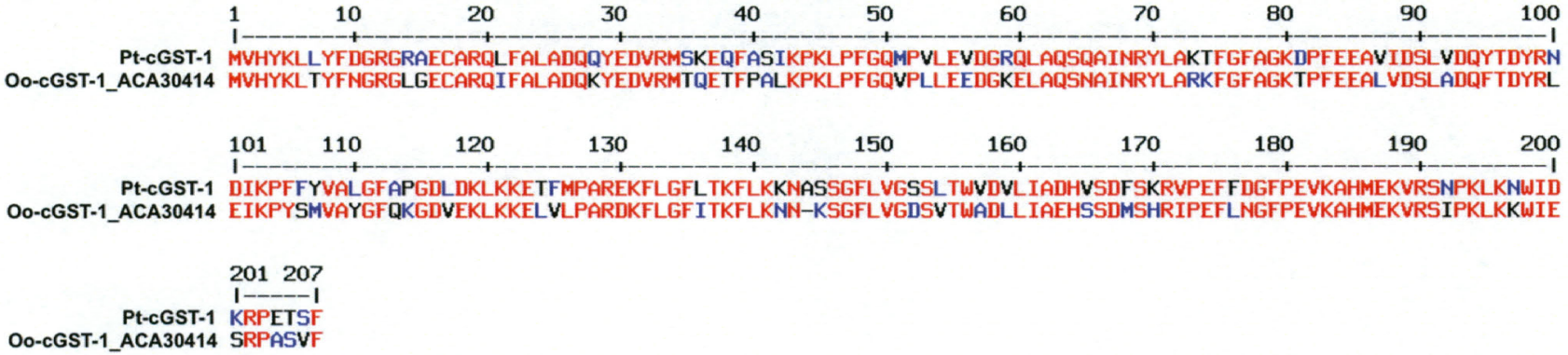


Figure A2-13 *P. tenuis* cytosolic glutathione-S-transferase (GST) has 71% identity with cytosolic GST of *Oesophagostomum dentatum*. Alignment of Pt-cGST-1 with *O. dentatum* cytosolic GST (ACA30414) was performed using the BLASTp program from NCBI. The amino acids are displayed in standard single-letter code and identical residues are in red.

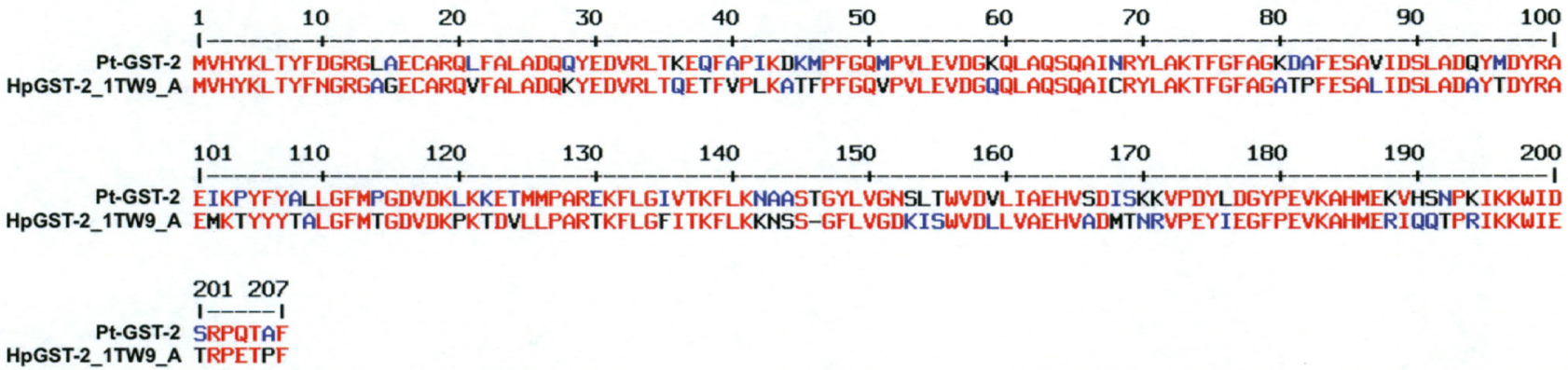


Figure A2-14 *P. tenuis* glutathione-S-transferase (GST) has 68% identity with GST of *Heligmosomoides polygyrus*. Alignment of Pt-GST-2 with *H. polygyrus* GST (1TW9_A) was performed using the BLASTp program from NCBI. The amino acids are displayed in standard single-letter code and identical residues are in red.

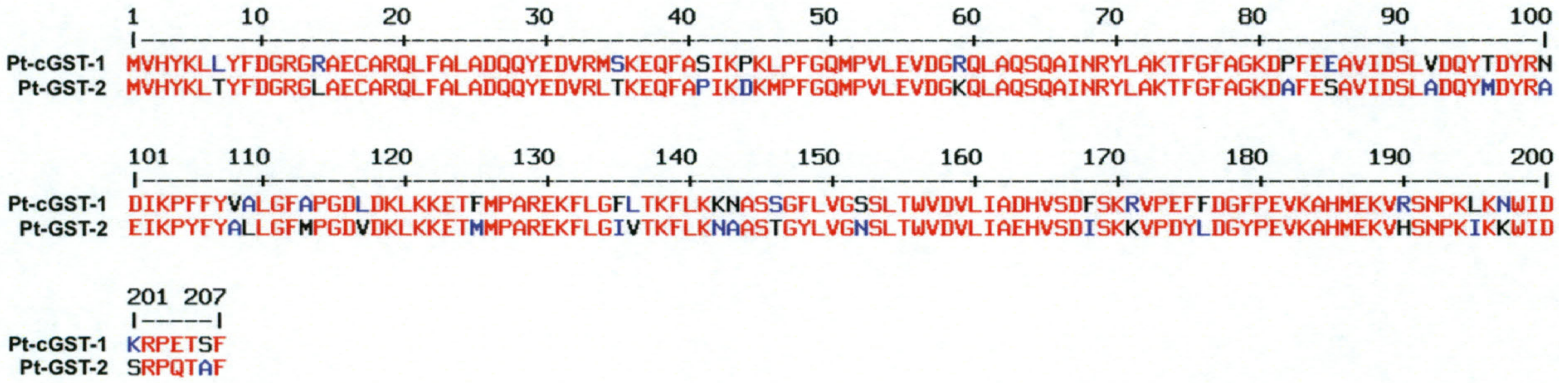


Figure A2-15 *P. tenuis* glutathione-S-transferase paralogues have 86% identity with each other. The alignment graphic of Pt-cGST-1 with Pt-GST-2 was developed using the MultAlin sequence alignment program. The amino acids displayed are in standard single-letter code and identical residues are in red.

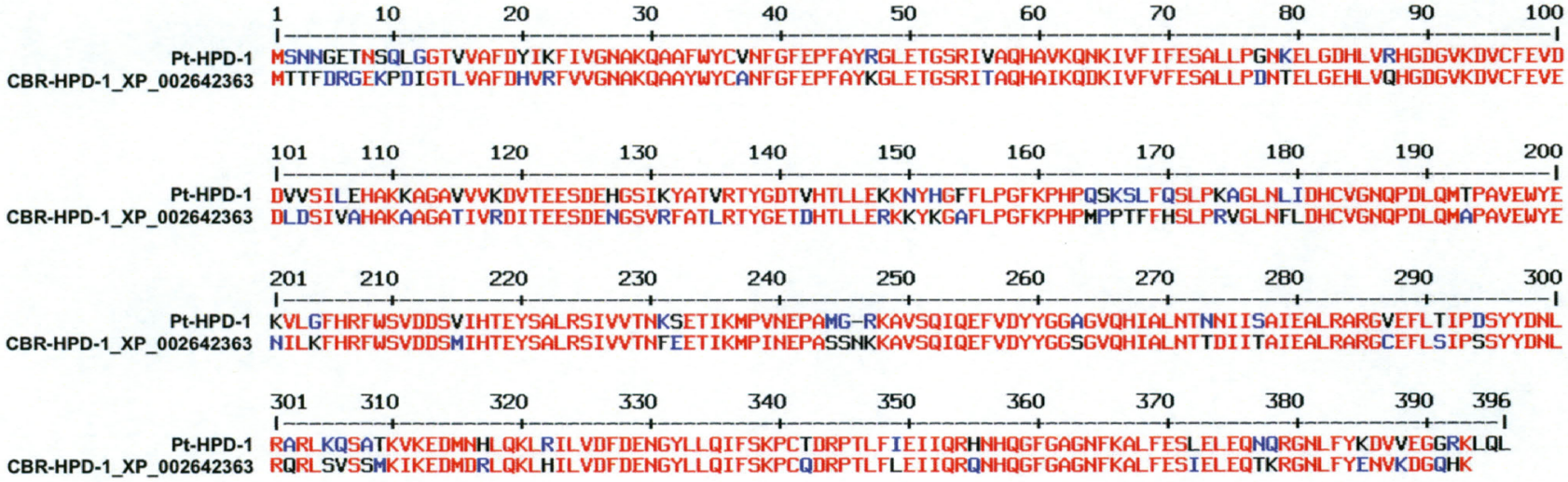


Figure A2-16 *P. tenuis* 4-hydroxyphenylpyruvate dioxygenase (HPPD) has 77% identity with HPPD of *Caenorhabditis briggsae*. Alignment of Pt-HPD-1 with *C. briggsae* HPPD (XP_002642363.1) was performed using the BLASTp program from NCBI. The amino acids are displayed in standard single-letter code and identical residues are in red.

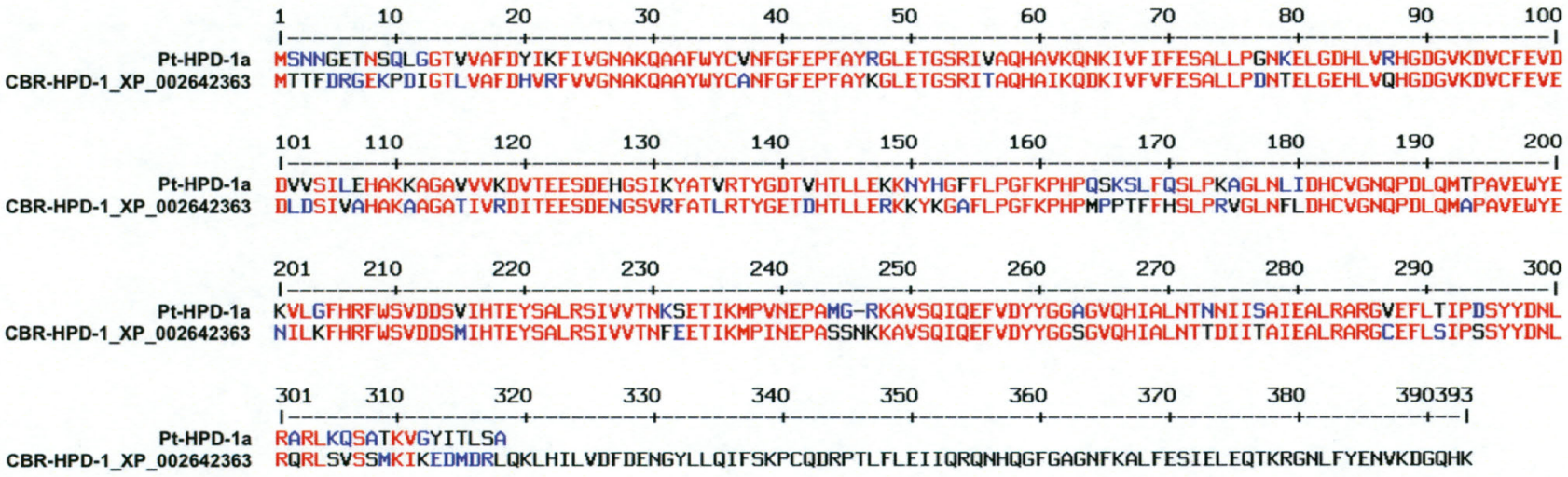


Figure A2-17 *P. tenuis* 4-hydroxyphenylpyruvate dioxygenase (HPPD) has 76% identity with HPPD of *Caenorhabditis briggsae*. Alignment of Pt-HPD-1a with *C. briggsae* HPPD (XP_002642363.1) was performed using the BLASTp program from NCBI. The amino acids are displayed in standard single-letter code and identical residues are in red.

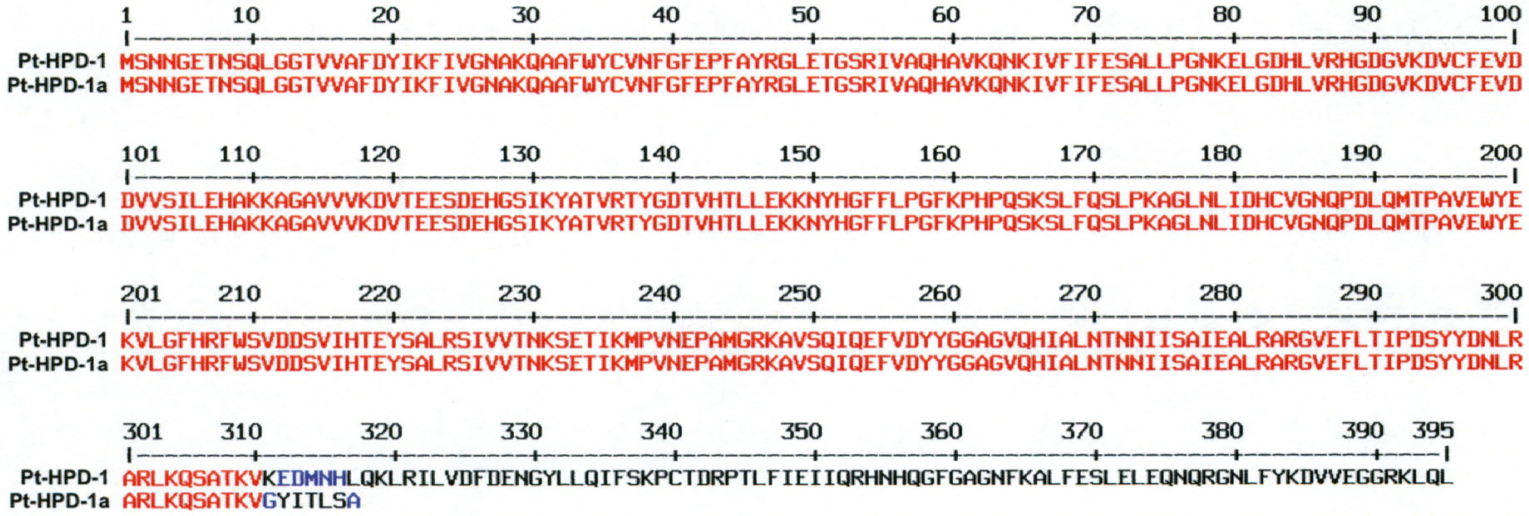


Figure A2-18 *P. tenuis* 4-hydroxyphenylpyruvate dioxygenase (HPPD) paralogues have 98% identity with each other. The alignment graphic of Pt-HPD-1 with Pt-HPD-1a was developed using the MultAlin sequence alignment program. The amino acids displayed are in standard single-letter code and identical residues are in red.

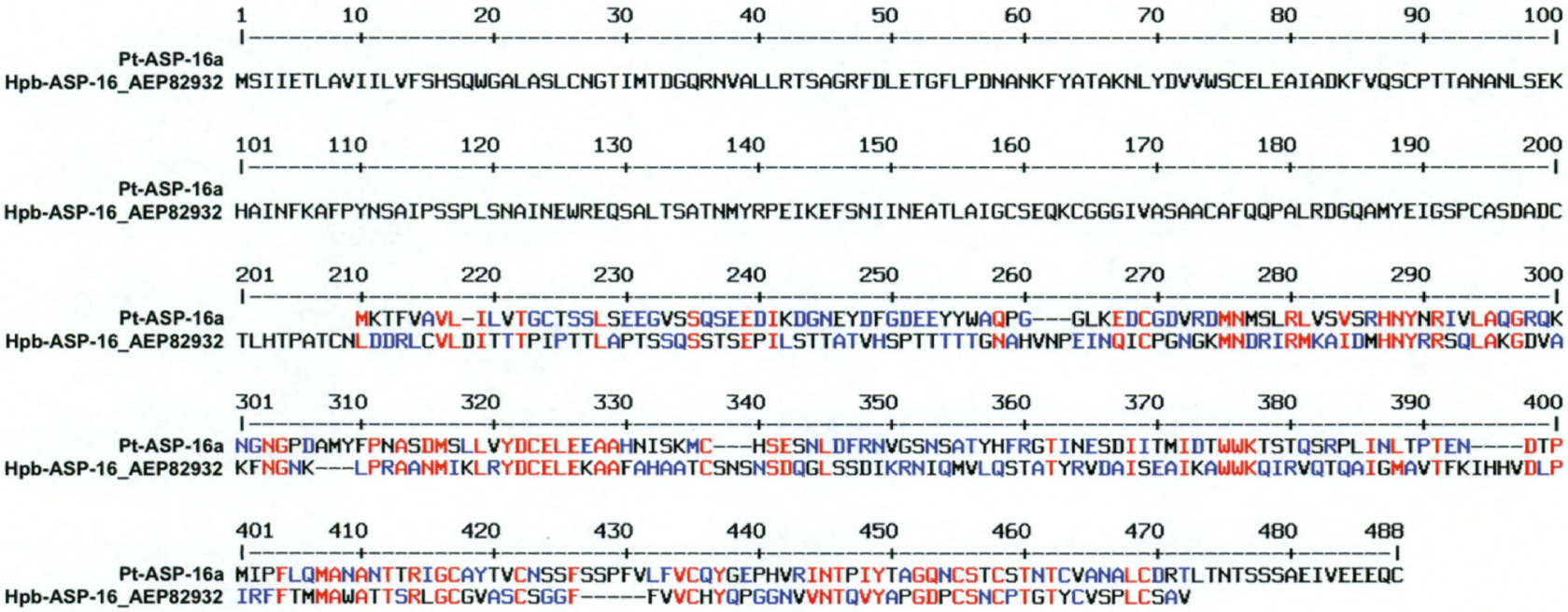


Figure A2-19 *P. tenuis* Ancylostoma secreted protein (ASP) has 32% identity with ASP of *Heligmosomoides polygyrus bakeri*. Alignment of Pt-ASP-16a with *H. polygyrus bakeri* ASP (AEP82932.1) was performed using the BLASTp program from NCBI. The amino acids are displayed in standard single-letter code and identical residues are in red.

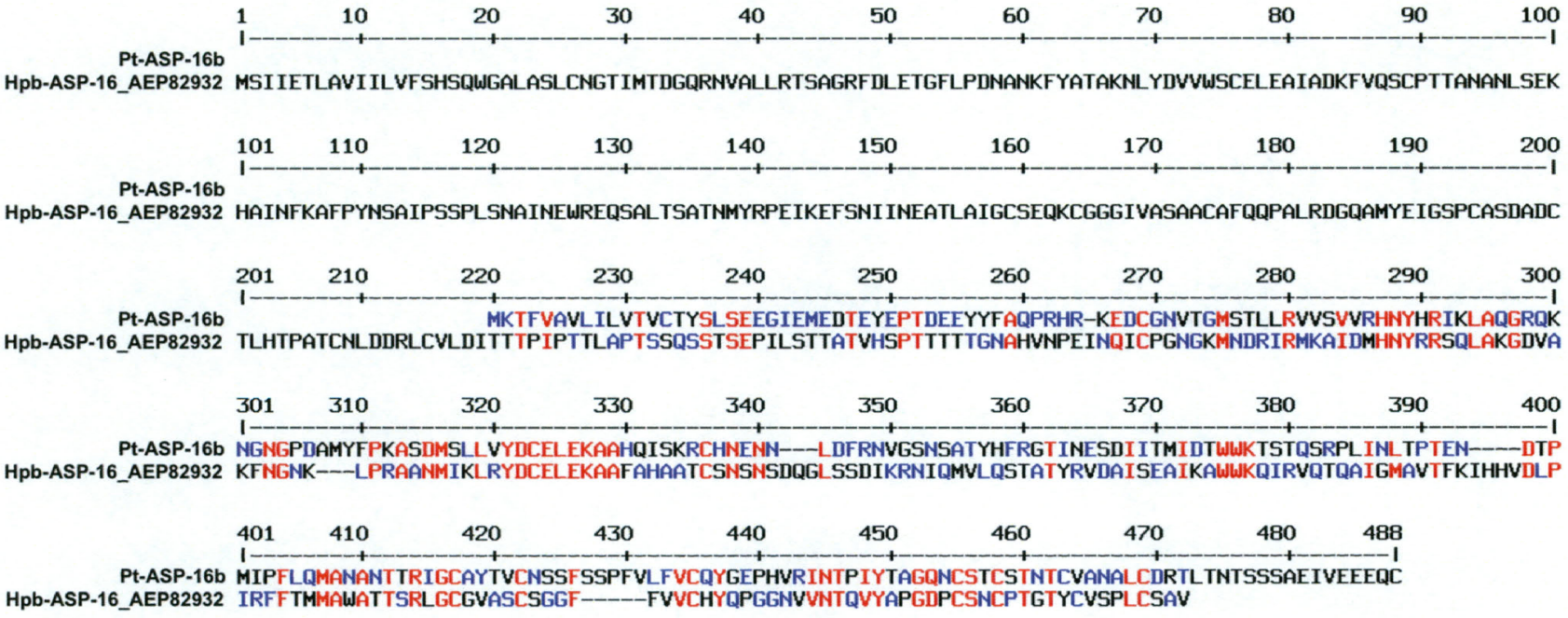


Figure A2-20 *P. tenuis* Ancylostoma secreted protein (ASP) has 32% identity with ASP of *Heligmosomoides polygyrus bakeri*. Alignment of Pt-ASP-16b with *H. polygyrus bakeri* ASP (AEP82932.1) was performed using the BLASTp program from NCBI. The amino acids are displayed in standard single-letter code and identical residues are in red.

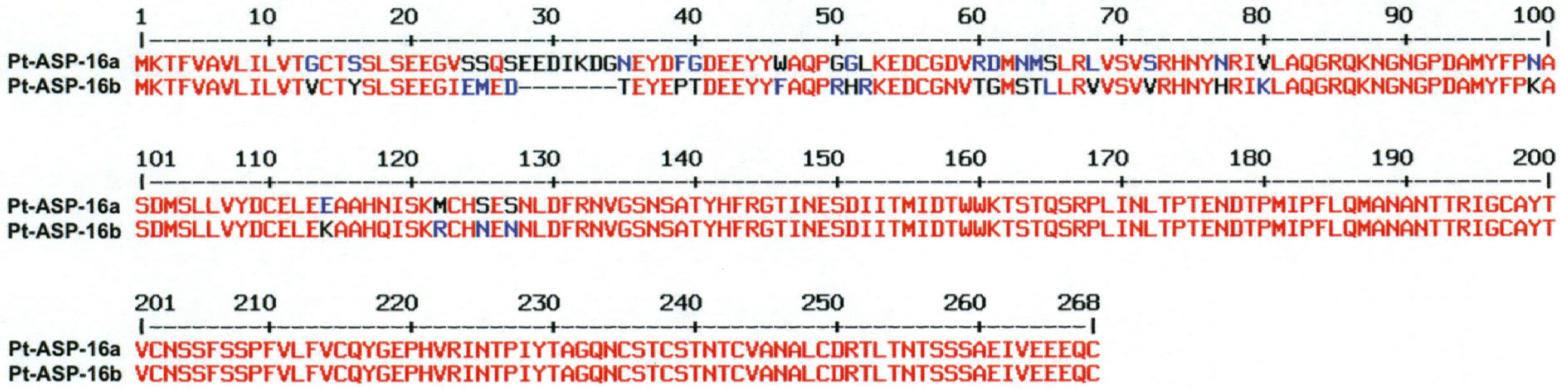


Figure A2-21 *P. tenuis* Ancylostoma secreted protein (ASP) paralogues have 88% identity with each other. The alignment graphic of Pt-ASP-16a with Pt-ASP-16b was developed using the MultAlin sequence alignment program. The amino acids displayed are in standard single-letter code and identical residues are in red.

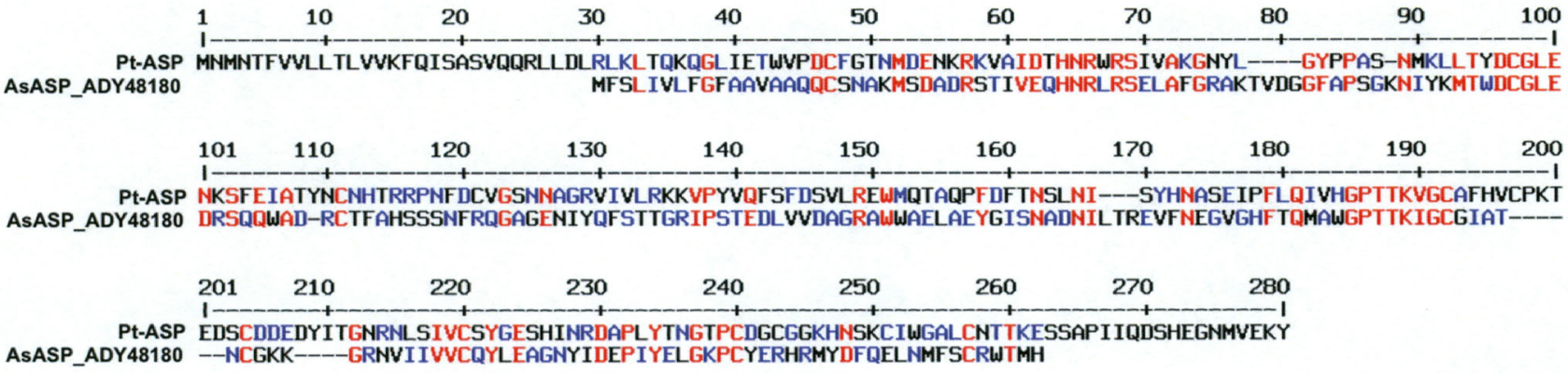


Figure A2-22 *P. tenuis* Ancylostoma secreted protein (ASP) has 28% identity with ASP of *Ascaris suum.* Alignment of Pt-ASP with *A. suum* ASP (ADY48180.1) was performed using the BLASTp program from NCBI. The amino acids are displayed in standard single-letter code and identical residues are in red.

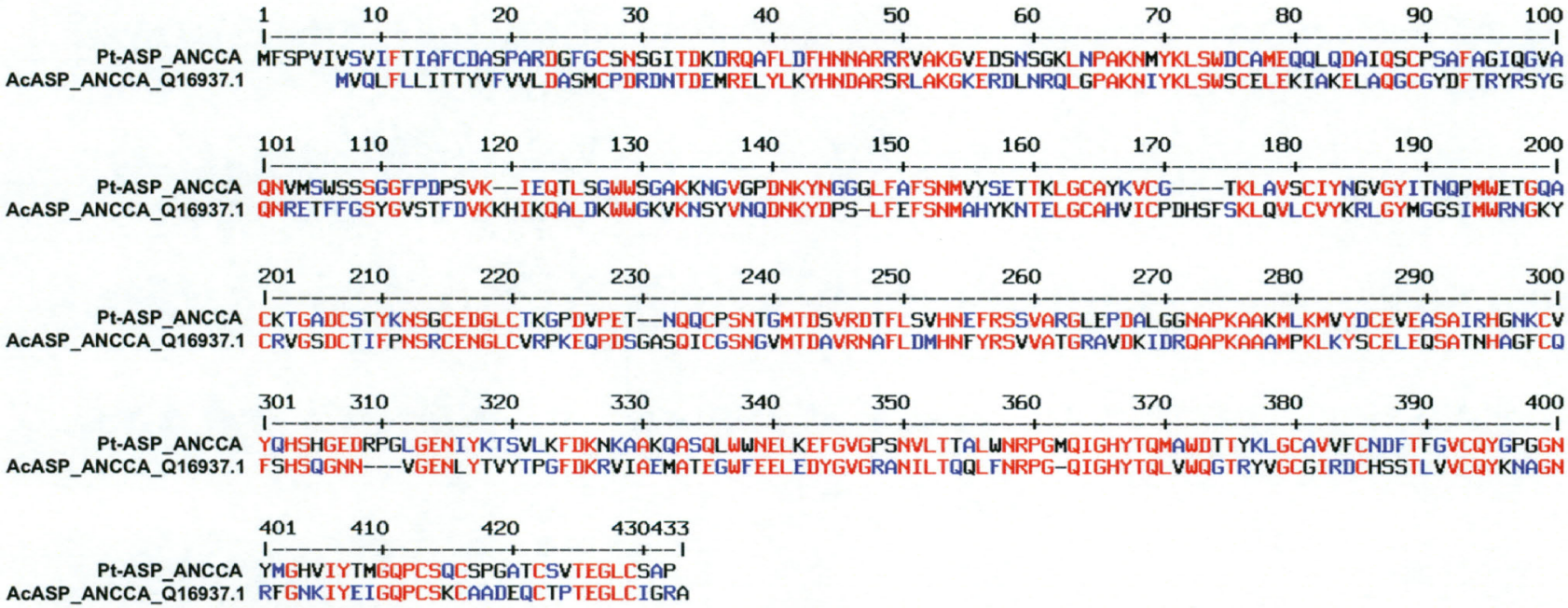


Figure A2-23 *P. tenuis* Ancylostoma secreted protein (ASP) has 42% identity with ASP of *Ancylostoma caninum.* Alignment of Pt-ASP_ANCCA with *A. caninum* ASP (Q16937.1.1) was performed using the BLASTp program from NCBI. The amino acids are displayed in standard single-letter code and identical residues are in red.

Curriculum Vitae
Candidate's full name: Jennifer Lee Fitzpatrick

Universities attended:
Dalhousie University (2008)
Bachelor of Science
Biochemistry & Molecular Biology and Microbiology & Immunology

University of New Brunswick (2013)
Master of Science
Biology

Conference Presentations:

***Fitzpatrick J.,** S. Belfry, E. Rideout, M.S. Duffy. 2012. Improved Localization of the Alpha-Gal Epitope in the Adult Parasite, *Parelaphostrongylus tenuis* Using Immunogold Labeling. 2012 Annual Meeting of the Microscopical Society of Canada, Dalhousie University, Halifax, Nova Scotia. June 5-8th, 2012. (Expanded Abstract)

***Fitzpatrick, J.,** E. Rideout, M.S. Duffy. 2012. Identification of excretory/secretory proteins from adult *Parelaphostrongylus tenuis*. Atlantic Canada Association of Parasitologists Annual Meeting, Pictou, Nova Scotia, Canada, October 26-28, 2012.

*Rideout, E., **J. Fitzpatrick**, M.S. Duffy. 2012. Localization of glycosylated reproductive proteins from *Parelaphostrongylus tenuis* with a potential role in molecular mimicry. 22nd Annual APICS Atlantic Universities Biology Conference, Mount Allison University, Sackville, N.B., March 9-11, 2012.

***Fitzpatrick J.,** S. Belfry, M.S. Duffy. 2011. Fortuitous re-identification of secretory cells with undefined roles in parasitism. 50th Annual Meeting, Canadian Society of Zoologists, University of Ottawa, Ottawa, Ontario. May 16-20th, 2011

*Leger, K., **J. Fitzpatrick,** G. Forbes, M. Burt, M.S. Duffy. 2011.Observations on the incidence and interrelationships of *Parelaphostrongylus tenuis* in moose and deer in New Brunswick. 50th Annual Meeting, Canadian Society of Zoologists, University of Ottawa, Ottawa, Ontario. May 16-20th, 2011

***Fitzpatrick, J.,** M.S. Duffy. 2011. Characterization of *Parelaphostrongylus tenuis* secreted glycoproteins. Atlantic Canada Association of Parasitologists Annual Meeting, Pictou, Nova Scotia, Canada, December 2 – 4, 2011.

*Leger, K., **J. Fitzpatrick**, G. Forbes, D. McAlpine, M.D.B. Burt, M.S. Duffy. 2011. Experimental design for quantifying larval *P. tenuis* in gastropods: considering ecological, logistical, and statistical constraints. Atlantic Canada Association of Parasitologists Annual Meeting, Pictou, Nova Scotia, Canada, December 2 – 4, 2011.

*Bedford, R., **J. Fitzpatrick**, M.S. Duffy. 2010. Molecular conservation of a novel sugar used by parasites for immune evasion. 20th Annual APICS Atlantic Universities Biology Conference, Fredericton, New Brunswick. March 5-7th, 2010.

***Fitzpatrick J.,** R. Bedford, M.S. Duffy. 2010. Alpha-Gal modifications of parasite glycoproteins: Immune evasion via molecular mimicry. 49th Annual Meeting, Canadian Society of Zoologists, University of British Columbia, Vancouver, British Columbia. May 17-21st, 2010.

***Fitzpatrick, J.,** R. Bedford, M.S. Duffy. 2010. Conservation of the alpha-Gal epitope among Metastrongyloid nematodes. Atlantic Canada Association of Parasitologists Annual Meeting, Pictou, Nova Scotia. October 22-24th, 2010.

*Leger, K., **J. Fitzpatrick,** G. Forbes, M. Burt, M.S. Duffy. 2010. Sampling for determination of abundance of *P. tenuis* in deer, moose and gastropods. Atlantic Canada Association of Parasitologists Annual Meeting, Pictou, Nova Scotia. October 22-24th, 2010.

***Fitzpatrick, J.**, M.S. Duffy. 2009. Alpha-Gal modification of glycoproteins; A novel role in immune evasion via molecular mimicry. Alantic Canada Association of Parasitologists Annual Meeting, Pictou, Nova Scotia. October 23-25th, 2009.

*Bedford, R., **Fitzpatrick, J.,** Duffy, M.S. 2009. The phylogenetic distribution of alpha-Gal among Metastrongyloid nematodes. Atlantic Canada Association of Parasitologists Annual Meeting, Pictou, Nova Scotia. October 23-25th, 2009.

Publications (in preparation):

Fitzpatrick, J., E. Rideout, S. Belfry, M.S. Duffy. Observations on the ultrastructure of the excretory gland of adult *P. tenuis* and improved localization of the alpha-Gal epitope. In preparation for International Journal for Parasitology.